

Photocopy and Use Authorization

In presenting this thesis in partial fulfillment of the requirements for an advanced degree at Idaho State University, I agree that the Library shall make it freely available for inspection. I further state that permission for extensive copying of my thesis for scholarly purposes may be granted by the Dean of the Graduate School, Dean of my academic division, or the University Librarian. It is understood that any copying or publication of this thesis for financial gain shall not be allowed without my written permission.

Signature _____

Date _____

Characterization of a Bone-Targeting Angiotensin-(1-7) Conjugate and
Studying Its Stability, Pharmacokinetics' and Pharmacodynamics' Properties

by

Sana Khajeh pour

A dissertation

submitted in partial fulfillment

of the requirements for the degree of

Doctor of Philosophy in the Department of Biomedical and Pharmaceutical

Sciences

Idaho State University

Fall 2022

Committee Approval

To the Graduate Faculty:

The members of the committee appointed to examine the dissertation of Sana Khajeh pour find it satisfactory and recommend that it be accepted.

Dr. Ali Aghazadeh-Habashi,
Major Advisor

Dr. Marvin Schulte,
Committee Member

Dr. Jared Barrott,
Committee Member

Dr. Srinath Pashikanti,
Committee Member

Dr. René Rodriguez,
Graduate Faculty Representative

Animal Welfare Research Committee Approval



Office for Research - Research Outreach & Compliance
921 S. 8th Avenue, Stop 8046 • Pocatello, Idaho 83209-8046

March 5, 2019

Ali Habashi, PhD
921 S. 8th Ave
Stop 8333
Pocatello, ID 83209

RE: Your application dated 3/5/2019 regarding study number 772: Pharmacokinetics and Pharmacodynamics Study of Small Molecule and Peptide Conjugate Anti-inflammatory Drugs in Adjuvant Arthritis Rat Model

Dear Dr. Habashi:

Thank you for your response to requests from a prior review of your application for the new study listed above. Your study is eligible for Designated Member Review under OLAW guidelines.

This is to confirm that your application is now fully approved. The protocol is approved through 3/5/22.

You are granted permission to conduct your study as most recently described effective immediately. The study is subject to annual review on or before 3/5/2020, unless closed before that date.

Please note that any changes to the study as approved must be promptly reported and approved. Some changes may be approved by expedited review; others require full board review. Contact Tom Bailey (208-282-2179; fax 208-282-4723; email: anmicare@isu.edu) if you have any questions or require further information.

Sincerely,

A handwritten signature in black ink, appearing to read "Curt Anderson", written over a horizontal line.

Curt Anderson, PhD
IACUC Chair

Phone: (208) 282-1336 • Fax: (208) 282-4723 • isu.edu/research

ISU is an Equal Opportunity Employer



February 8, 2021

Ali Habashi, PhD
Pharmacy
921 S. 8th Ave., Stop 8333
Pocatello, ID 83209

RE: AMENDMENT regarding study number 772: *Pharmacokinetics and Pharmacodynamics Study of Small Molecule and Peptide Conjugate Anti-inflammatory Drugs in Adjuvant Arthritis Rat Model*

Dear Dr. Habashi:

Your request for revision of the study listed above was reviewed at the 2/8/21 meeting of the Idaho State University IACUC.

The requested revision involves including both sexes in the animal study and investigate the gender effect on the its outcome. This is to confirm that your application for revision has been approved.

You are granted permission to conduct your study as revised effective immediately. The date for the next annual review remains unchanged at 3/5/21, unless the study closes before that date.

Please note that any further changes to the study must be promptly reported and approved. Contact Tom Bailey (anmlcare@isu.edu; 208-282-2179) if you have any questions or require further information.

Sincerely,

A handwritten signature in blue ink, appearing to read 'ERIN RASMUSSEN', written over a horizontal line.

Erin Rasmussen, PhD
IACUC Chair



September 22, 2021

Ali A. Habashi, PhD, PharmD
Biomedical & Pharmaceutical Sciences
921 S. 8th Ave., Stop 8333
Pocatello, ID 83209

RE: AMENDMENT regarding study number 772: *Pharmacokinetics and Pharmacodynamics Study of Small Molecule and Peptide Conjugate Anti-inflammatory Drugs in Adjuvant Arthritis Rat Model*

Dear Dr. Habashi:

Your request for revision of the study listed above is eligible for Veterinary Verification and Consultation (VVC) per OLAW guidelines.

The requested revision involves studying the effect of drinking hydrogenated water on alleviation of adjuvant arthritis sign and symptoms in SD rats. The whole procedure of arthritis induction and animal group assignments will be followed similarly to the original protocol with a simple modification on drug treatment. The animals will drink hydrogenated water instead of receiving drug treatment by injection. The H2 Therapeutics device will produce hydrogenated water, and animal water bottles will be filled to let animals drink hydrogenated water daily for three weeks. The rest of the procedure will follow as described under "Procedure, subsection: PD study." This is to confirm that your application for revision has been approved. Please coordinate with Mia Benkenstein to make sure the appropriate supplies are available when needed.

You are granted permission to conduct your study as revised effective immediately. This study is set to expire on 3/5/22. If work needs to continue past that date, you will need to submit a new protocol at least a month in advance of the expiration date to avoid any gaps.

Please note that any further changes to the study must be promptly reported and approved. Contact Tom Bailey (anmlcare@isu.edu; 208-282-2179) if you have any questions or require further information.

Sincerely,

A handwritten signature in blue ink, appearing to read 'ERIN RASMUSSEN', written over a horizontal line.

Erin Rasmussen, PhD
IACUC Chair

Idaho State UNIVERSITY

Office for Research - Research Outreach & Compliance
921 S. 8th Avenue, Stop 8046 • Pocatello, Idaho 83209-8046

June 15, 2020

Ali Habashi, PhD, PharmD
Biomedical & Pharmaceutical Sciences
921 S. 8th Ave. Stop 8333
Pocatello, ID 83209

RE: Designated Member Review regarding study number 790: *Pharmacokinetics and Pharmacodynamics of PEGylated-Bone Targeting Peptide Conjugates and Small Molecules*

Dear Dr. Habashi:

Thank you for your responses to a full-board review of the study listed above. Your responses are eligible for Designated Member Review (DMR) per OLAW guidelines. This is to confirm that your protocol has been approved.

You are granted permission to conduct your study as submitted effective immediately. The date for annual review is 6/15/21, unless the study closes before that date.

Please note that any further changes to the study must be promptly reported and approved. Contact Tom Bailey (anmlcare@isu.edu; 208-282-2179) if you have any questions or require further information.

Sincerely,



Erin Rasmussen, PhD
IACUC Chair

Phone: (208) 282-1336 • Fax: (208) 282-4723 • isu.edu/research

ISU is an Equal Opportunity Employer



February 26, 2021

Ali Habashi, PhD, PharmD
Biomedical & Pharmaceutical Sciences
921 S. 8th Ave., Stop 8333
Pocatello, ID 83209

RE: DMR regarding study number 798: *Pharmacokinetics and Pharmacodynamics of PEGylated-Bone Targeting-Small Peptide Conjugates*

Dear Dr. Habashi:

Thank you for your responses to a full-board review of the study listed above. Your responses are eligible for Designated Member Review (DMR) per OLAW guidelines.

This is to confirm that your application for revision has been approved. The date for annual review is February 26, 2022, unless the study closes before that date.

Please note that any further changes to the study must be promptly reported and approved. Contact Tom Bailey (anmlcare@isu.edu; 208-282-2179) if you have any questions or require further information.

Sincerely,

A handwritten signature in blue ink, appearing to read 'Erin Rasmussen', with a long horizontal line extending to the right.

Erin Rasmussen, PhD
IACUC Chair



April 14, 2021

Ali Habashi, PhD, PharmD
Pharmacy
921 S. 8th Ave., Stop 8333
Pocatello, ID 83209

RE: AMENDMENT regarding study number 798: *Pharmacokinetics and Pharmacodynamics of PEGylated-Bone Targeting-Small Peptide Conjugates*

Dear Dr. Habashi:

Your request for revision of the study listed above is eligible for Administrative Review per OLAW guidelines.

The requested revision involves adding Caleb Wilson as personnel to the protocol. This is to confirm that your application for revision has been approved.

You are granted permission to conduct your study as revised effective immediately. The date for annual review remains unchanged at 2/26/22, unless the study closes before that date.

Please note that any further changes to the study must be promptly reported and approved. Contact Tom Bailey (anmlcare@isu.edu; 208-282-2179) if you have any questions or require further information.

Sincerely,

A handwritten signature in blue ink, appearing to read 'E. Rasmussen', with a long horizontal flourish extending to the right.

Erin Rasmussen, PhD
IACUC Chair



June 14, 2021

Ali Habashi, PhD, PharmD
Biomedical & Pharmaceutical Sciences
921 S. 8th Ave., Stop 8333
Pocatello, ID 83209

RE: AMENDMENT regarding study number 798: *Pharmacokinetics and Pharmacodynamics of PEGylated-Bone Targeting-Small Peptide Conjugates*

Dear Dr. Habashi:

Your request for revision of the study listed above is eligible for Veterinary Verification and Consultation (VVC) per OLAW guidelines.

The requested revision involves performing routine animal urine collection using standard metabolic cages and adding Logan Cano as personnel to the study. This is to confirm that your application for revision has been approved.

You are granted permission to conduct your study as revised effective immediately. The date for annual review remains unchanged at 2/26/22, unless the study closes before that date.

Please note that any further changes to the study must be promptly reported and approved. Contact Tom Bailey (anmlcare@isu.edu; 208-282-2179) if you have any questions or require further information.

Sincerely,

A handwritten signature in blue ink, appearing to read 'ERIN RASMUSSEN', written over a horizontal line.

Erin Rasmussen, PhD
IACUC Chair



March 15, 2022

Ali Habashi, PhD, PharmD
Biomedical & Pharmaceutical Sciences
921 S. 8th Ave., Stop 8333
Pocatello, ID 83209

RE: DMR regarding study number 805: *Pharmacokinetics and Pharmacodynamics Study of Chemical and Peptide Conjugate Anti-inflammatory Drugs in Adjuvant Arthritis Rat Model*

Dear Dr. Habashi:

Thank you for your responses to a full-board review of the study listed above. Your responses are eligible for Designated Member Review (DMR) per OLAW guidelines.

This is to confirm that your protocol has been approved.

You are granted permission to conduct your study as revised effective immediately. The date for annual review is 3/15/23, unless the study closes before that date.

Please note that any further changes to the study must be promptly reported and approved. Contact Tom Bailey (anmlcare@isu.edu; 208-282-2179) if you have any questions or require further information.

Sincerely,

A handwritten signature in blue ink, appearing to read 'ERIN RASMUSSEN', written over a horizontal line.

Erin Rasmussen, PhD
IACUC Chair

Dedication

This dissertation is a dedication to my mom, brother and my dad who encouraged and supported me and always believed that I could do it. I would like to dedicate this dissertation to brave people of Iran.

Acknowledgments

I would like to thank those that made the completion of this dissertation possible. First, I would like to express my special thanks to my major advisor, Dr. Ali Aghazadeh-Habashi, for his continued support, invaluable guidance, constant encouragement, useful discussion and peerless criticisms throughout this research. He pushed and challenged me to produce projects I am proud of. I am highly grateful to Dr. Jared Barrott, Dr. Srinath Pashikanti, Dr. René Rodriguez, and Dr. Marvin Schulte, my committee members, who enabled me to facilitate my research work and for their insightful feedback.

Secondly, I would like to thank my former and current lab mates, Arina Ranjit, Biwash Ghimire, Matt Kirkham, and undergraduate interns, Zach Capps, Preston Baker, Kaden Lee, Maria Blaser, Emma Summerill, Megan Condie, and Adriene Pavek whose support, and help have been reflected in the completion of this research.

Thirdly, I would like to thank my mom, and my brother, Sina, for their unfailing moral and emotional support and continuous encouragement throughout my years of research

Lastly, I would like to thank everybody else in my personal life who accompanied me during this journey in Idaho, USA. It has been a life-changing experience which marks an important chapter of my life and their presence made it unforgettable. A special thanks to the people who were far from me all this time, but their words and motivation were my driving force every day.

This dissertation research was supported by Idaho State University internal support and a grant from and awards granted to A A-H and SST from the National Institutes of

Health under grants No. P20 GM103408 (sub-award No. SI3394-SB-825944) and 5U54GM104944-07 (sub-award No. GR09455), respectively.

Table of Contents

List of Figures.....	xx
List of Tables.....	xxv
List of Abbreviations.....	xxvi
List of Symbols.....	xxviii
Abstract.....	xxix
1 Chapter I: Introduction to Bone Structure and Bone Drug Delivery.....	1
1.1 The Renin-Angiotensin (Ang) System (RAS).....	1
1.2 Bone Structure and Bone Drug Delivery.....	5
1.3 Inflammation.....	7
1.3.1 Pathophysiology of Inflammation.....	7
1.3.2 Effects of Inflammation.....	9
1.4 Arthritis.....	11
1.4.1 Epidemiology of RA.....	12
1.4.2 Pathophysiology of RA.....	12
1.4.3 Causes and risk factors of RA.....	13
1.4.4 Symptoms of RA.....	14
1.4.5 Diagnosis of RA.....	14
1.4.6 Complications of RA.....	15
1.4.7 Therapeutic Strategies for the Treatment of RA.....	16
1.5 RA and the RAS.....	17
2 Chapter II: Characterization, Validation, Stability, and HA binding Properties of Ang-(1-7) and Ang. Conj.	20

2.1	Hypothesis and Objectives	20
2.2	Experimental Method and Materials	20
2.2.1	HPLC-Photodiode Array Detector (DAD) Analysis of Ang. Conj.....	21
2.2.2	Stability of Ang. Conj.....	22
2.2.3	HA Binding	22
2.2.4	Statistical Analysis	23
2.3	Results	23
2.3.1	Characterization of Ang. Conj.	23
2.3.2	Stability of Ang. Conj.....	25
2.3.3	HA Binding	27
2.4	Discussion.....	28
2.5	Conclusion	30
3	Chapter III: Plasma Angiotensin Peptides as Biomarkers of Rheumatoid Arthritis are Correlated with Anti-ACE2 Auto-Antibodies Level and Disease Intensity.....	32
3.1	Background.....	32
3.1.1	RAS and Inflammation	32
3.1.2	Anti-ACE2 Autoantibodies	32
3.2	Rationale.....	33
3.3	Hypothesis and Objectives	34
3.4	Experimental Methods and Materials.....	34
3.4.1	Defining the RA stage	34
3.4.2	Plasma Sample Collection, Solid-phase Extraction, and LC-MS/MS analysis of the Ang Peptides	35

3.4.3	Enzyme-linked Immunoassay (ELISA) for the Detection of Anti-ACE2 Autoantibodies in Plasma	36
3.4.4	Statistical Analysis	37
3.5	Results	38
3.5.1	Patients' Demographics and RA Staging	38
3.5.2	Plasma Levels of Ang Peptides	39
3.5.3	ELISA Scores for Plasma Anti-ACE2 Autoantibodies	39
3.5.4	Ang Peptides, Anti-ACE2 Autoantibodies, and RA Biomarkers Correlations	40
3.6	Discussion	41
3.7	Conclusions	44
4	Chapter IV: Improved Pharmacokinetics of Angiotensin-(1-7) peptide through Bisphosphonate Conjugation	45
4.1	Background	45
4.1.1	The RAS Components	45
4.1.2	Ang-(1-7) Peptide Actions in the Body	45
4.2	Experimental Methods and Materials	46
4.2.1	Dose Calculation	46
4.2.2	Animal Handling, Cannulation, and Sample Collection	46
4.2.3	Sample Preparation, Extraction, and LC-MS/MS Analysis for Ang-(1-7) Peptide Measurement	47
4.2.4	Pharmacokinetic Modeling and Analysis	49
4.3	Results	49

4.4	Discussion.....	52
4.5	Conclusion	52
5	Chapter V: Anti-Inflammatory Effects of Ang-(1-7) Bone-Targeting Conjugate in an Adjuvant-Induced Arthritis Rat Model.....	53
5.1	Background.....	53
5.1.1	Inflammation and RAS	53
5.1.2	Inflammation and Arachidonic Acid (ArA) Pathway	53
5.2	Rationale.....	57
5.3	Hypothesis and Objectives	58
5.4	Experimental Methods and Materials.....	58
5.4.1	Dose Calculation	58
5.4.2	Adjuvant Arthritis Induction, Assessment, and Animal Handling	58
5.4.3	SS Induction.....	60
5.4.4	Sample Collection	61
5.4.5	Colorimetric Assay for Nitrite and Nitrate Measurement.....	62
5.4.6	Plasma Sample Collection, Solid-phase Extraction, and LC-MS/MS analysis of the Ang Peptides	63
5.4.7	Quantitative Polymerase Chain Reaction (qPCR) Analysis of the RAS Components	63
5.4.8	Western Blot Analysis of the RAS Components and Caspase-3.....	65
5.4.9	Sample Preparation, Simultaneous Extraction, and LC-MS/MS Analysis of Ang Peptides	67
5.4.10	Sample Preparation and LC-MS/MS Analysis of ArA Metabolites.....	68

5.4.11	Statistical Analysis	71
5.5	Results	72
5.5.1	Effect of Ang. Conj. Treatment on Body Weight and Arthritis Index	72
5.5.2	Serum Nitrate and Nitrite Levels	74
5.5.3	Measuring the Plasma Levels of Ang-(1-7) and Ang. Conj.	75
5.5.4	Measuring the Plasma Levels of ArA Metabolites	77
5.5.5	Gene Expression of the RAS Components in Different Tissues	80
5.5.6	Protein Expression of the RAS Components in Different Tissues	82
5.5.7	Statistical Analysis	83
5.6	Discussion.....	84
5.7	Conclusions.....	87
6	Chapter VI: <i>In vitro</i> and <i>In vivo</i> Pharmacodynamics of Ang. Conj. in Cancer	88
6.1	Background.....	88
6.1.1	The RAS and Cancer.....	88
6.1.2	Synovial Sarcoma (SS).....	90
6.1.3	Osteosarcoma (OS).....	92
6.1.4	Breast Cancer	93
6.2	Rationale.....	95
6.3	Hypotheses and Objectives	96
6.4	Experimental Methods and Materials.....	96
6.4.1	Cancer Cell Lines and Culture Media	96
6.4.2	MTT Cell Viability Assay	98
6.4.3	RealTimeGlo™ MT Cell Viability Assay.....	98

6.4.4	Dose Calculation	100
6.4.5	Sample Collection	100
6.4.6	Statistical Analysis	101
6.5	Results	101
6.5.1	Cell Proliferation Assay of SS and OS Cell Lines	101
6.5.2	RealTime MT Assay on Breast Cancer Cell Lines	102
6.5.3	Tumor Size Change in SS-bearing Mice.....	104
6.5.4	The RAS Gene Expression in Tumor Tissue from SS-bearing Mice ..	104
6.5.5	The RAS and Apoptosis Marker Protein Expression in Tumor Tissue from SS-bearing Mice.....	105
6.6	Discussion.....	106
6.7	Conclusions.....	108
7	Summary	110
7.1	General Conclusions.....	110
7.2	Future Directions.....	111
7.3	Strength and Limitations	112
8	References	113

List of Figures

Figure 1. The RAS pathway and its opposing arms. Adapted from reference (44) with permission.	4
Figure 2. Schematic illustration of Ang. Conj. chemical synthesis using Fmoc-mediated solid-phase peptide synthesis. Adapted from reference (69) with permission.	6
Figure 3. The schematic view of bone drug conjugates binding to the bone surface and releasing their cargo.	7
Figure 4. Semi-Prep HPLC chromatogram (a) and MALDI-TOF mass spectrum of Ang. Conj. (b). Adapted from reference (69) with permission.	24
Figure 5. Representative analytical HPLC-DAD individual chromatograms of (A) blank, internal standard (IS), Ang-(1-7), and Ang. Conj. standard solutions and (B) Ang. Conj. solution (plus IS) in the different media after 28 days at room temperature. Adapted from reference (69) with permission.	27
Figure 6. The binding capacity of Ang-(1-7) and Ang. Conj. in the different media. N=3 for each group, *Significantly different from Ang-(1-7), $p < 0.05$. Adapted from reference (69) with permission.	28
Figure 7. An illustration of ACE2 inactivation by its specific autoantibodies. Adapted from reference (44) with permission.	33
Figure 8. Ang-(1-7) and Ang II plasma concentration (ng/mL) in the active (n=5) and remission (n=7) groups (A), and the ratio of Ang-(1-7)/Ang II (B). Data are presented in mean \pm SEM, *significantly different from the remission group, $p < 0.05$. Adapted from reference (44) with permission.	39

Figure 9. The plasma anti-ACE2 autoantibodies ELISA scores of RA patients in the active and remission stages. Data are presented as mean \pm SD, *significantly different from the remission group, $p < 0.05$. Adapted from reference (44) with permission.	40
Figure 10. Correlation between the (A) Ang II concentration, anti-ACE2 autoantibodies ELISA, and RAPID3 scores, (B) Ang II plasma concentration, CRP levels, and anti-ACE2 autoantibodies ELISA score, (C) Ang-(1-7)/Ang II ratio, anti-ACE2 autoantibodies ELISA score, CRP levels, and RAPID3 scores. Adapted from reference (44) with permission.	41
Figure 11. Mean \pm SD plasma concentration-time profile of Ang-(1-7) after Ang-(1-7) (n=3) Ang. Conj. (n=3) i.v., and Ang. Conj. (n=3) s.c. administration in healthy rats (A). Plasma concentration-time profiles of Ang-(1-7) for individual rats after Ang-(1-7) (n=3) Ang. Conj. (n=3) i.v., and Ang. Conj. (n=3) s.c. administration.	51
Figure 12. Arachidonic acid pathway. Hydroxyeicosatetraenoic acids; HETEs, epoxyeicosatrienoic acids; EETs, dihydroxyeicosatrienoic acids; DHTs.	55
Figure 13. The schematic overview of the RAS and ArA pathways and their interactions.	57
Figure 14. Effect of AIA and treatment with Ang-(1-7) and Ang. Conj. on the percentage change of body weight (A) and the arthritis index (B) in the rats (n = 5-6). The percentage change in the right joint (C), right paw (D), left joint (E), and left paw (F) diameters compared to day 0. Different letters denote significant differences between groups ($p < 0.05$), one-way ANOVA followed by Tukey's post hoc test. Adapted from reference (186) with permission.	74

Figure 15. Effect of AIA and Ang-(1-7) or Ang. Conj. treatment on serum NO concentrations (n = 5-6). Different letters denote significant differences between groups ($p < 0.05$), one-way ANOVA followed by Tukey post hoc test. Adapted from reference (186) with permission. 75

Figure 16. Ang-(1-7) (A), Ang II (B), levels and their ratio in plasma in control (n=6), inflamed (n=6), Ang-(1-7)-treated (n=5), and Ang. Conj.-treated (n=5) groups. Values are reported as mean \pm SEM, and statistical analysis was done using one-way ANOVA with the Tukey post hoc test. Different letters denote significant differences between groups ($p < 0.05$). Adapted from reference (186) with permission. 76

Figure 17. Total EETs (A), DHTs (B), and 20-HETE (C) levels in rat plasma samples from control (n=6), inflamed (n=6), Ang-(1-7)-treated (n=5), and Ang. Conj.-treated (n=5) rats. Ratio of the total EETs to 20-HETE in the same groups (D). Correlation between the RAS peptide and ArA metabolites (E&F). Values are reported as mean \pm SEM, and statistical analysis was done using one-way ANOVA with the Tukey post hoc test. * Significantly different from another group, $p < 0.05$. Adapted from reference (188) with permission. 80

Figure 18. Gene expression of ACE1, ACE2, MasR, and AT1R levels in the heart (A), lung (B), liver (C), kidney (D) tissues, and the ratio of ACE2/ACE1 and MasR/AT1R in those tissues (E) in control (n=6), inflamed (n=6), Ang-(1-7)-treated (n=5), and Ang. Conj.-treated (n=5) groups. ACE1; angiotensin-converting enzyme 1, ACE2; angiotensin-converting enzyme 2, MasR; Mas receptor, AT1R; angiotensin II type 1 receptor. Values are reported as mean \pm SEM, and statistical analysis was done using

one-way ANOVA with the Tukey post hoc test. Different letters denote significant differences between groups ($p < 0.05$). Adapted from reference (186) with permission.. 81

Figure 19. Protein expression of ACE1, ACE2, MasR, and AT1R, levels in the heart (A), lung (B), liver (C), kidney (D) tissues, and the ratio of ACE2/ACE1 and MasR/AT1R (E) in control (n=6), inflamed (n=6), Ang-(1-7)-treated (n=5), and Ang. Conj.-treated (n=5) groups. ACE1; angiotensin-converting enzyme 1, ACE2; angiotensin-converting enzyme 2, MasR; Mas receptor, AT1R; angiotensin II type 1 receptor. Values are reported as mean \pm SEM, and statistical analysis was done using one-way ANOVA with the Tukey post hoc test. Different letters denote significant differences between groups ($p < 0.05$). Adapted from reference (186) with permission..... 83

Figure 20. Effect of Ang. Conj. treatment on HSSY-1 and SJSA-1 cancer cells proliferation after 72 hours of a single administration of vehicle, Ang-(1-7) 10 μ M, or Ang. Conj. 10 μ M. 102

Figure 21. Cell proliferation in 4T1.2 (A), T47D (B), and MCF7 (C) breast cancer cell lines after 72 hours of a single administration of vehicle, Ang-(1-7) 10 μ M, or Ang. Conj 10 μ M. Results are reported as mean \pm SEM. * Significant different with $p < 0.05$ 103

Figure 22. Effect of vehicle, Ang-(1-7), and Ang. Conj. treatment on percentage tumor size change compared to day one in SS-bearing mice. Different letters show significant difference between groups. Data are presented as relative to the value of control (mean \pm SD), * $p < 0.05$ 104

Figure 23. Effects of vehicle, Ang-(1-7) and Ang. Conj. treatment on the RAS components gene expression in tumor tissue from SS-bearing mice. Different letters

show significant difference between groups. Data are presented as relative to the value of control (mean \pm SD), $p < 0.05$ 105

Figure 24. Effect of vehicle, Ang. Conj. and Ang-(1-7) on the RAS and apoptosis maker protein expression in tumor tissue from SS-bearing mice. Different letters show significant difference between groups. Data are presented as relative to the value of control (mean \pm SD), * $p < 0.05$ 106

List of Tables

Table 1. Intra- and inter-day precision (coefficient of variation, CV) and accuracy for HPLC assay of Ang. Conj. in three different media. Adapted from reference (69) with permission.	25
Table 2. Percentage of Ang. Conj. remaining after four weeks of storage in different media. Adapted from reference (69) with permission.	26
Table 3. Baseline demographic and clinical characteristics of RA patients. Adapted from reference (44) with permission.	38
Table 4. Ang-(1-7) pharmacokinetic parameters of Ang-(1-7) (n=3) Ang. Conj. (n=3) after i.v., and Ang. Conj. (n=3) after s.c. administration in healthy rats. ^a Significantly different from Ang-(1-7), $p<0.05$, ^b Significantly different from Ang. Conj., $p<0.05$	50
Table 5. Primer sequences used in a reverse transcription-quantitative polymerase chain reaction (qPCR) analysis of genes.	64
Table 6. Compound parameters for arachidonic acid metabolites, and their internal standard with MRM in negative electrospray ionization mode.	70
Table 7. The percentage change in paw and joint diameters in different treatment groups at the end of the experiment compared to day 0. Adapted from reference (186) with permission.	73
Table 8. Inter- and intra-day precision and accuracy of Ang peptides. Adapted from reference (187) with permission.	75
Table 9. Inter- and intra-day precision and accuracy of ArA metabolites. Adapted from reference (187) with permission.	77

List of Abbreviations

ACE	Angiotensin converting enzyme
ACE2	Angiotensin converting enzyme 2
ACEI	Angiotensin converting enzyme inhibitor
AI	Arthritis index
AIA	Adjuvant-induced arthritis
Ang	Angiotensin
Ang. Conj.	Angiotensin-(1-7) pegylated bisphosphonate conjugate
ArA	Arachidonic acid
ARB	Angiotensin II receptor blocker
AT1R	Angiotensin II type 1 receptor
AT2R	Angiotensin II type 2 receptor
BAL	Broncho alveolar lavage
BP	Bis-phosphonate
CFA	Complete Freund's adjuvant
COX	Cyclooxygenase
DAD	Photodiode array detector
DKK-1	Dickkopf-1
ER	Estrogen receptor
GPCR	G protein-coupled receptors
HA	Hydroxyapatite
HLA	Human Leukocyte Antigen

HPLC	High-performance liquid chromatography
i.v.	Intravenously
MasR	Mas receptor
MAPK	Mitogen-activated protein kinases
MI	Myocardial infarction
MMP	Matrix metalloproteinases
MTT	3-(4,5-dimethylthiazol-2-yl)-2,5-diphenyl-2H-tetrazolium bromide
NSAIDs	Non-steroidal anti-inflammatory drugs
OD	Optical density
OS	Osteosarcoma
PBS	Phosphate buffer saline
PEG	Poly-ethylene glycol
PR	Progesterone receptor
qPCR	Quantitative polymerase chain reaction
RA	Rheumatoid arthritis
RANKL	Receptor activator of nuclear factor kappa-B ligand
RAS	Renin-angiotensin system
RNS	Reactive nitrogen species
ROS	Reactive oxygen species
s.c.	Subcutaneously
SD	Standard deviation
SEM	Standard error of mean
SS	Synovial sarcoma

List of Symbols

α	Greek small letter Alpha
β	Greek small letter Beta
g	Gram
k	Kilo
λ	Greek small letter Lambda
L	Liter
μ	Greek small letter Micro
m	Milli
M	Molar
n	Nano
p	Pico

CHARACTERIZATION OF A NOVEL BONE-TARGETING ANGIOTENSIN-(1-7)
CONJUGATE AND STUDYING ITS STABILITY, PHARMACOKINETICS' AND
PHARMACODYNAMICS' PROPERTIES

Dissertation Abstract--Idaho State University (2022)

The renin-angiotensin (Ang) system (RAS) is an enzymatic cascade that controls many body functions. It consists of classical and protective arms counteracting each other. Chronic imbalances of them are seen in different pathophysiological conditions. As part of the protective arm, Ang-(1-7) is extensively known for its beneficial actions in different body systems, including anti-inflammation, and anti-proliferation. However, enzymatic instability and short half-life, leading to its low bioavailability, hamper Ang-(1-7) beneficial effects. To address this shortcoming, we have employed a bisphosphonate (BP) conjugation strategy by conjugating Ang-(1-7) to a non-nitrogenated BP moiety through a polyethylene glycol (PEG) linker (Ang. Conj.).

We hypothesize that formation of the Ang. Conj. can improve its stability which can present with an improved pharmacokinetic, and longer half-life. Therefore, it will outperform the native Ang-(1-7) peptide in different diseases. Our objectives were to show Ang. Conj. is capable of reducing signs and symptoms of inflammation in models of arthritis and cancers.

Several methods were designed to test these hypotheses. chromatography method was used to quantify Ang-(1-7) and Ang. Conj. and to study Ang. Conj. stability, and pharmacokinetic, and pharmacodynamic. Fluorescent spectrometry was used to compare the hydroxy apatite binding of Ang. Conj. and compare it to the native peptide *in vitro*. MTT assays were done to measure the cancer cell viability. To perform the

animal study of RA, Sprague-Dawley rats were treated with vehicle or test articles. Body weights and arthritis indices were measured during the study and nitric oxide colorimetric assay, and the RAS components in tissues were analyzed.

Our results suggest that Ang. Conj. has more bioavailability and bone targeting capacity compared to native Ang-(1-7). Moreover, administration of Ang. Conj. decreased edema, weight loss, and nitrite/nitrate, and it balanced the RAS components' levels in an RA rat model and SS model in mice.

We concluded that inflammatory diseases have detrimental effects on the RAS. We highlight the feasibility of a novel class of bone-targeting peptides for RA and other inflammatory conditions and prolonging the half-life of Ang-(1-7), enhances its therapeutic effects. Our approach represents a novel therapeutic opportunity for using natural peptides in inflammatory conditions.

Keywords: The renin-angiotensin system, Bone drug delivery, Pharmacokinetics, Pharmacodynamics

1 Chapter I: Introduction to Bone Structure and Bone Drug Delivery

1.1 The Renin-Angiotensin (Ang) System (RAS)

The discovery of renin about 80 years ago resulted in remarkable advances in scientists' understanding of the RAS (Fig. 1). This system has several critical physiological actions (1). It is involved in several enzymatic reactions through the activity of its enzymes, peptides, and receptors components (2). The pharmacological actions of the RAS have been shown to be on a wide range of body tissues, including the kidneys, heart, brain, gastrointestinal tract and reproductive organs (3). Diverse actions of Ang peptides as part of the locally acting RAS are present in almost all tissues of the body. The RAS that is distributed in tissues contributes to many metabolic diseases (4), in tandem with the centrally-acting RAS that controls blood pressure and body fluid homeostasis (5, 6). As a major regulator of body homeostasis, the RAS has two counter-regulatory axes: "the classical RAS" composed of Ang converting enzyme (ACE)/Ang II/Ang type 1 receptor (AT1R) axis. On the other hand, "the protective arm" is composed of ACE2/Ang-(1-7)/Mas receptor (MasR) which promotes anti-proliferation, anti-angiogenesis, and vasodilation effects (7). Ang-(1-7) inhibits arginine-vasopressin release from rat hypothalamo-neurohypophysial to control blood pressure in the CNS, increases the synthesis of nitric oxide in heart (8) in addition to protective effects in cardiovascular system (9), renal dysfunction (10), asthma and pulmonary fibrosis, and regulating the pancreatic hormones, liver, and skeletal muscle functions (9). The positive role of this pathway in different cancers have shown as well (11). These two

arms are maintained in a dynamic balance (12) in healthy individuals; however, when the RAS is activated, the balance shifts toward the classical arm (13). Ang II, which was known to be the effector peptide of this system, is produced enzymatically from Ang I in plasma and various tissues by the action of ACE1 (14). This peptide can directly act on the AT1R or exert its actions indirectly through aldosterone stimulation. AT1R activation via Ang II will result in vasoconstriction, cardiac hypertrophy, remodeling, inflammation, fibrosis (15), proliferation, and metastasis of several cancers (16-18). Formation and stimulation of reactive oxygen (ROS) and nitrogen species (RNS) stimulated by the AT1R cause pathophysiological conditions (19, 20). The formation of the ROS activates many signaling pathways that trigger mitogen-activated protein kinases (MAPK), tyrosine kinases, phosphatases, calcium channels, and redox-sensitive transcription factors resulting in cell growth, and pro-inflammatory gene expression (21). Moreover, the chymase enzyme can generate Ang II, a non-ACE1 enzyme that hydrolyzes angiotensinogen to Ang-(1-12) (22). Chymase is produced and distributed in many organs, including the heart (23). Recent studies have demonstrated that Ang II is not the final product of the RAS, and other peptides affect different bodies' systems and mechanisms (24). The opposite arm of the classical pathway regulates the cardiovascular, central nervous system, gastrointestinal, musculoskeletal, and immune systems (25). Functioning as a carboxypeptidase, ACE2 was discovered two decades ago and converts Ang II to Ang-(1-7). Being a member of the G protein-coupled receptors (GPCR) (26), MasR is a specific receptor for Ang-(1-7), but not Ang II (27). Another side of the protective arm is the stimulation of the AT2R, a functional AT1R antagonist, by Ang II, which results in vasodilation, anti-proliferation, anti-inflammatory,

and anti-fibrotic. Although some controversy exists regarding its beneficial role, new studies suggest a protective role for AT₂R activation, especially in renal diseases and injuries (28, 29).

There are some other enzymes involved in the RAS. Other than renin, some acid peptidases, including cathepsins E and D, and aspartic proteinases, are capable of forming Ang I from angiotensinogen (30-32). Cathepsin D is found in lysosomes, whereas cathepsin E is an endoplasmic reticulum, endosomes and other cell compartments enzyme. Formation of various peptide precursors are done by both cathepsin enzymes (31). Formation of Ang I can also be done by two neutral peptidases in the brain: elastase and proteinase 3 (33, 34). Furthermore, generation of Ang II can be performed directly from angiotensinogen through the action of two neutral peptidases cathepsin G and tonin, together with elastase and proteinase 3, without Ang I production as an intermediate. This is done by the cleavage of the peptide bond between the Phe⁸–His⁹ residues (35, 36). Aminopeptidases have traditionally been thought to be inactivators of Ang II (37). In the brain, it has been suggested that aminopeptidase A activity is essential for formation of an active Ang III peptide which plays a key role in central control of arterial blood pressure (38). Metabolization of Ang II can also be done by endopeptidases, such as neprilysin, thimet oligopeptidase, and neutral endopeptidase. They cleave the Tyr⁴–Ile⁵ bond and form two tetrapeptides (39, 40). Moreover, all these endopeptidases are able to cleave Ang I to form Ang-(1-7) (39, 41). Neprilysin is a neutral endopeptidase and a member of the membrane-bound, zinc-dependent metalloproteases. It cleaves peptide bonds on the amino acid side of hydrophobic amino acid residues (42, 43).

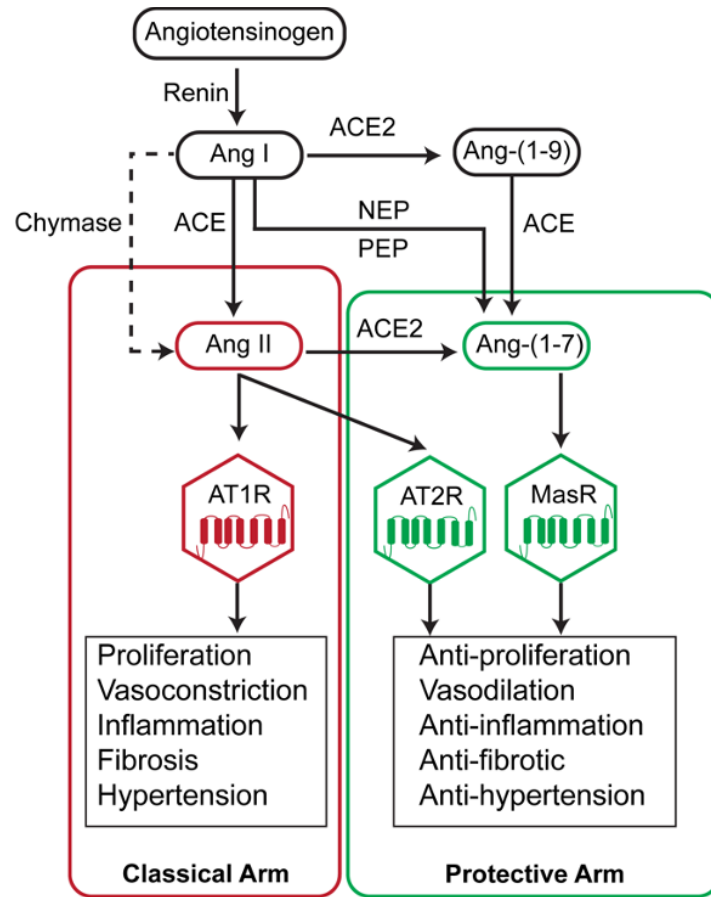


Figure 1. The RAS pathway and its opposing arms. Adapted from reference (44) with permission.

Targeting different components of the RAS has been an interesting topic. It led to significant discoveries of ACE1 inhibitors (ACEIs), and Ang II receptor blockers (ARBs) mainly for treating cardiovascular disorders. Accumulating evidence supports that targeting the protective arm components, such as Ang-(1-7), counteracts the Ang II action (25). Ang-(1-7) has been tested in different pathological conditions, such as diabetes (45), diabetic nephropathy (46), cardiovascular (47) and pulmonary diseases (48), rheumatoid arthritis (RA) (49), Alzheimer's disease (50, 51) and cancer (52-55). However, its low bioavailability due to systemic enzymatic degradation hampers its beneficial effects. Different strategies extend its short circulation half-life, including

structural modifications or appropriate drug delivery systems. For example, in an effort, Ang-(1-7) is incorporated in hydroxypropyl β -cyclodextrin for a long-term oral formulation of the peptide (56, 57). Hay et al. fabricated a glycosylated Ang-(1-7) with improved pharmacokinetic parameters to treat vascular cognitive impairment and inflammation-related memory dysfunction (58). A liposomal formulation of Ang-(1-7) was fabricated to slow-release the peptide for a long-lasting cardiovascular effect (59). A structurally-modified acetylated and aminated Ang-(1-7) was made for the purpose of treating lung cancer and it showed an increased peptide stability with improved pharmacokinetic parameters and half-life (60). These approaches enhanced the therapeutic efficacy of peptide drugs in general and Ang-(1-7) in specific (61). In a different strategy, we utilized the bone as a target for drug delivery, which will be discussed in detail in the following section.

1.2 Bone Structure and Bone Drug Delivery

Bone is essential for numerous vital functions in the body and is necessary for life. It provides a rigid framework of our skeletal system, allows the movement of limbs by interacting with muscle, protects internal organs, generates and maintains various blood cells, and is a source of essential minerals such as calcium and phosphorus (62). Strategies for different drug deliveries provide the benefit of improving the active pharmaceutical ingredients delivery to the site of drug action. The power of targeting drugs to the bone surface has been known since the mid-1970s, when radioactive technetium BP conjugation was used for the diagnostic imaging of bone metabolism (63) (Fig. 2). Using BP conjugation as a foundation for enhanced and novel drug delivery of small molecules to bone has been explored by several researchers (64, 65).

However, proteins and peptides conjugation strategies are being tested by different groups, recently. This approach has faced several challenges in controlling the site-directed coupling of bisphosphonate moieties to the peptide backbone while continuing to maintain the therapeutic abilities of the active biological component (66-68) (Fig. 3).

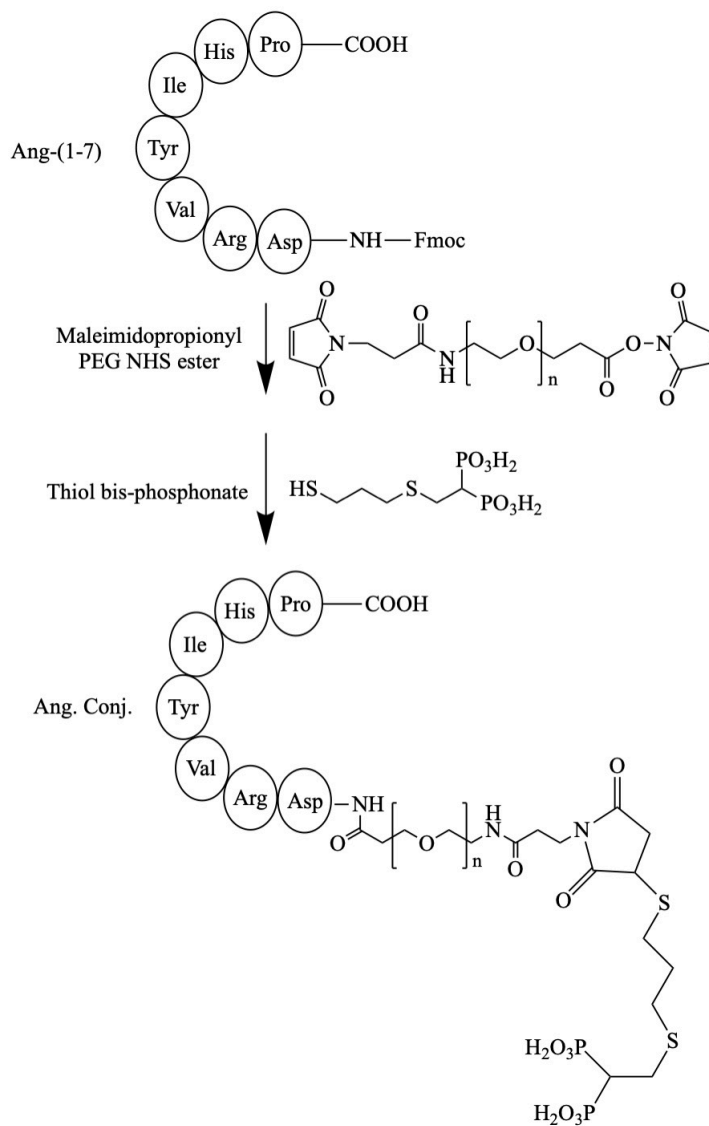


Figure 2. Schematic illustration of Ang. Conj. chemical synthesis using Fmoc-mediated solid-phase peptide synthesis. Adapted from reference (69) with permission.

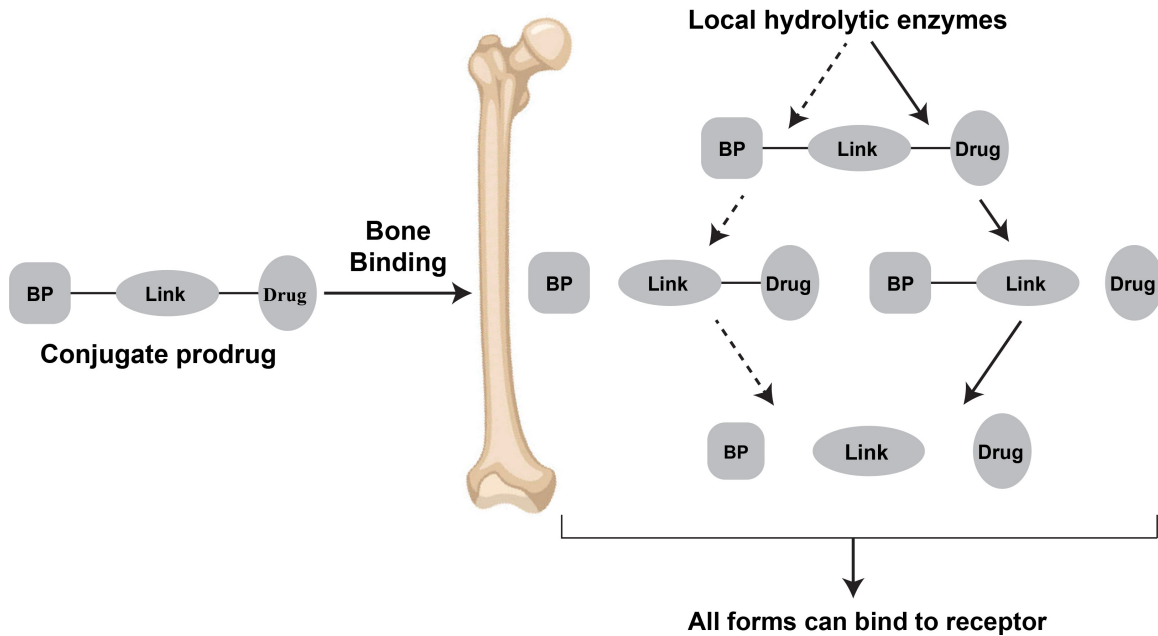


Figure 3. The schematic view of bone drug conjugates binding to the bone surface and releasing their cargo.

1.3 Inflammation

Inflammation is considered a body physiological response and a protective mechanism against harmful stimuli, damage to its cells, and/or invasion by a pathogen. It prevents the spread of infection, eliminates pathogens, disposes of dead cells, and sets the stage for healing and repair. Complex physiological mechanisms are involved in the process of inflammation, including activation of the immune system, release of chemical mediators, and tissue response. These are all considered as the body's biological response towards harmful stimuli (70).

1.3.1 Pathophysiology of Inflammation

Multiple systems and a series of processes in the body coordinate the biological mechanisms behind the inflammatory response. Such processes can be classified into three types of responses: vascular, cellular, and immune.

The inflammatory mediators' initial release results in vascular response marked by small blood vessels vasoconstriction in the inflamed area followed by vasodilation of the arterioles, increased vascular permeability, and increased blood flow. These result in redness, radiation of heat, swelling, and fluid formation in the inflamed area (71).

The cellular response begins with the leucocyte's infiltration in the inflamed area and is evident with the progression of inflammatory symptoms and tissue remodeling. The cellular response is completed in four distinct steps: 1) pavement: a process of antigen recognition, pooling of blood and release of inflammatory mediators; 2) emigration: infiltration of leucocytes; 3) chemotaxis: increase in the local population of leucocytes and macrophages at the site of inflammation; and 4) phagocytosis: involving the actual process of digestion of microbes or dead cells by the immune cells (71-73).

Lastly, the immune response involves a response against the invading microbe by coordinating T-cell-mediated cellular immunity and antibody-mediated humoral immunity. Initially, T-cells are activated for antigen recognition and releasing chemotaxis mediators to activate the B-cells in turn. Upon activation, B-cells produce antibodies against the antigen. T-cells act as the regulators of the immune response as they control the recruitment of immune cells at the site of inflammation (74).

The tissue repair process starts after the harmful stimuli removal, which is marked by the appearance of fibroblasts in the inflamed area. First, the fibrin and collagen fibers separate the inflamed area from the surrounding healthy tissue and provide an environment for the digestion of the dead cells and further tissue repair by providing a favorable inside environment. There are different stages in this process, including a loss of tenderness, resistance to stretch, and immobilization, as the tissue adapts and

recovers from the removal of dead cells and harmful stimuli. It may take several months to years for the tissue to regain its steady state and resume normal function (71-73).

1.3.2 Effects of Inflammation

The more we understand the inflammatory processes, inflammatory mediators, and involvement of body mechanisms in inflammatory responses, it has very important to investigate the effect of inflammation in different body organs.

Local effects of inflammation: When the inflammation happens, its local effects include an increased blood supply, increased vascular permeability of the capillaries, and leaking of the blood vessels. This would pool the fluids and leads to edema, redness, heat radiation, and swelling in the inflamed area. This will help with toxins dilution, help antibodies to reach the antigens and neutralize them, and help the lymphatic system with taking up the dead cells' debris.

Systemic effects of inflammation: When inflammation happens in the body, it is not limited to the inflamed area only and involves multiple organs and systems. Various systemic effects will be resulted from the release of inflammatory mediators in the circulation during inflammation. This is when the preliminary symptoms develop into systemic signs, including pyrexia, weight loss, nausea, anorexia, leukocytosis, increased erythrocyte sedimentation rate, amyloidosis, and many other hematological changes. Other systemic consequences of inflammation consist of compromised organs function such as reduced renal function, changes in hepatic metabolism, and altered ischemic reconditioning (75).

Pyrexia happens when the body's temperature increases caused by bioactive proteins (pyrogen) that are released by leucocytes in the process of digesting the invading bacteria. The thermoregulatory center is affected by these pyrogens and some prostaglandins, resulting in increased body temperature (75).

Another common systemic effect of inflammation consequences is weight loss caused by the negative nitrogen balance during the process of inflammation, indicating the consumption of energy. Reactive hyperplasia of the reticuloendothelial systems and swelling or enlargement of the systemic lymph nodes is also common in acute and chronic inflammation (75).

Hematological changes are non-specific inflammation consequences including an increase in the erythrocyte sedimentation rate. These are assumed to be caused by the release of cytokines, thromboxane, and leukotrienes by immune cells, which increase the thrombogenic potential of blood (75).

Longstanding chronic inflammation also causes elevated levels of serum amyloid-A protein abnormal shredded protein fragments that can result in plaque formation and leads to systemic (reactive) amyloidosis, organ failure, and death (76).

Diseases associated with inflammation: Among all the inflammatory cytokines (e.g., interleukin-1 (IL-1) and -6, tumor necrosis factor- α , C-reactive protein (CRP)), CRP high level is found to be associated with cardiovascular diseases. High levels of inflammatory markers are also seen in depression, dementia, and Alzheimer's disease (77). There are several other diseases that are associated with inflammation, too, including asthma, RA, diabetes, immune disorders, Crohn's disease, hepatitis, and tuberculosis (78). In what follows, RA, as one of the inflammatory disorders, will be discussed in detail.

1.4 Arthritis

Arthritis is the inflammation of the joints and a musculoskeletal disorder that describes various rheumatic conditions that affect joints, tissues around joints, ligaments, cartilage, and connective tissue. It is considered one of the most common chronic diseases in the world that affects one-third of the population of over 45-year-old individuals in the United States. These patients, at some point, suffered from objective joint pain, swelling, and loss of mobility due to arthritis (79). A significant number of the youth (< 25 years) is also affected despite the fact that it is considered a disease of the elderly. Arthritis has been found to be more prevalent in females in comparison to males, and it has a substantial impact on the quality of life as a chronic disorder (80).

There are many types of arthritis that range from mild forms (e.g., tendonitis, bursitis, and fibromyalgia) to severe and systemic forms (e.g., osteoarthritis and RA). Arthritis's exact trigger is not known, but some of its risk factors are autoimmunity, microbial infection, genetics, environment, smoking, and physical or emotional stress (81).

Arthritis is classified into different types: 1) Infectious arthritis (e.g., arthritis secondary to bacterial and viral infections); 2) degenerative arthritis (e.g., diffuse idiopathic skeletal hyperostosis); 3) RA (e.g., RA, juvenile arthritis); 4) traumatic arthritis (e.g., work-related trauma to joints, radiation-induced arthritis, Raynaud's disease); 5) metabolic arthritis (e.g., gout and pseudo-gout) (82).

RA is an autoimmune disease affecting 1% of the population worldwide. It has an unknown origin and is characterized by the production of antibodies directed against the body's own synovial tissues, cartilage, and bone. This results in joint and surrounding

tissue inflammation, pain, and swelling. Despite the fact that RA is a joint disorder, its signs and symptoms may spread to other organs, such as fever, loss of renal function, and cardiovascular abnormalities (83).

1.4.1 Epidemiology of RA

RA is prevalent in 0.1-1% of the general population and is considered to be one of the leading causes of disability in the world (84). RA is predominantly considered a disease of the elderly (more than half of new RA cases occur between ages 40 and 70 years); however, the younger population aged between 25-50 years old are also affected, and women develop this disease three times more than men (81). In 2005, it was estimated that 1.3 millions of the United States population are reported to have RA, and it imposes a total of \$128 billion to the United States economy through the direct and indirect cost of treatment (85). Overall, 50% of people with RA are work-disabled, and this is expected to increase in the next 30 years (86).

1.4.2 Pathophysiology of RA

The body's immune system plays an important role in producing antibodies against its own cells, referred to as autoimmunity. These antibodies attack the synovial lining and membranes around the joints resulting in inflammation, swelling, and pain in joints. The RA characterization is the thickening of the synovium, stiffness of joints, loss of mobility, and loss of alignment. The pathophysiology of RA involves an immune cell complex reaction between humoral immunity (87). The synovial membrane is either damaged during RA or infiltrated by the inflammatory cytokines released by inflammatory cells. The subsequent activation result of these cytokines is the activation of antigen-specific

macrophages and T-cells. As a result, T-helper cells are recruited at the site of inflammation, followed by triggering the humoral immunity by activating B-cells. Subsequently, the activated B-cells will secrete antibodies against the synovial membrane (88). This auto-antibodies production in tandem with the release of cytokines in the synovial fluid creates an inflammatory environment in the joints that causes RA (89).

1.4.3 Causes and risk factors of RA

Although the exact cause of RA is still not known, both genetic and environmental factors are suspected of triggering the immune system leading to RA. Genetically, a specific Human Leukocyte Antigen (HLA) gene polymorphism is reported to increase the risk of developing RA by five times in comparison to the general population (90). HLA is responsible for controlling the immune response against an antigen; thus, any abnormality. Moreover, there are other genes polymorphism that is suspected to be involved in RA but can only explain a part of the causes (91, 92).

Other risk factors include gender (mostly happens in women), use of oral contraceptives, microbial infections, menstrual history, physical and emotional stress or trauma, obesity, breastfeeding, and hormone replacement therapy. Environmental factors such as smoking, air pollution, insecticides, mineral oil, and pollens could also play an important role in RA development and progression (93).

1.4.4 Symptoms of RA

RA's primary symptoms are swollen joints, redness, and pain. Larger joints are most affected (e.g., wrists, knees, fingers, and ankles) simultaneously on both sides of the body. The onset of the disease often happens slowly together with joint stiffness and pain, further developing into morning stiffness, tender, and warm joints becoming stiff over time. Morning stiffness usually lasts for one hour after waking up and wears off as the joint and tendons warm up during the day. Additionally, chest pain, shortness of breath, finger numbness, burning and tingling of extremities, and sleep disturbances are other symptoms of RA (87-93).

1.4.5 Diagnosis of RA

Although RA's early symptoms are non-specific (e.g., malaise, weakness, muscle soreness, and low-grade fever) and hard to diagnose. Its diagnosis should ideally be made at the onset of the disease within six months of the preliminary symptoms. To further prevent the emergence of greater damages, the appropriate treatment should be started (93).

Diagnosis of RA should include the following:

Medical history: Asking for personal habits, recent and current symptoms (e.g., early morning stiffness, inflamed nodules, low-grade fever, and restricted movement) followed by a physical examination of the joints looking for any involved joints, pain, and swelling.

Blood tests: A complete blood test along with erythrocyte sedimentation rate and specific inflammatory markers of RA (e.g., CRP) for confirmation.

Imaging tests: An ultrasound, X-ray, or magnetic resonance imaging of areas that are affected should be done for differential diagnosis and measuring the extent of erosion and damage to the bone (93).

1.4.6 Complications of RA

1- Cardiovascular diseases: Cardiovascular diseases are the most common diseases found in conjunction with RA, especially congestive heart failure and myocardial infarction. Cardiovascular complications associated with an estimated 40% of the deaths in RA patients.

2- Infections: Infections are common in RA patients, including tuberculosis being the second leading cause of death in RA patients. However, it is still unclear if the underlying cause of this infection is the immune system dysfunction due to RA or the anti-rheumatic drugs side effects targeted to suppress the immune system.

3- Central nervous system diseases: Reports of anxiety and depression is prevalent in patients suffering from RA.

4- Malignancies and cancer: RA patients at some point in their lives suffer from malignancies such as lymphomas, leukemia, multiple myelomas, and cancer.

5- Carpal tunnel syndrome: RA can affect the nerves supplying to the hands at advanced stages of the disease leading to curving of fingers and hands, a condition called carpal tunnel syndrome.

6- Lung diseases: RA patients experience dramatic hemodynamic changes and accumulation of fluids exudate in the lungs resulting in significant loss of surface area, leading to shortness of breath, asthma, and scarring (93).

1.4.7 Therapeutic Strategies for the Treatment of RA

There are several pharmacological and non-pharmacological strategies suggested for the RA that can improve the disease condition, avoid further complications, and improve the quality of life. The overall goals of RA therapy are relieving symptoms, preventing joint damage, improving physical function, and preventing complications.

Non-pharmacological approaches include physical activities that are properly designed, including walking, cycling, swimming, and jogging. If the patients do these exercises properly and regularly, they can reduce pain and fatigue, improve mobility, counter depression, strengthen the joints, and improve quality of life. It is recommended that the RA patient 150 minutes per week moderate physical activity, combined with resistance training two times per week. In addition to that the next step is to make sure to advice the patient that physical activity is safe, and can improve the main RA symptoms. This should be implemented by RA practitioner in every visit (94).

Pharmacological interventions include administration of non-steroidal anti-inflammatory drugs (NSAIDs), glucocorticoids, disease modifying anti-rheumatic drugs, and biologics. NSAIDs inhibit prostaglandin synthesis by inhibition of cyclooxygenase (COX) enzymes. They are classified into non-selective and selective COX-2 inhibitors based on their COX-2 selectivity (95).

Glucocorticoids are used to treat RA due to their immune-suppressive, and anti-inflammatory properties. They suppress the immune system, and block the RA inflammatory mediators. This class of drug, such as prednisolone, is used only in extreme situations and for short-term because of their side effects, including weight gain, thinning of the bones, and infections due to immune suppression (96).

Disease modifying anti-rheumatic drugs modify the immune system and slow down the RA progression by protecting joints from further damage. Examples of this category of drugs are methotrexate, sulfasalazine, cyclophosphamide, gold salts, minocycline, and penicillamine (97).

Biological response modifiers or biologics are monoclonal antibodies or anti-inflammatory cytokines fusion proteins, and T-cell antigens (98). They are usually well-tolerated but they have high-cost and are injectables, so their use is reserved for severe conditions and for those patients who are non-responsive to regular medications (99).

1.5 RA and the RAS

Between all the mechanisms related to the pathogenesis of RA, the RAS plays a crucial role in that. For example, Ang II, known as a cytokine and growth factor, actively contributes to many inflammatory effects (100). RAS is shown to be functional locally in many organs and tissues, including chondrocytes, synovial tissue, and synovial fluid (101). In the pathological synovium of RA patients, the existence of a locally activated RAS is verified by showing a high level of ACE1 and active renin concentrations in the synovial fluid in RA patients, proposing that inactive renin becomes active in the RA (101). When the RAS becomes highly activated, Ang II is formed in high amounts in the RA, and is believed to have a great contribution to the disease initiation, progression and inflammatory responses. Ang II is responsible for the activation of NF- κ B resulting in an increase in tissue damage (102) plus enhances the production of pro-inflammatory cytokines including IL-1, IL-6, and TNF- α . IL-6 upregulates the expression of vascular AT1R causing further endothelial dysfunction, vasoconstriction, oxidative stress, and inflammatory events (103). Ang II also induces the ROS by AT1R activation and

upregulating the NAPDH activity in osteoblasts, vascular smooth muscle cells, and neutrophils (104). All these effects are confirmed by studies that administered AT1R antagonists in animal models of RA and observed a potent anti-inflammatory effect (105). For example, the co-administration of azilsartan, AT1R blocker, with etanercept for the active RA treatment, resulted in a greater improvement of the disease condition compared to the etanercept alone (102).

The expression and activity of ACE1, as another role key player in the pathology of RA, was seen to be higher in RA patients' synovia (106) and the administration of the ACEIs, such as captopril, improved arthritis symptoms, clinical scores, plasma viscosity, and the CRP level in patients with active RA (107).

Ang II action through AT1R can cause angiogenesis by stimulating the migration of inflammatory mediators and cytokine release (108) in addition to local VEGF production (109). The expression of the VEGF in synovial fluid in RA patients is significantly high. Similarly, the Ang II peptide level, as a classical arm component, is high in RA patients' synovial fluid. As a result, it can be inferred that the level of the activated RAS components, such as Ang II is positively correlated with the expression of VEGF and its involvement in the process of angiogenesis and cartilage degeneration (100).

The classical RAS shown to be an important cause of osteopenia in RA through different pathways. The activated RAS impairs the balance between osteoclastogenesis and osteoblastogenesis (110) through receptor activator of nuclear factor kappa-B ligand (RANKL), Dickkopf-1 (DKK-1), and matrix metalloproteinases (MMPs) pathways. RANKL pathway activation leads to osteoclastogenesis and joint inflammation by the expression of NF- κ B (111). DKK-1 is a glycoprotein that inhibits the Wnt/ β -catenin

signaling which is essential for osteoblast formation and inhibiting osteopenia (112). Classical RAS upregulates DKK-1 by increasing its expression through AT1R activation (104). MMPs, including MMP-13, MMP-9, and MMP-14 appear to be the most important in degradation and apoptosis in the synovial tissue which are overly expressed by the action of Ang II via AT1R in osteoblasts (113).

We hypothesized that the bone-targeted Ang-(1-7) has higher stability, bone binding capacity, improved pharmacokinetics parameters, and pharmacodynamics outcomes compared to the native peptide.

2 Chapter II: Characterization, Validation, Stability, and HA binding Properties of Ang-(1-7) and Ang. Conj.¹

2.1 Hypothesis and Objectives

We hypothesized that Ang. Conj. is stable and presents with improved pharmacokinetic parameters and longer half-life compared to Ang-(1-7) native peptide (Chapter 1).

The objective of this novel approach was to characterize the Ang. Conj. via analytical instruments, to test its stability in different media and temperatures, and to investigate the preclinical pharmacokinetics and profiles of Ang-(1-7) after Ang-(1-7) and Ang. Conj. administration in healthy rats. Pharmacokinetic properties of Ang-(1-7) was examined after single i.v. bolus and s.c. injections.

2.2 Experimental Method and Materials

The Ang. Conj. was synthesized through a standard method of Fmoc-mediated solid-phase peptide synthesis as explained in previously published works (69). The compound was successfully characterized using an HPLC-DAD instrument as explained below.

The HPLC method was validated for specificity, linearity, accuracy, and intra-day, and inter-day variations. The working calibration curves were prepared in three different

¹ This work has been previously published in Amino Acids journal. Aghazadeh-Habashi A, Khajehpour S. Improved pharmacokinetics and bone tissue accumulation of Angiotensin-(1-7) peptide through bisphosphonate conjugation. Amino Acids. 2021 May;53(5):653-64. DOI: <https://doi.org/10.1007/s00726-021-02972-2>.

media by serial dilution of Ang. Conj. in double-distilled (DD) water, acetate buffer (pH 5.5), and PBS (pH 7.4). Stock solution was (500 µg/mL) used to achieve standard samples concentrations of 0, 50, 75, and 100 µg/mL. The standard curves were constructed by plotting the analyte/internal standard peak area ratio against each compound's given concentration. Three calibration curves were constructed on the same day or three different days to determine intra- and inter-day variabilities. The accuracy percentage was determined from observed concentration \times 100/added concentration. The coefficient of variation (CV%) was used to estimate the assay precision.

2.2.1 HPLC-Photodiode Array Detector (DAD) Analysis of Ang. Conj.

An Agilent 1220 Infinity II HPLC system (Santa Clara, CA, USA), configured to include a degasser, a dual pump, an autosampler, a column oven, and a photodiode array detector, was used in this assay. Chromatographic separation was carried out using a Security Guard Cartridge Polar RP (KJ0-4282, 4.0 mm \times 3.0 mm i.d.) and an Eclipse XRD-C18 analytical column (4.6 \times 150 mm i.d. 5 µm) (Agilent Technologies, Santa Carla, CA, USA). The signal detection was monitored and integrated by the OpenLab CDS software version 2.2.0 (Agilent Technologies, Santa Carla, CA, USA). The mobile phases were composed of two solvents, A: 0.1% trifluoroacetic acid (TFA) in water and B: 0.1% TFA in acetonitrile. The mobile phases were delivered using a gradient elution program. The initial composition of the mobile phases ($t = 0$) was set at 10% B, which was increased linearly to 60% B over 5 min and then maintained at 60% for an additional 5 min. The gradient was then returned to 10% B over 3 min for column recalibration before the next sample injection. The sample run time was 13 min, and the

column oven was set at 30 °C. The analytes were detectable at different wavelengths; however, 220 nm was chosen as the optimal wavelength for detection due to better sensitivity.

2.2.2 Stability of Ang. Conj.

Three different concentrations of 50, 75, and 100 µg/mL of Ang. Conj. were prepared in DD water, acetate buffer (pH 5.5), and PBS buffer (pH 7.4) and stored at room temperature (25 °C), refrigerator (2-8 °C) and freezer (-20 °C). After 1, 3, 7, 10, 15, and 30 days, 100 µL of the solutions was sampled and analyzed by HPLC-DAD to monitor the stability of Ang. Conj. over time under different storage conditions.

2.2.3 HA Binding

The affinity of the Ang. Conj. to the bone mineral, HA, was evaluated using a HA binding assay according to a published protocol with some modifications (114). 20 µg of Ang-(1-7) or an equivalent amount of Ang. Conj. was mixed with 5 mg of HA powder in 750 µL of the binding buffer. The buffers that were used in this study were double-distilled water, 10 mM PBS buffer; pH 7.4, 50 mM PBS buffer; pH 7.4, and acetate buffer; pH 5.5. Negative controls were prepared by mixing an equal amount of Ang-(1-7) or Ang. Conj. in corresponding buffers without HA, and the mixtures were shaken at room temperature for one hour. Then, tubes were centrifuged at 10,000 revolutions per minute for five minutes. The supernatant was separated and assayed for unbound drug, using a fluorescent spectrometer (λ_{Ex} 215 nm, λ_{Em} 305 nm). The percentage of HA binding was calculated as $(\text{Intensity of control} - \text{the intensity of supernatants}) / \text{Intensity of control} \times 100\%$. Each experiment was measured in triplicate.

2.2.4 Statistical Analysis

The results are shown as mean \pm SD unless stated otherwise. All statistical analysis were done using GraphPad Prism[®] 9.3.0 statistics software 2021 (GraphPad Software, Inc. La Jolla, CA 92037 USA). The significance level was set at $p < 0.05$.

The mean values of HA binding study for Ang-(1-7) was compared with mean of Ang. Conj. using two-tailed Students t-test.

2.3 Results

2.3.1 Characterization of Ang. Conj.

Ang. Conj. was successfully synthesized using solid-phase peptide synthesis (Fig. 4), HPLC isolation (Fig. 4a), and MALDI-TOF confirmed the (Fig. 4b). A single conjugate with a molecular weight of 2650.1 Da was produced. The representative HPLC–UV chromatographic representation of Ang. Conj. has a single peak with more than 90% purity (Fig. 4a). Mass spectrum determined by MALDI-TOF shows negative ion: $m/z = 1324.24$ (M_2H^-), validating the mass predicted for Ang. Conj (Fig. 4b).

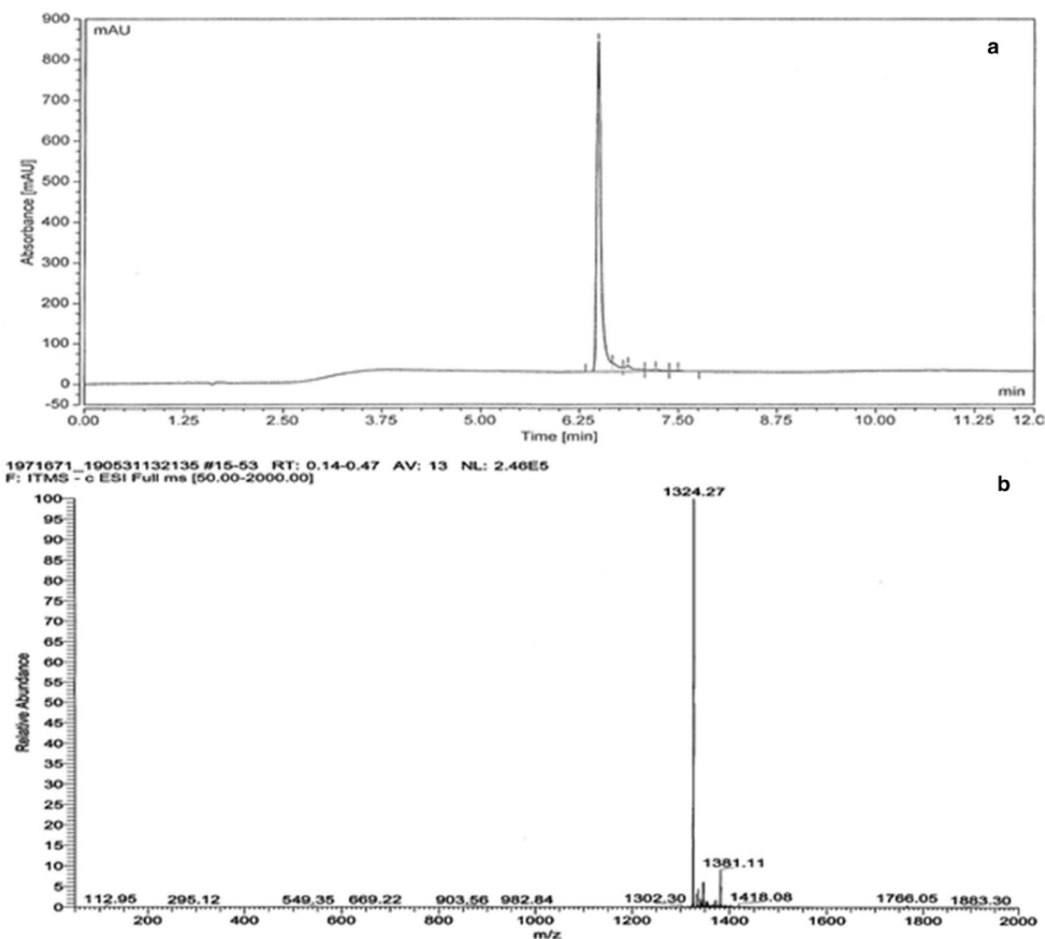


Figure 4. Semi-Prep HPLC chromatogram (a) and MALDI-TOF mass spectrum of Ang. Conj. (b). Adapted from reference (69) with permission.

The HPLC-DAD method was validated for its specificity, linearity, precision, intra-day and inter-day variations. The working calibration curves were constructed in three different media: DD water, acetate buffer [pH 5.5], and PBS [pH 7.4] by serial dilution of the Ang-(1-7) and Ang. Conj. stock solutions (500 $\mu\text{g}/\text{mL}$), yielding standard samples containing 0, 50, 75, and 100 $\mu\text{g}/\text{mL}$ of each compound. The standard curves were created by graphing the ratio of analyte peak area to internal standard peak area versus the concentration of each compound. To determine intra- and inter-day variances, three calibration curves were generated on the same day or on three different days. The

accuracy% was determined from observed concentration \times 100/added concentration.

The coefficient of variation (CV%) was used to estimate the assay precision (Table 1).

Table 1. Intra- and inter-day precision (coefficient of variation, CV) and accuracy for HPLC assay of Ang. Conj. in three different media. Adapted from reference (69) with permission.

Medium	Conc. ($\mu\text{g/mL}$)	Intra-day		Inter-day	
		(CV%)	Accuracy%	(CV%)	Accuracy%
DD water	50	≤ 2.44	91.7 ± 6.7	≤ 0.99	99.6 ± 6.9
	75	≤ 1.31	101.1 ± 2.3	≤ 7.25	105.6 ± 12.6
	100	≤ 2.10	97.4 ± 2.7	≤ 6.23	106.8 ± 8.2
PBS buffer	50	≤ 2.81	91.5 ± 8.3	≤ 3.24	104.4 ± 12.6
	75	≤ 0.38	98.8 ± 0.7	≤ 8.37	107.8 ± 10.5
	100	≤ 2.90	100.7 ± 3.9	≤ 7.83	102.5 ± 10.4
Acetate Buffer	50	≤ 1.53	94.3 ± 4.0	≤ 3.86	98.7 ± 11.5
	75	≤ 5.59	88.0 ± 10.2	≤ 10.36	102.7 ± 10.4
	100	≤ 1.05	99.3 ± 1.4	≤ 10.03	106.5 ± 10.1

2.3.2 Stability of Ang. Conj.

The stability of Ang. Conj. was examined in three matrices: DD water, acetate buffer (pH 5.5), and PBS (pH 7.4). This test was conducted at three temperature storage conditions: (i) room temperature (25 °C), (ii) refrigerator (2–8 °C), and (iii) freezer (-20 °C) for four weeks to make sure that the conjugate did not degrade during the duration of the investigation.

Results reveal that Ang. Conj. is more stable in an acidic medium under all three storage conditions for a period of four weeks (Table 2). The representative chromatograms depict the peaks of the internal standard, Ang. Conj. and Ang-(1-7), after 28 days of storage in various matrices and under varied circumstances (Fig. 5).

Table 2. Percentage of Ang. Conj. remaining after four weeks of storage in different media. Adapted from reference (69) with permission.

Temperature	25 °C		4 °C		-20 °C	
	5	28	5	28	5	28
Acetate buffer (pH 5.5)	94.3	93.3	98.4	98.0	99.8	99.5
DD water	90.6	64	95.9	92.4	99.5	99.1
PBS buffer (pH 7.4)	72.8	22.6	91.9	79.2	99.2	98.9

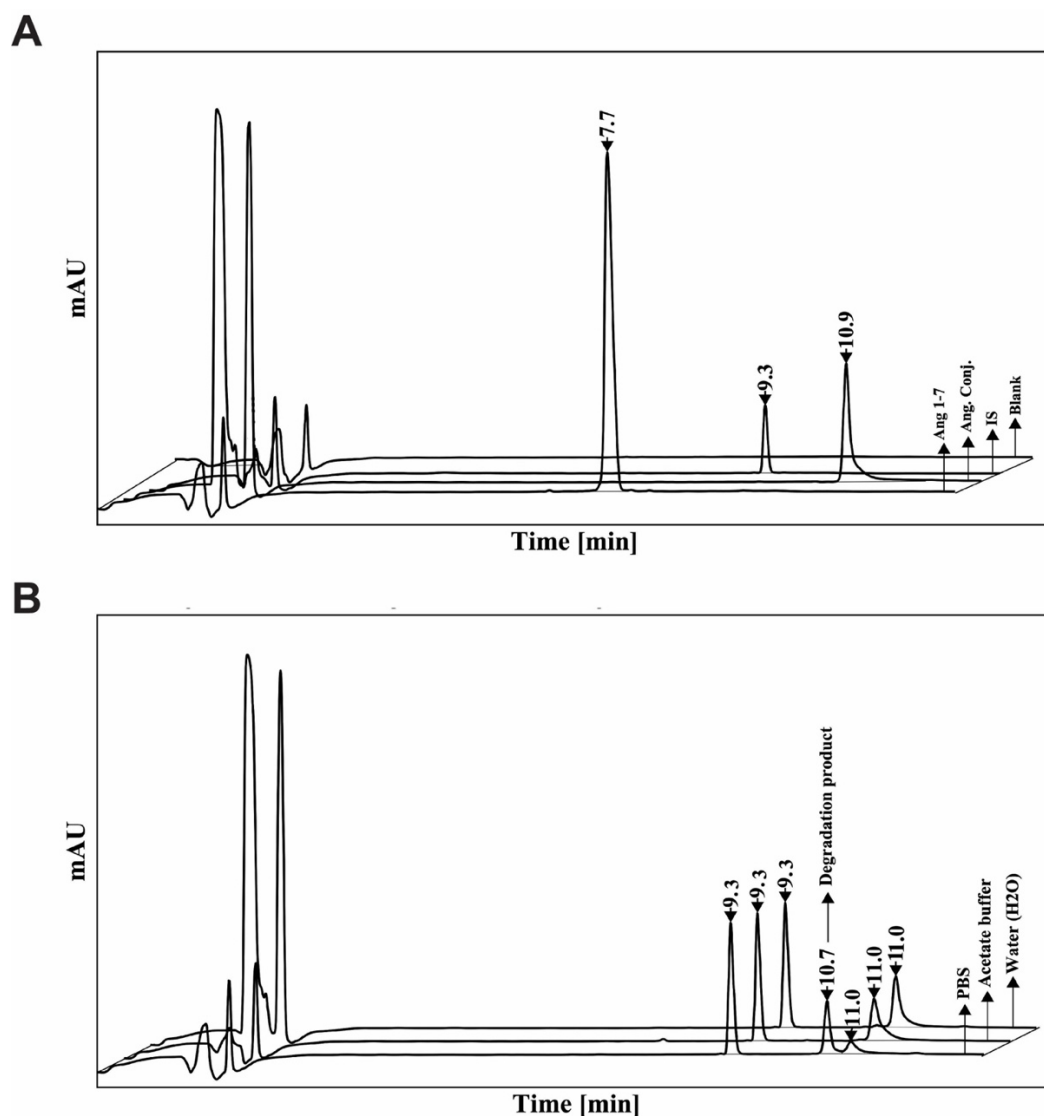


Figure 5. Representative analytical HPLC-DAD individual chromatograms of (A) blank, internal standard (IS), Ang-(1-7), and Ang. Conj. standard solutions and (B) Ang. Conj. solution (plus IS) in the different media after 28 days at room temperature. Adapted from reference (69) with permission.

2.3.3 HA Binding

The bone mineral affinity of the bone-targeting Ang. Conj. is evaluated and compared to the Ang-(1-7) peptide. As it is shown in Fig. 6, Ang-(1-7) exhibited $4.2 \pm 0.1\%$, $3.7 \pm 0.6\%$, $4.4 \pm 0.2\%$, and $2.6 \pm 0.4\%$ binding capacity in DD water, PBS 50 mM, PBS 10 mM, and acetate buffer, respectively. In comparison, the corresponding figures for

Ang. Conj. were $20.4 \pm 0.5\%$, $6.8 \pm 0.6\%$, $8.4 \pm 0.2\%$, and $11.6 \pm 0.5\%$. These results indicate that the binding capacity of Ang. Conj. in each medium was substantially higher than that of Ang-(1-7). In addition to pH and phosphate ion presence and concentration, pH and phosphate ion presence also affected the binding capacity. Higher binding was seen at an acidic pH (pH 5.5 vs. pH 7.4) with a lower concentration of phosphate ion (10 mM vs. 50 mM) (Fig. 6).

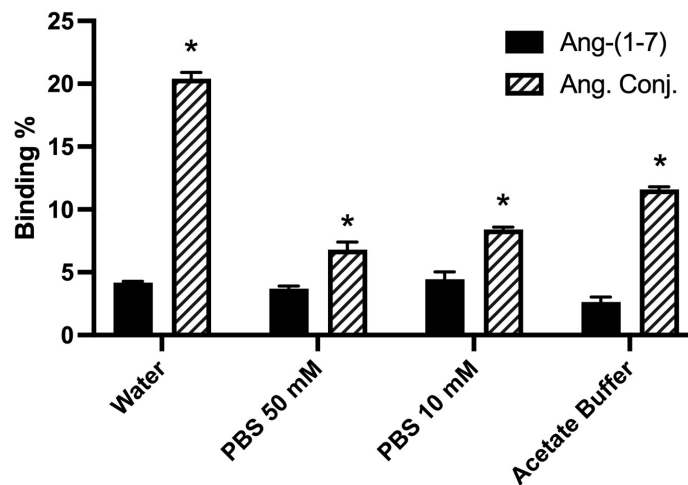


Figure 6. The binding capacity of Ang-(1-7) and Ang. Conj. in the different media. N=3 for each group, *Significantly different from Ang-(1-7), $p < 0.05$. Adapted from reference (69) with permission.

2.4 Discussion

The RAS is a desirable target for therapeutic research due to the roles that its counter-regulating arms play and how they affect different pathological conditions and its protecting arm of ACE2/ Ang-(1-7)/ MasR has attracted a lot of interest. Numerous studies have examined the Ang-(1-7) peptide to show its beneficial effects in counterbalancing the negative effects of Ang II in cardiovascular (47, 115, 116), renal (105, 117), pulmonary (48, 118), arthritis (49), cancer (52-55), diabetes (45, 46, 119), and neurological disorders (50, 51, 120). However, the stability and short biological half-

life is a key challenge for peptides that are biologically active and are considered to be promising therapeutic agents. The active peptide, Ang-(1-7), which has a number of advantageous effects, is not an exception. To avoid such limitations, continuous infusion of Ang-(1-7) is used in some recent clinical trials to treat different pathological conditions (121-123), which is not considered patient compliant. So, numerous attempts have been made to enhance the peptide stability, particularly Ang-(1-7). For example, a lanthionine-stabilized Ang-(1-7) known as cyclized Ang-(1-7) was shown to be fully resistant to ACE1 and other peptidases and was presented with improved stability and half-life and efficacy against type 2 diabetes mellitus (124). In several attempts by researchers, Ang-(1-7) was included in β -cyclodextrin to treat myocardial infarction post-inflammation and prevent hyperglycemia in type 2 diabetes mellitus (56). However, none of these applications addressed the peptide short half-life for oral administration. A simple and effective method of producing an alternative Ang-(1-7) analog was introduced by Ma et al. (60) with N and C termini protected by acetylation and amination (Ang-AA). Ang-AA pharmacokinetics and toxicity results in significantly reduced Ang-(1-7) hydrolysis in mice and longer half-life in rats with preserving the specific binding of Ang-AA to the MasR. Ang-AA had greater inhibitory effects on proliferation, migration, and invasion in the A549 cell line than Ang-(1-7). Using an Ang-(1-7)-bioexpressing bacteria, Carter et al. showed that it can increase the Ang-(1-7) and decrease Ang II levels compared to Ang-(1-7) s.c. administration and can reduce the neuro-inflammation in prefrontal cortex (125). In the current study, we synthesized a stable PEGylated bone-targeting conjugate of Ang-(1-7), called Ang. Conj. while preserving its biological activity (126). When compared with native Ang-(1-7) peptide, Ang. Conj. exhibits greater

stability in various matrices and a longer biological half-life (69). The MALDI-TOF spectrum of the final compound matches the anticipated molecular weight and verifies the successful conjugation of Ang-(1-7) and synthesis of Ang. Conj. (Fig. 4). Higher stability was obtained by using PEG as a spacer in the conjugate structure (Table 4 and Fig. 5). After exposure to HA in solution in different media, the bone-targeting efficacy of Ang. Conj. increased. Ang. Conj. displayed more than fourfold higher bone HA binding capacity when compared with native Ang-(1-7) in DD water [pH 6.0]. By decreasing the pH from 4 to 6, its affinity decreased from 20% to 11.6% (acetate buffer pH 4). However, the binding capacity was still greater in PBS solution pH 7.5 (Fig. 6). The ability of the conjugate to bind to the bone in various media may be explained by the phosphate group's ionization status on the BP moiety and the existence of competing phosphate ions. The effects of competing ions were more noticeable when phosphate buffers with varying molarities were utilized. The HA binding data show that pH and the ionization state of phosphate groups of the BP moiety have less of an effect on the conjugate HA binding than the presence of competing phosphate ions in the matrix.

2.5 Conclusion

In conclusion, characterization and pharmacokinetic studies of Ang. Conj. confirm the idea that it can target the bone and use it as a reservoir for maintaining a therapeutic plasma level of active peptide by conjugating Ang-(1-7) with bone-seeking BP. High solution stability and significant prolongation of the Ang. Conj. plasma half-life following i.v. and s.c. administrations demonstrate the efficacy of our strategy in enhancing peptide chemical and biological stability. The capacity of Ang. Conj. to target bone led to a longer circulatory half-life and greater potency of Ang-(1-7) compared to the original

peptide. The findings of this study point to Ang. Conj. as a potentially effective therapeutic alternative for the treatment of inflammatory bone disease associated with activated RAS, including osteoporosis, osteoarthritis, RA, Paget's disease, and malignancies with bone metastases.

3 Chapter III: Plasma Angiotensin Peptides as Biomarkers of Rheumatoid Arthritis are Correlated with Anti-ACE2 Auto-Antibodies Level and Disease Intensity²

3.1 Background

3.1.1 RAS and Inflammation

See section 1.5. (Chapter 1).

3.1.2 Anti-ACE2 Autoantibodies

ACE2 is one of the main components of the RAS, which converts pro-inflammatory Ang II to tissue-protective Ang-(1-7). The urinary or plasma-circulating ACE2 was shown to be associated with different disease conditions such as renal (127), cardiovascular (128), and metabolic disorders (129). Many studies correlate plasma ACE2 levels with hypertension (128), heart failure, microalbuminuria, and nephropathy in diabetic patients (129). Although those patients had a higher plasma level of ACE2, they presented with reduced ACE2 activity and had considerable level of circulating anti-ACE2 autoantibodies (130) (Fig. 7). Herein, we investigated the production of anti-ACE2

² This work has been previously published in *Inflammopharmacology* journal. Khajeh Pour S, Scoville C, Tavernier SS, Aghazadeh-Habashi A. Plasma angiotensin peptides as biomarkers of rheumatoid arthritis are correlated with anti-ACE2 auto-antibodies level and disease intensity. *Inflammopharmacology*. 2022 May 26:1-8. DOI: <https://doi.org/10.1007/s10787-022-01008-9>.

autoantibodies in inflammatory conditions, impacting Ang peptides levels. All in all, the classical RAS has an important contribution to the pathology of RA and its inhibition improves the sign and the most specific hallmarks of disease in animal models of RA.

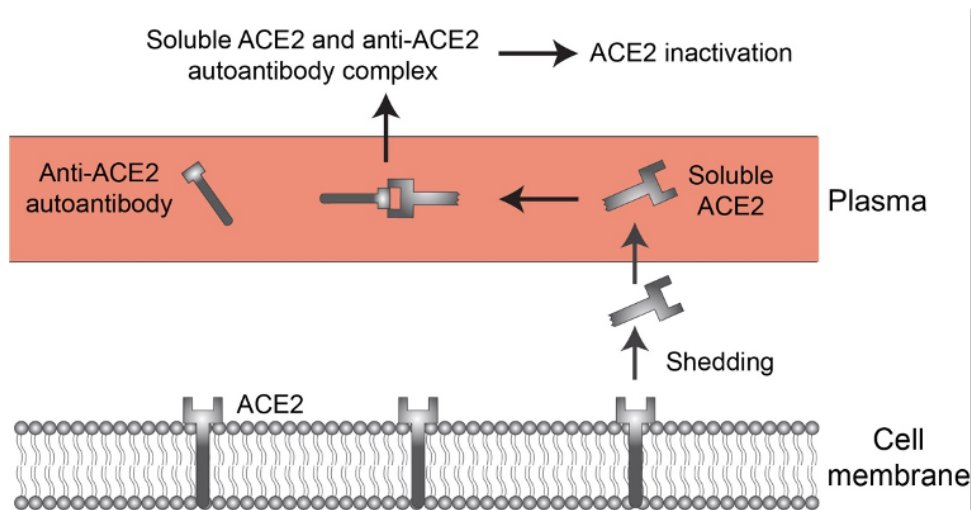


Figure 7. An illustration of ACE2 inactivation by its specific autoantibodies. Adapted from reference (44) with permission.

3.2 Rationale

Activation of the RAS due to different etiologies results in chronic imbalances can be seen in different pathological conditions such as RA.

The urine or plasma circulating ACE2 has been linked to a variety of diseases, including renal (127), cardiovascular (128), and metabolic problems (129). Numerous studies connect plasma ACE2 levels with hypertension, heart failure, microalbuminuria, and nephropathy in diabetic patients (128, 129). Despite having a greater plasma level of ACE2, these individuals exhibited a decreased ACE2 enzyme activity and a high level of anti-ACE2 autoantibodies (130). In this study, we evaluated the impact of anti-ACE2 autoantibodies on Ang peptide levels in inflammatory conditions. Therefore, Ang-(1-7) level as a product of ACE2 activity and assessment of the Ang II/Ang-(1-7) ratio coupled

with anti-ACE2 autoantibodies could provide accurate diagnostic and prognostic biomarkers for individuals with various inflammatory disorders such as RA.

This investigation was an exploratory pilot study in which 12 patients with RA were enrolled using a convenience sampling approach at the time of the study. Patients were categorized into the “active” and “remission” groups based on the disease diagnosis criteria explained below. The Institutional Review Board approved this study through the IRB-FY2020-273 protocol. Written informed consent was obtained from all patients before admission to the study.

3.3 Hypothesis and Objectives

We hypothesized that the RAS classical arm is augmented and the protective arm is suppressed in RA. As a result, the stage of the diseases is inversely related to the Ang-(1-7) level and directly related to the Ang II levels and the presence of anti-ACE2 autoantibodies. Moreover, we hypothesized that higher systemic levels of Ang-(1-7) could modulate and put the disease into remission and protect the patient from long-term consequences of RA.

This study aimed to explore a correlation between plasma Ang II/ (1-7) ratio, anti-ACE2 autoantibodies level and disease activity in RA patients.

3.4 Experimental Methods and Materials

3.4.1 Defining the RA stage

The RA activity staging was made using a Routine Assessment of Patient Index Data

3 (RAPID3) questionnaire (131) and measurement of CRP. RAPID3 questionnaire includes the three patient-reported American College of Rheumatology (ACR) Core Data Set and is a self-reporting index. RAPID3 measures RA based on physical function, pain, and the global patient status estimate (131). Each of these criteria is scored 0 to 10, for a total of 0 to 30 scores. On the other hand, CRP is an RA acute phase protein and it is commonly measured in clinical practice. Its elevation happens at a very early stage of inflammation and can be a valid marker for inflammation and infection. Furthermore, CRP is widely used as an index of disease activity in rheumatological and other connective tissue diseases, except for systemic Lupus Erythematosus (132).

In this study, CRP level above 10 mg/L correlated with elevated RAPID3 measurements. Thereby confirming active RA disease in certain patients. Those patients with less disease activity or disease remission had CRP levels below 10 mg/L.

3.4.2 Plasma Sample Collection, Solid-phase Extraction, and LC-MS/MS analysis of the Ang Peptides

Two mL of blood was obtained from each patient and transferred to test tubes containing 100 μ L iced-cold protease inhibitor cocktail solution for inactivation of the peptidases based on the manufacturer's protocol. No heparin was added to the samples, and EDTA was used as an anticoagulant. Samples were then centrifuged for 10 min at 2500 \times g at 4 $^{\circ}$ C and plasma samples were collected into several tubes to avoid repeated freeze and thaw cycles and were stores at -80 $^{\circ}$ C until analysis.

The extraction of the Ang II and Ang-(1-7) was done using a previously established method (133) with minor changes. Briefly, 200 μ L of plasma samples were treated with

50 μ L of the 20 ng/mL IS ([Asn¹, Val⁵] Ang II), and formic acid to the final concentration of 0.5%. Extraction was done using Waters C18 SPE column. They were preconditioned with 2 mL ethanol and 4 mL DI water. Samples were then loaded onto the cartridge, followed by 3 mL of DL water for washing. The vacuum was applied to further dry the cartridges and Ang peptides were eluted with 2.5 mL of methanol containing 5% formic acid. The samples were dried using a Savant 200 SpeedVac system (Thermo Fisher Scientific, Waltham, MA, USA). The dried samples were reconstituted in 50 μ L 16% acetonitrile in water containing 0.1% formic acid, and 10 μ L of samples were injected into the LC-MS/MS to measure the Ang peptides concentrations, using a standard curve for Ang peptides. The LC-MS/MS analysis of the Ang peptides are explained in previous sections.

3.4.3 Enzyme-linked Immunoassay (ELISA) for the Detection of Anti-ACE2

Autoantibodies in Plasma

The presence of anti-ACE2 autoantibodies in the sera of patients suffering from RA was measured using an ELISA method described by Takahashi et al. with some modifications (130). The recombinant human ACE2 was purchased from Abcam (ab151852, Cambridge, United Kingdom). About 10 μ g/mL of recombinant ACE2 was made in carbonate-bicarbonate buffer pH 9.6 and 200 μ L of that was added to each well in a 96-well ELISA plate. The plate was covered with an adhesive plastic and kept at 4 °C overnight. The next day, it was blocked with a blocking buffer (5% skim milk in PBS) for 2 hours at room temperature. Then, it was washed 3 times with the washing buffer containing 0.1% Tween-20. Two-hundred μ L of the sera of the patients were added to each well in triplicates and incubated for one hour at room temperature on a horizontal

shaker. Bound anti-ACE2 autoantibody was detected using 200 μ L of horseradish peroxidase-conjugated anti-human IgG (secondary antibody) (Novus Biologicals, Littleton, CO, USA) diluted in the wash buffer (1:1000). The plate was incubated at room temperature for 2 hours and then washed 3 times with the wash buffer. Two-hundred μ L ready-to-use of SureBlue™ TMB peroxidase substrate (Kirkegaard & Perry Laboratories Inc., Gaithersburg, MD, USA) was added to each well and kept at room temperature for 30 minutes to develop the yellow color and the reaction was stopped with 50 μ L of stopping solution (3 M hydrochloric acid). Addition of the stop solution increases absorbance values 2-3-fold. The optical density (OD) values were read on a VarioscanLux™ microplate reader (Thermofisher Scientific, Waltham, MA, USA) at 450 nm (134). All samples were tested in triplicates.

3.4.4 Statistical Analysis

Data distribution for the human study was tested for their normality. The one-tailed Student's t-test was used to analyze the demographics. The Mann-Whitney U and two-tailed Student's t-test was used for anti-ACE2 ELISA scores, and correlations. to determine significant differences at $p < 0.05$ using GraphPad Prism 8.0 software (San Diego, CA, USA). The Pearson correlation coefficient between variables was calculated using SAS Studio online version.

The results of ELISA analyses are presented as mean \pm SD of OD450 nm of anti-ACE2 autoantibody in the human plasma. The mean values obtained for the remission RA group are compared with mean of active RA group using two-tailed Students t-test.

3.5 Results

3.5.1 Patients' Demographics and RA Staging

Table 3 presents the demographics of patients with RA in remission (n=7) and active (n=5) groups. Each group contained an equal number of males and females. Age, body mass index (BMI), medication use, and comorbidities exhibited no statistically significant differences. However, the score values for CRP and RAPID3 between the two groups were significantly different (Table 3).

The American College of Rheumatology (ACR) includes RAPID3 among the indices used to quantify RA disease activity (135). Based on the CRP levels and RAPID3 scores, five patients have active RA and seven patients are in remission.

Table 3. Baseline demographic and clinical characteristics of RA patients. Adapted from reference (44) with permission.

Variable	Remission group (Mean ± SD)	Active group (Mean ± SD)	p-value
Age	68.29 ± 12.05	68.80 ± 15.22	ns ^a
BMI	28.57 ± 5.71	27.60 ± 5.46	ns ^a
Medication use	7.43 ± 3.78	7.40 ± 2.07	ns ^a
Comorbidities	1.71 ± 1.25	1.80 ± 0.84	ns ^a
CRP (mg/L)	1.59 ± 1.27	16.10 ± 10.97	0.0054*
RAPID3 score	8.29 ± 6.38	19.85 ± 7.64	0.0085*

*One-tailed t-test was performed, $p < 0.05$. ^ans; not significant.

3.5.2 Plasma Levels of Ang Peptides

The mean \pm SEM results of the levels of Ang-(1-7) and Ang II peptides are shown in Fig. 8A. The data indicate that Ang-(1-7) level in active RA (1.29 ± 0.81 ng/mL) is significantly lower than in remission RA (7.63 ± 2.61 ng/mL). In contrast to Ang-(1-7) levels, Ang II levels are significantly higher in active RA patients (5.43 ± 1.82 ng/mL) as in comparison to the remission group (0.87 ± 0.16 ng/mL).

The ratio of Ang-(1-7)/Ang II in remission and active group is shown in Fig. 8B. This ratio was significantly lower in the active (0.25 ± 0.12) than in the remission group (5.61 ± 0.67).

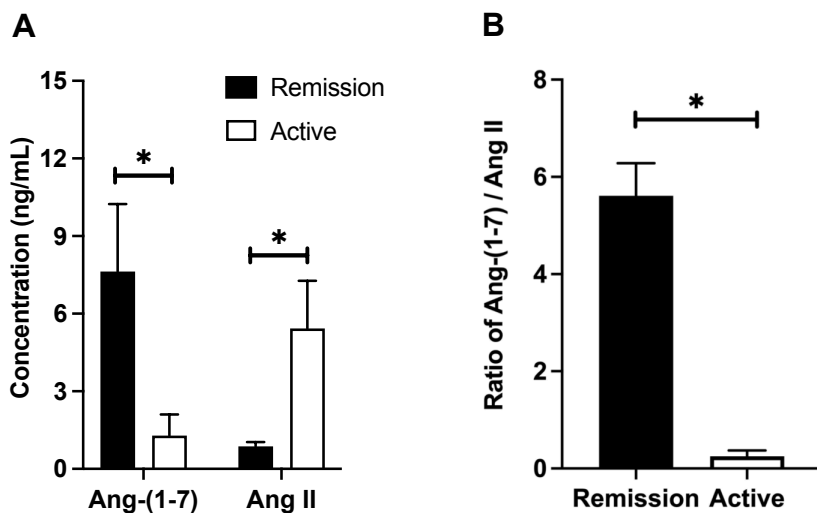


Figure 8. Ang-(1-7) and Ang II plasma concentration (ng/mL) in the active (n=5) and remission (n=7) groups (A), and the ratio of Ang-(1-7)/Ang II (B). Data are presented in mean \pm SEM, *significantly different from the remission group, $p < 0.05$. Adapted from reference (44) with permission.

3.5.3 ELISA Scores for Plasma Anti-ACE2 Autoantibodies

Samples from active and remission patients showed an ELISA reactivity to ACE2. The OD values were above the baseline level, and it was determined as the mean ELISA

score in those samples. The mean ELISA score was significantly higher in the active (1.81 ± 0.11) RA patients than in the remission (1.41 ± 0.11) RA patients (Fig. 9).

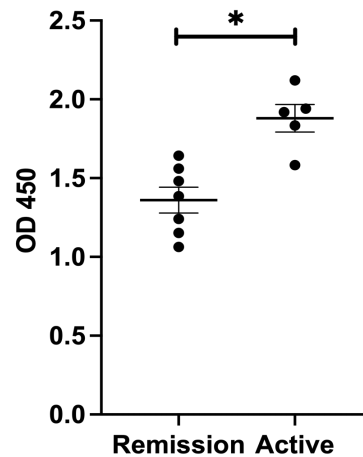


Figure 9. The plasma anti-ACE2 autoantibodies ELISA scores of RA patients in the active and remission stages. Data are presented as mean \pm SD, *significantly different from the remission group, $p < 0.05$. Adapted from reference (44) with permission.

3.5.4 Ang Peptides, Anti-ACE2 Autoantibodies, and RA Biomarkers Correlations

Fig. 10 illustrates the correlations between anti-ACE2 autoantibodies ELISA score, Ang II peptide level, Ang-(1-7)/Ang II ratio and RAPID3 score and CRP level. Anti-ACE2 autoantibodies ELISA score correlated positively with CRP level ($r = 0.7251$) and RAPID3 score ($r = 0.6132$). (Fig. 10A). In a similar fashion, Ang II level was positively correlated with anti-ACE2 autoantibodies ($r = 0.6796$), CRP levels ($r = 0.7820$), and Rapid 3 score ($r = 0.2555$), but only in the latter instance was this correlation significant. As shown in Fig. 10C, the sign of these relationships was negative for the Ang-(1-7)/Ang II ratio.

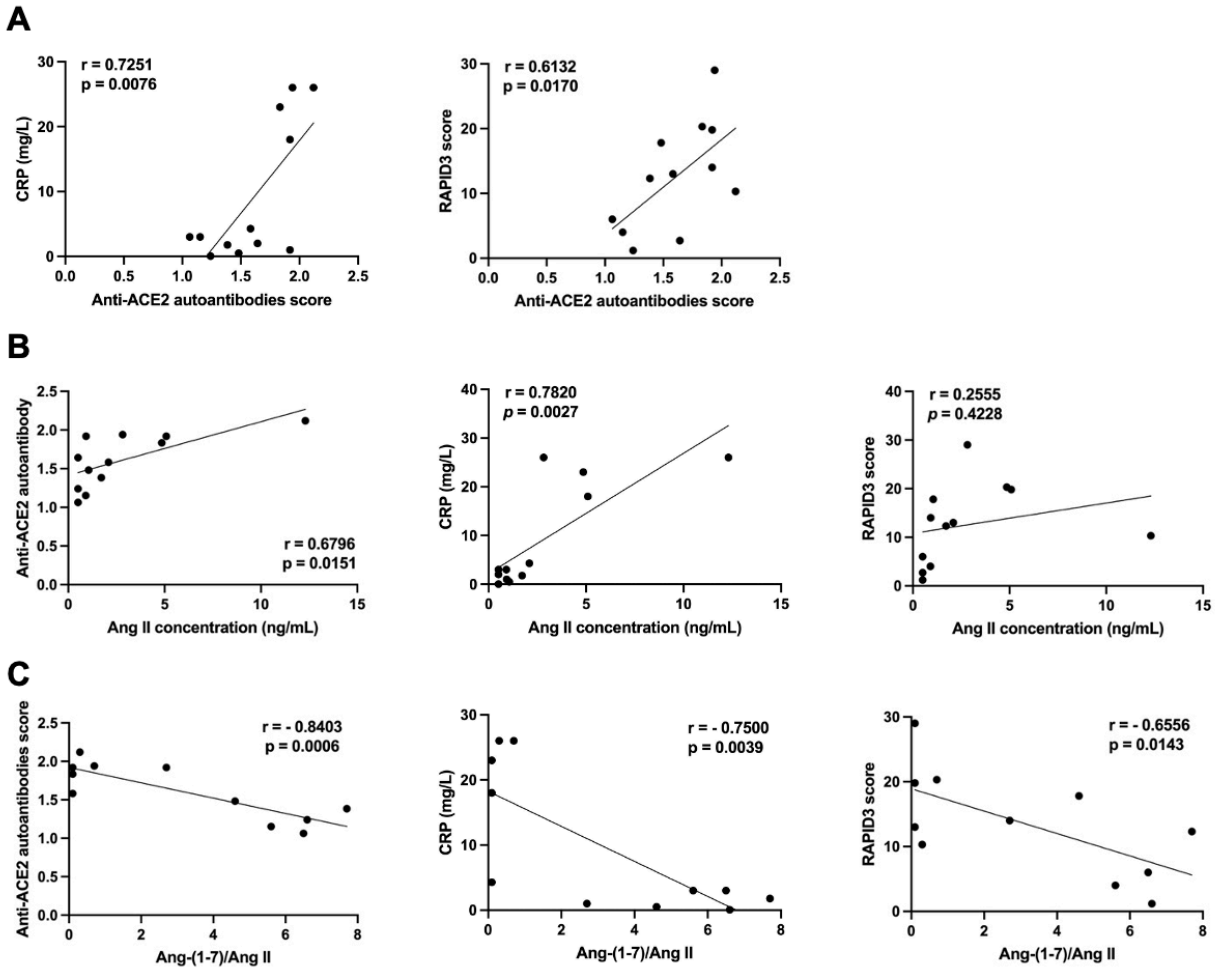


Figure 10. Correlation between the (A) Ang II concentration, anti-ACE2 autoantibodies ELISA, and RAPID3 scores, (B) Ang II plasma concentration, CRP levels, and anti-ACE2 autoantibodies ELISA score, (C) Ang-(1-7)/Ang II ratio, anti-ACE2 autoantibodies ELISA score, CRP levels, and RAPID3 scores. Adapted from reference (44) with permission.

3.6 Discussion

In patients with RA in active or remission groups, the Ang-(1-7), Ang II plasma levels, Ang-(1-7)/Ang II ratio, and anti-ACE2 autoantibodies ELISA scores were assessed and compared. The aim of human study was to establish whether the RAS systemic axes were unbalanced in RA. Ang-(1-7) levels were considerably lower in patients with active RA, whereas Ang II levels were significantly lower in patients in remission (Fig. 8).

Similarly, the mean ELISA score of anti-ACE2 autoantibodies in active RA patients was significantly greater (Fig. 8). As circulating soluble ACE2 is primarily responsible for the conversion of Ang II to Ang-(1-7), the lower Ang-(1-7)/Ang II ratio in active RA patients was attributed to the deactivation of ACE2 enzyme by greater levels of anti-ACE2 autoantibodies. This is consistent with the increased Ang II plasma levels observed in patients with active RA, and is positively linked with CRP levels and RAPID3 scores. It is worth mentioning the observed results indicate that both arms of the RAS are affected by RA. Accordingly, the higher score of anti-ACE2 autoantibodies in the active RA than in remission patients emphasizes the contribution of the classical and protective arm to the disease's status and intensity (Fig. 10). It was previously reported that the plasma anti-ACE2 autoantibodies in patients with inflammatory conditions such as pulmonary arterial hypertension (130) and COVID-19 (136) were associated with the intensity of the disease and poor prognostic outcome. The reported evidence aligns with the theory that anti-ACE2 antibodies can decrease soluble ACE2 activity and lower the Ang-(1-7)/Ang II ratio in inflammatory diseases. This phenomenon shifts the balance between the RAS arms toward the pro-inflammatory state and triggers observed arthritis symptoms in RA and cytokine syndrome in COVID-19 patients. This study is the first to report the RAS peptides and anti-ACE2 autoantibodies ELISA analysis associated with RA disease activity.

Braz et al. (137) measured and compared the RAS components plasma level in healthy and RA patients and correlated them with CV risk. The study failed to categorize the patients based on their RA state of being in the active or in remission stage and did not look at the plasma anti-ACE2 antibodies. In line with our study, Braz et al. reported an

association between CV risks of RA with the imbalance of the RAS arms. They also noticed an early, subclinical atherosclerotic disease in the cohort of female patients suffering from RA for at least 6 months. This group reported higher ACE1, Ang II, and Ang-(1-7) peptides in RA patients and observed positive control between Ang II levels and disease activity indices, such as Disease Activity Score in 28 joints (DAS28) and Clinical Disease Activity Index (CDAI). Similar to previously reported studies (128, 129, 138), the authors observed a higher level of ACE2 in RA patients. They also noted that Ang-(1-7) level was higher and Ang II/Ang-(1-7) ratio was lower in RA patients, which was interpreted as a compensatory mechanism of the protective arm of the RAS. The observed higher ACE1/ACE2 ratio has been reported in animal models of arthritis. In contrast to Braz et al.'s findings, such imbalance resulted in an expected higher Ang II/Ang-(1-7) ratio in plasma and heart tissues (139). The disparity in Braz et al study (a lower ratio of Ang II/ Ang-(1-7) in RA patients despite a larger ACE1/ACE2 ratio) may result from a number of study design-related factors. First, the disease state of the patient group (active vs. remission) is unclear. Our data indicate that the levels of RAS components and the ratio of Ang-(1-7)/Ang II are substantially linked with the severity of RA. Therefore, analysis of data without considering the disease stage could be misleading. In many inflammatory circumstances, it is known that inflammation activates the RAS and influences its enzyme, peptide, and receptor levels in favor of the classical arm (such as RA, diabetes, cancer, etc.) (140-142). This activation promotes disease progression by producing pro-inflammatory mediators through Ang II interaction with AT1R. Secondly, using ACEIs, ARBs, nonsteroidal anti-inflammatory drugs (NSAIDs), and other anti-inflammatory medications increases ACE2 expression and Ang-(1-7)

levels (139, 143). Therefore, such medications modulate the inflammation by restoring the imbalance of the RAS components, which could explain the Braz et al. reported-higher level of Ang-(1-7) beyond the componentry mechanisms. Third, despite the higher trend of ACE2 in RA patients, its activity could be compromised by developing anti-ACE2 autoantibodies, which have been observed in inflammatory diseases (130). Thus, if the patients in Braz et al study were classified based on their disease condition and their Ang II and Ang-(1-7) plasma levels were compared to their disease state, a comparable outcome to the present study could have been observed.

3.7 Conclusions

All in all, the results of the human study are consistent with the theory that in RA, the classical arm of the RAS is activated while the protective arm is inhibited. According to this study, larger systemic and maybe local Ang-(1-7) levels may be able to control the disease, induce remission, and protect the patient from RA's long-term effects. Future research should evaluate these predictions using longer-term, more in-depth follow-up studies and a more thorough analysis of the RAS components. Since the pathophysiology of RA is still largely unknown, it is crucial to pursue any leads that could shed light on this condition.

Overall, these findings confirm that the RAS is one of the major players in different inflammatory disease pathophysiology, including RA, and cancer. Therefore, utilizing the RAS components as the biomarkers of RA can serve as a reliable tool for early detection. This could also help clinicians evaluate the treatment success rate and determine disease prognosis to prevent long-term complications of RA.

4 Chapter IV: Improved Pharmacokinetics of Angiotensin-(1-7) peptide through Bisphosphonate Conjugation³

4.1 Background

4.1.1 The RAS Components

See section 1.1 (Chapter 1)

4.1.2 Ang-(1-7) Peptide Actions in the Body

As one of the RAS active peptides, Ang-(1-7) exerts its beneficial and protective effects via various pathways. Possessing such biological actions suggests the Ang-(1-7) peptide is an effective therapeutic agent for the treatment of a variety of diseases including: renal (105, 117) and cardiovascular diseases (47, 115, 116), diabetes (45, 52-54) (section 1.2, Chapter 1).

The short half-life of Ang-(1-7) due to rapid systemic clearance and enzymatic breakdown through proteolysis in the kidneys, liver, and blood circulation diminishes its therapeutic efficacy. These weaknesses collectively lead to the peptide's poor pharmacokinetics and low bioavailability. Various strategies, including cyclization (124) substitution with non-natural amino acid (144), and complexation with β -cyclodextrin

³ The pharmacokinetic study has been previously published in *Amino Acids* journal using a radiolabeled method. Here, we investigated the pharmacokinetic parameters using a different approach. Aghazadeh-Habashi A, Khajehpour S. Improved pharmacokinetics and bone tissue accumulation of Angiotensin-(1-7) peptide through bisphosphonate conjugation. *Amino Acids*. 2021 May;53(5):653-64. DOI: <https://doi.org/10.1007/s00726-021-02972-2>.

(56), have been employed to address this problem. By attaching a bone-targeting moiety to Ang-(1-7) peptide via a spacer, we enhanced its biological half-life. This innovative strategy was designed to analyze the preclinical pharmacokinetics of Ang-(1-7) PEGylated bisphosphonate conjugate in healthy rats. After single i.v. bolus and s.c. injections, the pharmacokinetic characteristics were evaluated.

4.2 Experimental Methods and Materials

4.2.1 Dose Calculation

The dose for the pharmacokinetic study was 1 mg/kg of the Ang-(1-7) or equivalent dose for Ang. Conj.

4.2.2 Animal Handling, Cannulation, and Sample Collection

Healthy Sprague-Dawley rats (male) weighing 250-300 g were purchased from Charles River (Wilmington, MA). Based on approved animal protocol #792, prior to any experimental procedure, the animals were acclimated for four days in the standard cages with two rats in each cage in a room with controlled temperature (25 ± 1 °C), humidity ($55 \pm 5\%$), and a 12-h light/dark cycle. Animals had access to a standard laboratory diet and water, ad libitum. After acclimatization, rats were randomly assigned to i.v., and s.c. groups (n = 4/group). They were anesthetized with oxygen/isoflurane (075/2%) and cannulated in the right jugular vein. After a 24-hr recovery, groups of animals were dosed with Ang-(1-7) (i.v.) or Ang. Conj. (i.v. or s.c.) with a dose of 1 mg/kg peptide and peptide conjugate equivalent through a i.v., or s.c. injections. The cannula was flushed with 200 μ L normal saline after i.v. dose administration.

Serial blood samples were collected at given time points. Sample collection for the rats in the Ang-(1-7) i.v. group was done at 0, 3, 5, 10, 20, 30, 60, 90, and 120 min and for the rats in the Ang. Conj. i.v. group was done at 0, 3, 5, 10, 20, 30, 60, 90, 120, 240, 360, 480, and 720 min, for the rats in the Ang. Conj. s.c. group was done at 0, 5, 10, 20, 30, 60, 90, 120, 240, 360, 480, 720, and 1440 min post-dose.

At each time point, 250 μ L of blood was collected and replaced with same volume of saline. Blood sample were added to a tube containing iced-cold protease inhibitor cocktail. Tubes were kept on ice for 10 minutes and centrifuged at 13,000 RPM for 10 minutes. Plasma was then harvested and transferred to a new tube, snap-frozen in liquid nitrogen, and kept at -80 $^{\circ}$ C until analysis. At 8 hr (for Ang-(1-7)) or 24 hr (for Ang. Conj.) post-dose, rats were euthanized by CO₂.

4.2.3 Sample Preparation, Extraction, and LC-MS/MS Analysis for Ang-(1-7)

Peptide Measurement

Ang-(1-7) peptide was extracted from plasma using a solid-phase extraction (SPE) method by Cui et al. with minor changes in the process (133). Briefly, to 100 μ L of plasma samples, 100 μ L of the [Asn¹, Val⁶] Ang II (IS) (250 ng/mL) was added and mixed. Final concentration of 0.5% formic acid was added and after vortex mixing, samples were loaded onto the 2-mL-ethanol and 2-mL-water preconditioned Waters C18 SPE cartridges (#WAT020805, Milford, MA), followed by 2 mL of deionized water for washing. A positive nitrogen flow was applied to dry the cartridges further. Then 2.5 mL of 5% formic acid in methanol was used to elute the Ang-(1-7). The eluted solutions were collected and dried under the stream of nitrogen. The dried samples were

reconstituted in 100 μ L of 16% acetonitrile in water containing 0.1% formic acid, and 30 μ L of samples were injected into the LC-MS/MS.

The level of Ang-(1-7) peptide, was measured using a validated LC-MS/MS method (133) in multiple reaction mode (MRM). The system was composed of liquid chromatography in tandem with mass spectrometry (Shimadzu, Columbia, MD, USA) with a controller (CBM-20A), two binary pumps (LC-30AD), an autosampler (SIL-30AC), and an AB Sciex (Foster City, CA, USA) QTRAP 5500 quadrupole mass spectrometer in positive electrospray ionization mode (ESI). The chromatograms were monitored and integrated by the Analyst 1.7 software (AB Sciex, Foster City, CA, USA).

LC separation was performed on an analytical reversed-phase column Kinetex[®] C18 100 \times 2.1 mm (1.7 μ m) (Phenomenex, Torrance, CA, USA) by a combination of A: 0.1% formic acid in water and B: 0.1% formic acid in acetonitrile as mobile phases at a flow rate of 0.2 mL/min. The mobile phase gradient started at 5% B and increased to 30% B in 5 minutes, kept at 30% B for 5 minutes., returned to 5% B in 3 minutes and held at 5% B for 2 minutes before the next injection for column re-equilibrium.

The positive ion ESI mass spectrometric parameters were as follow: capillary voltage; 5.5 kV, temperature; 300 $^{\circ}$ C, declustering potential (DP); 100 V, and collision cell exit potential (CXP); 15 V. LC-MS/MS was performed with MRM transitions of m/z 300.6 \rightarrow 371.2 (Ang-(1-7)) and m/z 516.5 \rightarrow 769.4 (IS). Nitrogen was used as collision gas, and the collision energies were set at 20-30 eV. A calibration curves using peak height ratio (analyte over IS) were constructed over the range of 0.5-40 ng/mL in plasma was used to measure the Ang-(1-7) levels in plasma samples.

4.2.4 Pharmacokinetic Modeling and Analysis

Pharmacokinetic indices of Ang-(1-7) was determined using non-compartmental analysis (NCA) (WinNonlin version 4.0, Pharsight, A Certara Company, CA, USA). Due to lack of validated LC-MS/MS method for quantification of the Ang. Conj. we used Ang-(1-7) levels as a surrogate to estimate the pharmacokinetic parameters of Ang. Conj. Drug doses were normalized based on animal body weight. The terminal elimination rate constant, K_e , for the native peptide concentration-time curve after i.v. administration was determined by the linear regression of at least three data points from the terminal portion of the plasma concentration-time plots. The terminal half-life calculated based on $t_{1/2} = 0.693/K_e$. The area under the plasma concentration-time curve (AUC_t) was calculated using the trapezoidal rule until the last measured plasma concentration, C_{last} . The $AUC_{0-\infty}$ was calculated by adding up the AUC_t and C_{last}/K_e . The total body clearance, CL, was determined by i.v. dose divided by $AUC_{i.v.}$. The terminal phase volume of distribution of the compounds was calculated from $V_d = CL/K_e$. Total body clearance and volume of distribution were corrected for bioavailability after s.c. injection, and presented as CL/F and V/F, respectively. The parameters were determined for each animal, and the sample population averages were calculated. The observed peak plasma concentration (C_{max}) and the time-to-peak concentration (T_{max}) were recorded.

4.3 Results

Analysis of mean \pm SD of NCA pharmacokinetic parameters of Ang-(1-7) (i.v.) (Fig. 11B) and Ang-(1-7) released from Ang. Conj. (i.v.) (Fig. 11C) and Ang. Conj. (s.c.) (Fig. 11D) are listed in Table 4. After i.v. administration, the level of Ang-(1-7) in both Ang-(1-7) i.v. and Ang. Conj. declined in a multi exponential fashion with a rapid initial

distribution phase followed by a slower elimination phase (Fig. 11). Ang-(1-7) absorption of Ang. Conj. after s.c. administration was rapid, as indicated by the occurrence of mean peak plasma concentrations in about 0.83 ± 0.29 hr (Fig. 11 and Table 4). There was a significant difference in mean values of $T_{1/2}$, V_d , K_e , and AUC values following i.v. of Ang-(1-7) and Ang. Conj. $T_{1/2}$ and AUC parameters of Ang-(1-7) significantly increased and CL decreased after s.c. injection of Ang. Conj. when compared with i.v. route demonstration of Ang-(1-7). The absolute bioavailability (F) for s.c. dose was 1.28.

Table 4. Ang-(1-7) pharmacokinetic parameters of Ang-(1-7) (n=3) Ang. Conj. (n=3) after i.v., and Ang. Conj. (n=3) after s.c. administration in healthy rats. ^a Significantly different from Ang-(1-7), $p < 0.05$, ^b Significantly different from Ang. Conj., $p < 0.05$.

PK Parameters	Ang-(1-7) (i.v.)	Ang. Conj. (i.v.)	Ang. Conj. (s.c.)
C_{max} ($\mu\text{g/mL}$)	-	-	23.47 (2.01)
T_{max} (hr)	-	-	0.83 (0.29)
$T_{1/2}$ (hr)	0.71 (0.1)	4.00 (0.87) ^a	4.91 (0.83) ^a
K_e (1/hr)	0.97 (0.12)	0.18 (0.04) ^a	0.14 (0.02) ^a
V_d (mL)	38.71 (5.09)	21.76 (5.06) ^a	-
CL (mL/hr)	43.97 (7.56)	3.35 (0.18) ^a	-
V_d/F (mL)	-	-	13.72 (2.94)
CL/ F (mL/hr)	-	-	2.05 (0.54)
AUC _{inf} ($\mu\text{g/mL}\cdot\text{hr}$)	5.81 (1.11)	86.50 (4.72) ^a	131.57 (26.60) ^{a,b}
AUC _t ($\mu\text{g/mL}\cdot\text{hr}$)	4.91 (0.70)	73.73 (9.40) ^a	127.09 (24.57) ^{a,b}
MRT _{inf} (hr)	0.91 (0.09)	6.45 (1.33) ^a	6.94 (0.77) ^a
F			1.28

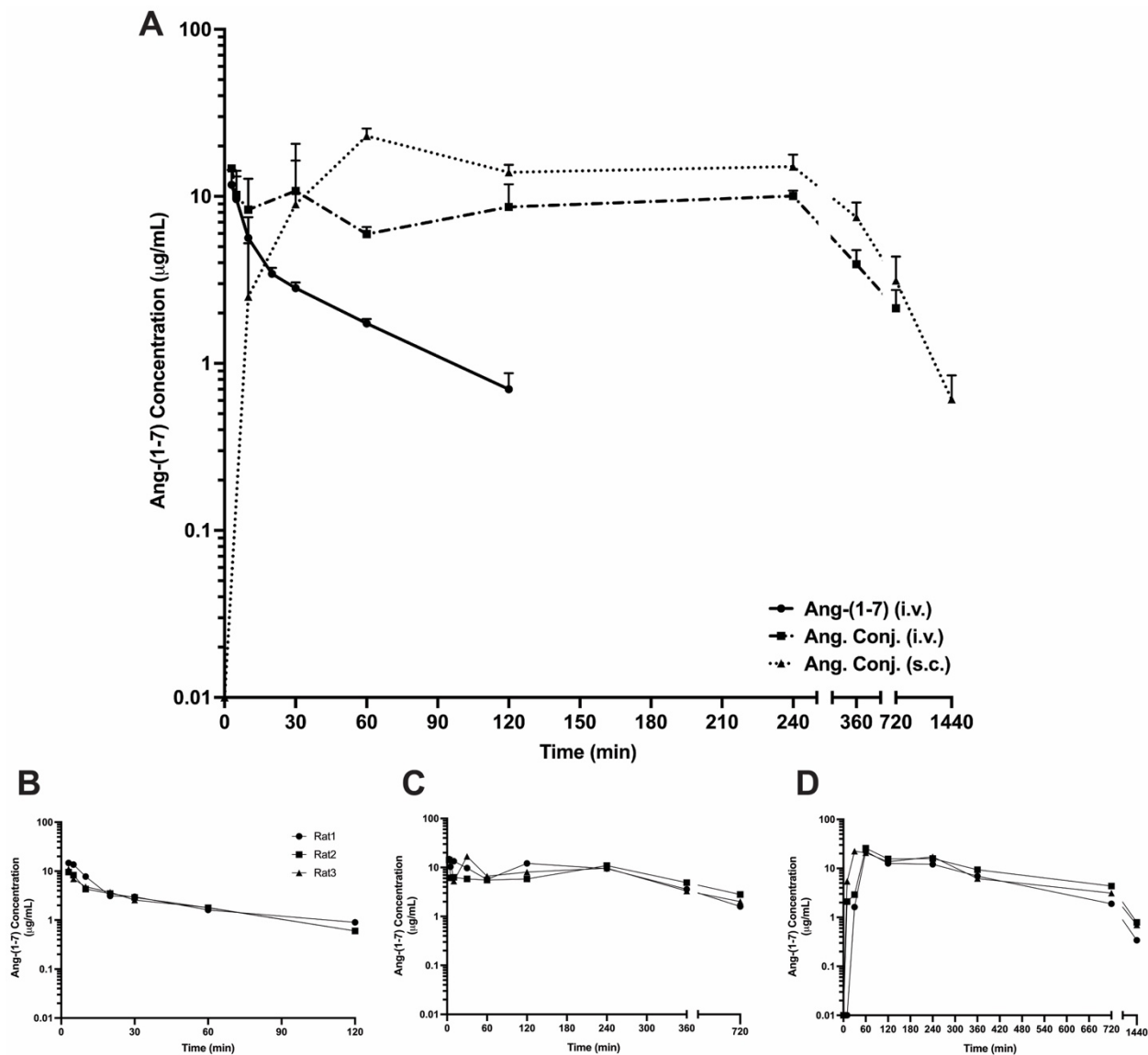


Figure 11. Mean \pm SD plasma concentration-time profile of Ang-(1-7) after Ang-(1-7) (n=3) Ang. Conj. (n=3) i.v., and Ang. Conj. (n=3) s.c. administration in healthy rats (A). Plasma concentration-time profiles of Ang-(1-7) for individual rats after Ang-(1-7) (n=3) Ang. Conj. (n=3) i.v., and Ang. Conj. (n=3) s.c. administration.

4.4 Discussion

The listed pharmacokinetic parameters of Ang-(1-7) and Ang-(1-7) released from Ang. Conj. after single i.v. and s.c. indicate that PEGylation and BP conjugation increased conjugate V_d and $t_{1/2}$ while decreasing its total body CL (Table 4 and Fig. 11).

4.5 Conclusion

The Ang. Conj. bone-targeting ability resulted in a prolonged circulation half-life. Overall, this study's results suggest that Ang. Conj. is a promising therapeutic option for treating the activated RAS-associated inflammatory bone diseases such as osteoporosis, osteoarthritis, RA, Paget's disease, and cancers with bone metastasis.

5 Chapter V: Anti-Inflammatory Effects of Ang-(1-7) Bone-Targeting Conjugate in an Adjuvant-Induced Arthritis Rat Model⁴

5.1 Background

5.1.1 Inflammation and RAS

See section 1.5 (Chapter 1).

5.1.2 Inflammation and Arachidonic Acid (ArA) Pathway

The ArA pathway is another important system for regulating the body functions.

Phospholipids as a major constituent of the cell membranes that are esterified to cell membrane glycerophospholipids, and are cleaved by phospholipases after stimulation by trauma, infection, or inflammation. Phospholipase A2 action liberates of ArA from membrane (145). Then, it becomes available for oxidative metabolism by multiple enzymes such as COX and lipoxygenase, or cytochrome P450 (CYP 450) to produce several metabolites. Many tissues including heart, kidney, liver, and lung express CYP enzymes (146, 147). ArA is a precursor of a variety of mediators and its metabolites are involved. ArA is metabolized to several eicosanoids by the action of enzymes. These eicosanoids include hydroxyeicosatetraenoic (HETEs) which is produced by the action

⁴ This work has been previously published in Pharmaceuticals journal. Khajeh pour S, Ranjit A, Summerill EL, Aghazadeh-Habashi A. Anti-Inflammatory Effects of Ang-(1-7) Bone-Targeting Conjugate in an Adjuvant-Induced Arthritis Rat Model. Pharmaceuticals. 2022 Sep 17;15(9):1157.. DOI: <https://doi.org/10.3390/ph15091157>.

of lipoxygenase (LOX), epoxyeicosatrienoic acids (EETs) which are considered as CYP P450 epoxygenase-derived metabolites, and dihydroxyeicosatrienoic acids (DHTs) which is the hydroxylated metabolites of the EET (Fig. 12) (148).

ArA metabolites are involved in different physiological and pathophysiological conditions in different tissues, such as the brain (149-152), cardiovascular system (153), kidneys (147, 154-157), liver (158, 159), and lungs (160, 161). The ArA metabolites are involved in physiological and pathophysiological processes and their intracellular signaling effects are seen in various diseases and inflammatory conditions, such as hypertension, renal disorders, atherosclerosis, stroke, diabetes, obesity, and cancer (162).

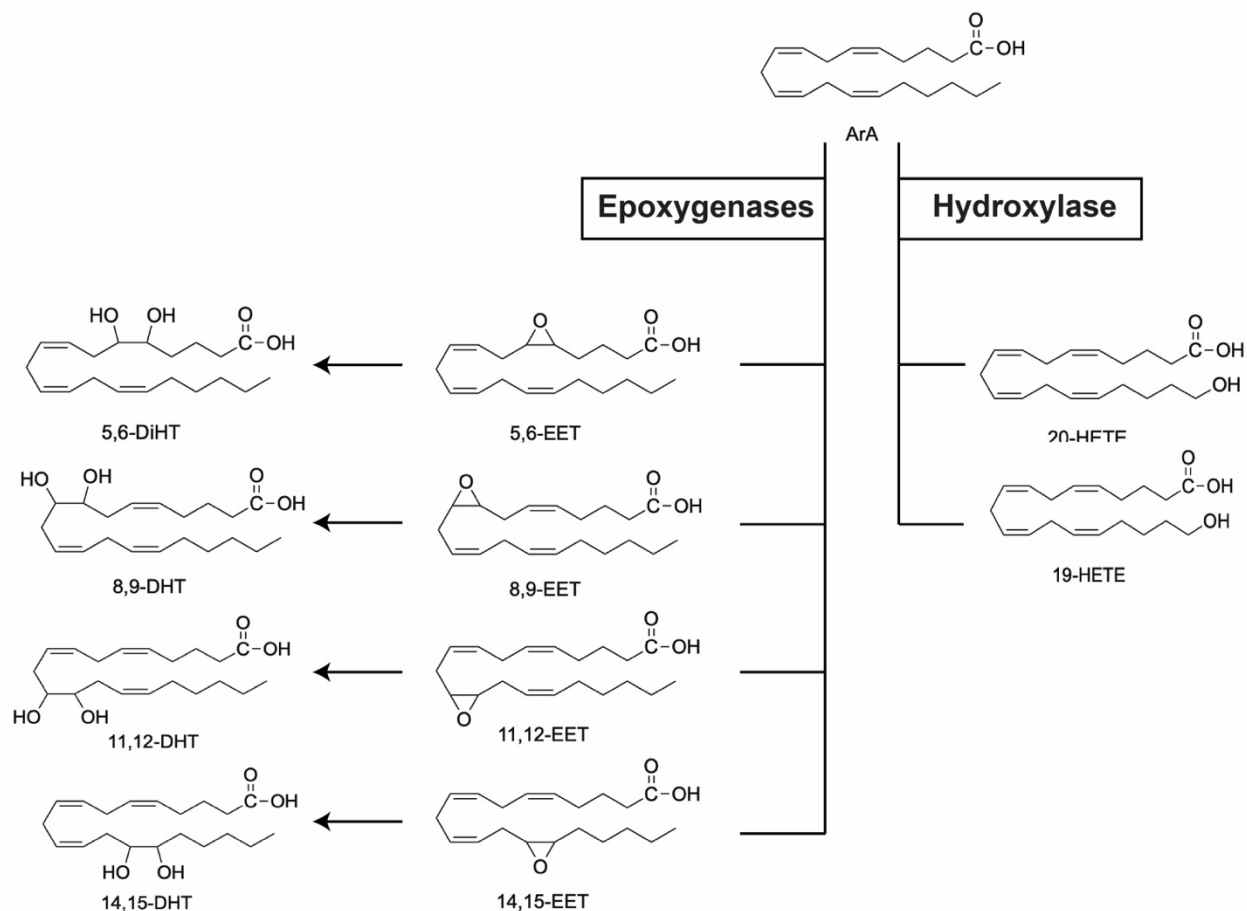


Figure 12. Arachidonic acid pathway. Hydroxyeicosatetraenoic acids; HETEs, epoxyeicosatrienoic acids; EETs, dihydroxyeicosatrienoic acids; DHTs.

Accumulating data suggest that ArA metabolites play an important role in triggering inflammation and inflammatory conditions. Several studies previously identified some of these ArA metabolites as potent pro-inflammatory agents and considered them as indices of inflammation (138, 163, 164). *In vitro* studies using an acute inflammatory model of lipopolysaccharide in mouse and rat have reported similar results (165). LOX catalyzes the insertion of one molecule of oxygen into the 5-, 12-, or 15- carbon position of ArA and is designated as 5-LOX, 12-LOX, or 15-LOX. 5S-, 12S-, or S-hydroperoxyeicosatetraenoic acid (5-, 12-, or 15-HPETE) are the main products, which

can be further reduced to hydroxy forms by glutathione peroxidase (5-, 8-, 12-, 15-HETE), respectively (166).

Multiple P450 enzymes can convert ArA to EETs, according to studies utilizing pure and/or recombinant P450 enzymes, however with varying catalytic efficiencies and the regioselectivity of EET production is P450 isoform-specific in general. CYP2C8, for example, produces 14, 15-EET and 11, 12-EET in a 1.3:1.0 ratio but no substantial levels of 8, 9-EET. Multiple P450s contribute to the biosynthesis of EETs in a given cell or tissue (167, 168). EETs, like other ArA metabolites with significant vasodilatory and anti-inflammatory properties, have been demonstrated to cause smooth muscle hyperpolarization and relaxation by activating several types of K⁺ channels (169). EETs are metabolized to DHTs by soluble epoxide hydrolase (sEH), which have less vasodilatory and anti-inflammatory activities than the parent EETs (170, 171).

As a major activator peptide within the RAS, Ang II has shown to be correlated with the metabolites from ArA pathway. ArA mimics the effect of Ang II (172). Ang II stimulates phospholipase A2 which releases ArA, and stimulates oxidase activity in vitro. Inhibiting ArA metabolism by its antagonists causes an attenuation of oxidase activation and inhibits Ang II-stimulated protein synthesis (173). Existing evidence show that Ang II stimulates the release of 20-HETE, suggesting the fact that CYP-450-derived HETEs may be important mediators in Ang II-induced vasoconstriction (174) (Fig. 13).

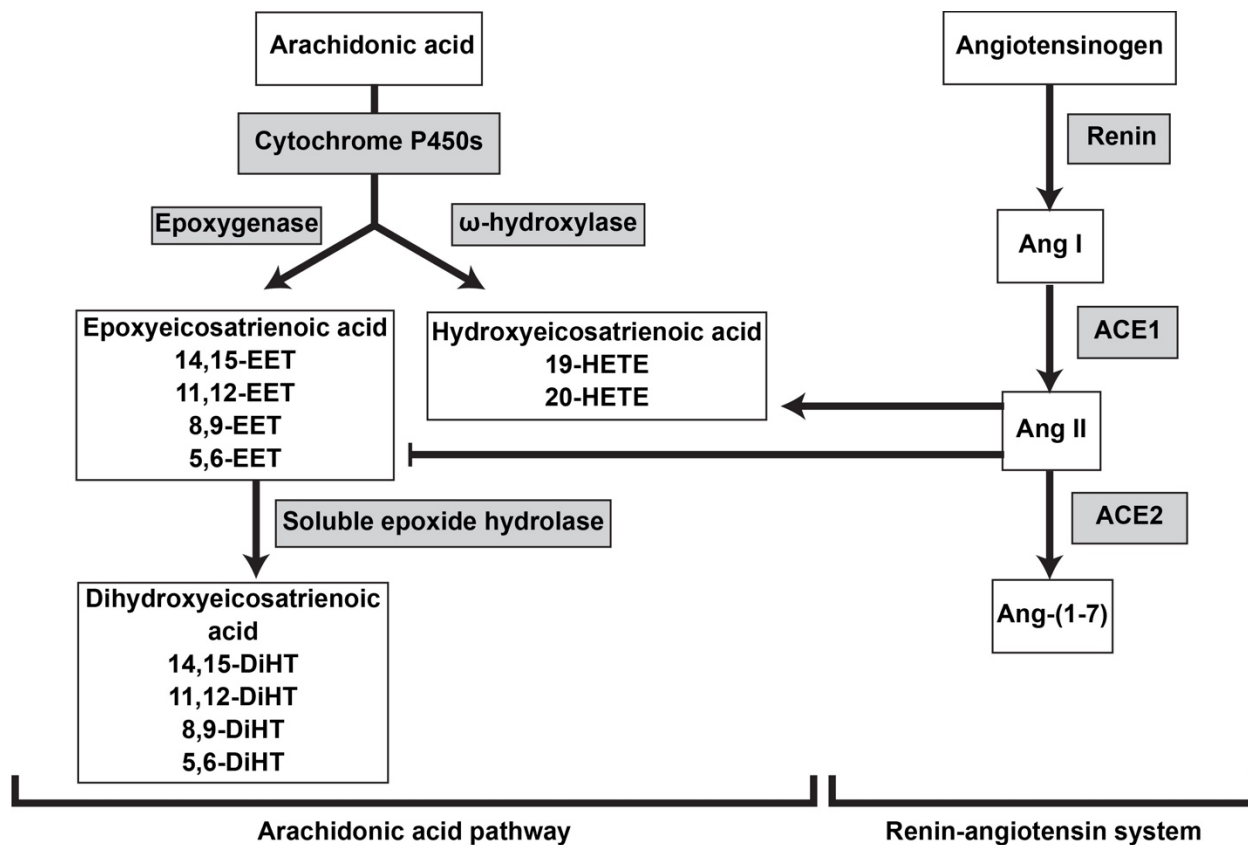


Figure 13. The schematic overview of the RAS and ArA pathways and their interactions.

5.2 Rationale

It is shown that the disturbance of the RAS arms is seen in many diseases such as RA and cancers. The rationale behind testing the Ang. Conj, in an animal model is that the evaluation of the effects of certain substances is more accurate in a complex *in vivo* model. You can easily view all the side effects that a substance produces in all parts of the body. The procedure may be easier as fewer variables need to be (or can be) controlled.

5.3 Hypothesis and Objectives

We hypothesized that inflammation resulted from arthritis disturbs the RAS balance.

Ang. Conj. can revert such imbalance in a greater extent compared to the native peptide at cellular and molecular level. We also hypothesized that such changes can improve the signs and symptoms of inflammation.

In this study, we focused on investigating the impact of the inflammation on the RAS in the heart, kidney, liver, and lung tissues at gene and protein levels and investigate the protective effects of Ang. Conj. treatment. We also evaluated Ang. Conj. systemic anti-inflammatory effects through assessment of serum concentration of NO, Ang-(1-7), Ang II, and ArA metabolites.

5.4 Experimental Methods and Materials

5.4.1 Dose Calculation

In case of *in vivo* pharmacodynamic studies.6 mg/kg or an equivalent dose of Ang. Conj. was administered s.c. every other day. In this study, all doses were weight-normalized and equivalent to their average therapeutic recommended dose for similar inflammatory diseases.

5.4.2 Adjuvant Arthritis Induction, Assessment, and Animal Handling

Animal protocol #772 for rats has been approved by Idaho State University Animal Care Facility, Pocatello, Idaho, USA. Adult male Sprague-Dawley rats (n=22) weighing 200-250 g were purchased from Charles River (Hollister, CA, USA). Animals were then housed in standard rat cages under controlled ambient temperature and humidity with

12-hour day and night cycles and free access to water and standard rat food. After three days of acclimatization, the rats were allocated into four groups, randomly, including healthy control treated with saline (n=6), inflamed treated with saline (n=6), inflamed treated with Ang-(1-7) (n=5), or Ang. Conj. (n=5).

To test our hypothesis (see section 6.3), an animal model of adjuvant-induced arthritis (AIA) was used based on previously-published studies. Snehalatha et al. tested the efficacy of the arthritis severity score and ankle diameter of using a complete Freund's adjuvant (CFA) via thermal imaging measurements. This method was shown to be effective in arthritis induction (96). AIA in rats is a commonly-used method for evaluating the test drugs with potential use for treatment of RA and other chronic inflammatory conditions. One of the methods is the injection of *Mycobacterium butyricum* suspended in mineral oil into rats' tail which causes an immune reaction. This immune reaction causes an inflammatory response that leads to distal cartilage and bone destruction concomitant with swelling of surrounding tissues (175). The induction of adjuvant arthritis in rats was done by injecting of 200 μ L of 50 mg/mL CFA containing *Mycobacterium butyricum* suspended in squalene into anesthetized the rats under isoflurane/oxygen mixture according to the manufacturer's protocol. The suspension was injected at the tail base. Rats in the control group were injected with sterile normal saline 0.9% solution instead. After 10-12 days, visible signs of inflammation associated with adjuvant arthritis were developed in rats. Rats in control and inflamed groups received blank normal saline (s.c.), whereas the rats in inflamed treated groups received the assigned treatment of either Ang-(1-7) or Ang. Conj. every other day (s.c.).

The emergence of arthritis and the progress of disease were measured by physical monitoring of the rats and recording signs and symptoms of adjuvant arthritis (176). After adjuvant inoculation, the physical signs of adjuvant arthritis were observed daily, including swelling of paws, joints, ankles, and involvement of tarsal, metatarsals, and front paws (177). Paw and joint diameters were measured using a micrometer caliper (Mitutoyo Canada Inc., Toronto, ON) every other day. The change in the rats' body weights was measured and recorded every other day using the animal balance. The arthritis index, a kind of disease score, was calculated according to published criteria (176). For each hind paw involved in swelling, we assigned a score between 0-4 (0=not involved, 1=single joint, 2=more than one joint, 3=several joints with moderate swelling, 4=several joints, ankles, and severe swelling). For each forepaw involved in swelling, a score between 0-3 was assigned (0=not involved, 1=single joint, 2=more than one joint, 3=involvement of wrists and joints with swelling). AI was calculated by adding all the scores from both hind paws and both forepaws together with a maximum of 14. A score of >5 was considered an emergence of signs and symptoms of disease, and treatment would be started. For biochemical assessments of arthritis, serum nitrate and nitrite were quantified using Griess reagent according to a published method (178).

5.4.3 SS Induction

Mouse animal were approved by the Animal Care Facility committee of the Idaho State University in accordance with legal and ethics standard. Human SYT-SSX2 cDNA was obtained by reverse transcription and the total of RNA was measured to generate the targeting vectors. Tumorigenesis was initiated in mice containing the SS18-SSX fusion

gene by the injection of TATCre which was shown to induce SS in a majority of mice, only after 3 months (179). Mice were injected with 30 μ L of 100 μ M TATCre into the quadriceps. Genotyping was carried out utilizing a PCR protocol.

5.4.4 Sample Collection

For the RA study, after dosing the animals for 14 days and after 24 h from the last dose, rats were anesthetized with isoflurane/oxygen and then euthanized. Blood samples were collected using heart puncture and further divided into three tubes. The heart, kidney, liver, lungs, and left joint tissues were surgically removed and processed for different experiments as described in the following paragraphs:

- 1) For the nitrites and nitrate measurement, a portion of freshly -collected blood samples were transferred in clean glass tubes and was kept at room temperature for 20 minutes. Tubes were further centrifuged for 10 minutes at 3,000 rpm for clearer serum. Serum was carefully separated using a micropipette in 1.7 mL Eppendorf tubes and snap-frozen in liquid nitrogen to be stored at -80 °C for further analysis of nitrite and nitrates using the commercial colorimetric assay kit.
- 2) For analysis of the RAS peptides, another portion of the blood was collected in clean glass tubes containing 50 μ L of Complete mini protease inhibitor cocktail (Roche Diagnostics GmbH, Mannheim, Germany) for each 1 mL of blood. The protease inhibitor cocktail was made using one Complete mini protease tablet in 10 mL isotonic normal saline. It inhibits a wide range of serine, cysteine, and metalloproteases in biological samples yielding 1 mM ethylene diamine tetra acetic acid (EDTA). Due to the interference with analysis, no heparin was added to these samples. Tubes were gently mixed and centrifuged at 3,000 revolutions

per minute at 4 °C for 10 minutes. The separation of the plasma in 1.7 mL Eppendorf tubes was done carefully using micropipettes. Tubes were snap-frozen using liquid nitrogen and then stored at -80 °C for further Ang peptides analysis

- 3) For the ArA metabolites measurement, a portion of blood was collected in glass tubes containing 60 USP units of sodium heparin (BD Diagnostics, NJ, USA). To every 1 mL of blood, 200 µL of 0.9% normal saline containing 0.113 mL butylated hydroxytoluene and 10 µM indomethacin (for inhibiting the cyclooxygenase enzymes and preventing chemical and enzymatic decomposition of fatty acids) was added. After gentle mixing, tubes were centrifuged at 3,000 revolutions per minute at 4 °C for 10 minutes. Then, plasma was gently separated, kept in 1.7 mL Eppendorf tubes, snap-frozen in liquid nitrogen, and kept in -80 °C for further HPLC analysis.
- 4) All other tissues were washed with normal saline collected in 2.0 mL labeled polypropylene tubes and snap-frozen with liquid nitrogen. They were then kept in -80 °C for further Western blot, qPCR, and histology tests.

5.4.5 Colorimetric Assay for Nitrite and Nitrate Measurement

For biochemical assessments of arthritis, serum nitrates and nitrites were quantified using Griess reagent according to a published method (178) using a commercial kit (Sigma Aldrich, St. Louis, MO, USA). The assay was done in a non-culture medium-treated 96-well plate. The standard solutions were added so that they generate 0, 20, 40, and 80 nmol/well standard. Standards were done in duplicates according to the manufacturer's protocol. For measuring both the nitrate and nitrite, 10 µL of nitrate

reductase and 10 μL of enzyme co-factors solution. The sample preparation was done by centrifuging the previously-collected serum in Amicon® Ultra-4 centrifugal unit with Ultracel®-10 membrane to remove hemoglobin and proteins. (Sigma Aldrich, MO, USA). 70 μL of the sample was added to each well in triplicates, and the buffer solution was used to bring the sample volume of 80 μL for nitrite and nitrate detection. The plate was mixed well on a horizontal shaker for two hours. 50 μL of Griess reagent A was added to each well and incubated for five minutes, following by the addition of the Griess reagent B and shaking for ten minutes. The absorbance was then measured at 540 nm in a microplate reader. After drawing a standard curve and determining the equation, each absorbance measurement was translated into the concentration of the nitrite and nitrate.

5.4.6 Plasma Sample Collection, Solid-phase Extraction, and LC-MS/MS analysis of the Ang Peptides

See section 3.5.2.

5.4.7 Quantitative Polymerase Chain Reaction (qPCR) Analysis of the RAS Components

Total RNA was isolated from the tumor, kidney, liver, lung, and heart tissues using a commercial kit according to the manufacturer's brochure. Briefly, frozen samples were kept at room temperature until they thawed. 50 mg of samples was weighed and added to an Eppendorf tube. Total RNA was extracted from fifty mg tissue samples using Quick-RNA™ Miniprep Plus kit (Zymo Research, Irvine, CA, USA) according to the manufacturer's protocol. Briefly, the samples were lysed into a yellow Spin-Away™

Filter in a collection tube and centrifuged to remove the genomic DNA. Then 95-100% ethanol was added to the flow through (1:1) and mixed well. This mixture was transferred into a green Zymo-Spin™ IICG Column in a collection tub and centrifuged. The flow-through was discarded. Following the DNase treatment, 400 µL of RNA Prep Buffer was added to the column, the solution was centrifuged, and flow-through was discarded. This process was repeated with 700 µL of RNA Wash Buffer. To ensure complete removal of the wash buffer, 400 µL of RNA Wash Buffer was added and the column, was centrifuged for 1 minute. The remaining solution was carefully transferred to a nuclease-free tube. Hundred µL of DNase/RNase-Free Water was added directly to the column matrix and centrifuged to elute the RNA.

Real-time qPCR mRNA analyses were performed on a system using SYBR green supermix (Bio-Rad, Hercules, CA, USA). Relative expression of all genes was determined by the comparative threshold cycle method using $2^{-\Delta\Delta Ct}$ normalized with GAPDH constitutive gene and expressed as fold change compared with control.

All primers were designed based on the rat species and a list of forward and reverse primers is shown in Table 5.

Table 5. Primer sequences used in a reverse transcription-quantitative polymerase chain reaction (qPCR) analysis of genes.

Gene	Primers	Sequences	Reference
ACE1	Forward (5'→3')	TTTGCTACACAAATGGCACTTGT	(180)
	Reverse (5'→3')	CGGGACGTGGCCATTATATT	
ACE2	Forward (5'→3')	ACCCTTCTTACATCAGCCCTACTG	(181)
	Reverse (5'→3')	TGTCCAAAACCTACCCCACATAT	
MasR	Forward (5'→3')	AGAAATCCCTTCACGGTCTACA	(182)
	Reverse (5'→3')	GTCACCGATAATGTCACGATTGT	

AT1R	Forward (5'→3')	CCTCTACAGCATCATCTTTGTGG	(183)
	Reverse (5'→3')	CACACTGGCGTAGAGGTTGA	
GAPDH	Forward (5'→3')	CCTGCACCACCAACTGCTTA	(184)
	Reverse (5'→3')	AGTGATGGCATGGACTGTGG	

5.4.8 Western Blot Analysis of the RAS Components and Caspase-3

Western blot analysis was done to measure the protein density of ACE, ACE2, AT1R, and MasR in the rat organs (heart, kidney, lung, liver) and ACE2, AT1R, and caspase-3 in the tumor tissue collected from mice. A published method with some modifications was used. Briefly, the previously-frozen samples were thawed at room temperature. Approximately 25 mg of tissue or tumor sample was weighed and homogenized in a commercially available RIPA buffer (Alfa Aesar, Ward Hill, MA, USA) (pH 7.4) also containing protease inhibitor cocktail (1 tablet Complete mini protease inhibitor with EDTA in 10 mL of buffer). The tissue homogenate was centrifuged at 10,000 revolutions per minute for 20 minutes at 4 °C following the collection of the supernatant in an Eppendorf tube with discarding the tissue debris. The total protein was measured in supernatant with fluorescence-based quantitation assay using a Qubit[®] protein assay kit (Invitrogen, Eugene, OR, USA). The protein concentrations ranged from 4-6 mg/mL. From each sample, a volume containing approximately 100 µg of protein was incubated with sample reducing buffer (Fisher Scientific, MA, USA) in a thermocycler at 95 °C for 8 minutes. Samples were electrophoresed at 100 mV for the first 15 minutes and 200 mV after that in 4-12% tris-glycine gels (Invitrogen, Eugene, OR, USA). The proteins were transferred to PVDF membranes previously soaked and washed in transfer buffer containing 0.1% Tween 20. Membranes were incubated in 10 mL blocking solution

containing 5% skimmed milk in washing buffer for 1 hour in room temperature on a horizontal shaker. Membranes were then incubated overnight at 4 °C with 10 mL of tris-buffered saline (pH 7.4) dilution of respective of primary antibody, as per manufacturer protocol. Primary and secondary antibodies were all supplied from Abcam (Cambridge, MA, USA).

The dilutions used for this purpose were: 1) anti-ACE monoclonal antibody (ab254222) at 1:100 dilution produced a 150 kDa band; 2) anti-ACE2 monoclonal antibody (ab151852) at 1:100 dilution produced a 92 kDa band; 3) anti-AT1R monoclonal antibody (ab124734) at 1:100 dilution produced a 42 kDa band; 4) anti-MasR monoclonal antibody (ab235914) at 1:100 dilution produced a 37 kDa band; 5) anti- α -tubulin monoclonal antibody (ab7291) at 1:100 dilution produced a 50 kDa band; 6) anti- β -actin monoclonal antibody (ab6276) at 1:100 dilution produced a 42 kDa band; 7) anti-caspase-3 monoclonal antibody (ab13847) at 1:100 dilution produced a 34 kDa band.

Following incubation with primary antibodies, the PVDF membranes were thoroughly wash with 15 mL washing buffer 4 times 10 minutes each. They were then incubated with secondary antibody (ab97051) in a dilution of 1:10,000 for 2 hours at room temperature. After that, the secondary antibody was removed and the membrane was slightly washed 4 times 10 minutes each on a horizontal shaker using the wash buffer. The secondary antibody binding was then visualized using a quantitative chemiluminescent substrate (Azure Biosystems, Dublin, CA, USA). Images were captured and scanned on a western blot imaging system (Azure Biosystems, Dublin,

CA, USA). The optical density of the bands was quantified by obtaining the ratio of the target protein to an optical density of bands loading control (α -tubulin or β -actin).

5.4.9 Sample Preparation, Simultaneous Extraction, and LC-MS/MS Analysis of Ang Peptides

Extraction of the Ang peptides was done using an established SPE method based on a method by Cui et al. with minor changes in the process (133). Briefly, to 200 μ L of plasma samples, 50 μ L of the [Asn¹, Val⁵] Ang II (IS) (100 ng/mL) was added and mixed. Final concentration of 0.5% formic acid was added and after vortex mixing, samples were loaded onto the 2-mL-ethanol and 2-mL-water preconditioned Waters C18 SPE cartridges (WAT020805, Milford, MA). Samples were then loaded onto the cartridge, followed by 2 mL of deionized water for washing. A positive nitrogen flow was applied to dry the cartridges further. Then 2.5 mL of 5% formic acid in methanol was added to elute Ang II. The eluted solutions were collected and dried under the stream of nitrogen. The dried samples were reconstituted in 100 μ L of 16% acetonitrile in water containing 0.1% formic acid, and 30 μ L of samples were injected into the LC-MS/MS. The level of Ang-(1-7) and Ang II peptides, as one of two important biomarkers of the protective, and classical arms of the RAS, respectively, was measured using a validated LC-MS/MS method (133) in multiple reaction mode (MRM). The system was composed of liquid chromatography in tandem with mass spectrometry (Shimadzu, Columbia, MD, USA) with a controller (CBM-20A), two binary pumps (LC-30AD), an autosampler (SIL-30AC), and an AB Sciex (Foster City, CA, USA) QTRAP 5500 quadrupole mass spectrometer in positive electrospray ionization mode (ESI). The chromatograms were monitored and integrated by the Analyst 1.7 software (AB Sciex, Foster City, CA, USA).

LC separation was performed on an analytical reversed-phase column Kinetex® C18 100 × 2.1 mm (1.7 μm) (Phenomenex, Torrance, CA, USA) by a combination of A: 0.1% formic acid in water and B: 0.1% formic acid in acetonitrile as mobile phases at a flow rate of 0.2 mL/min. The mobile phase gradient started at 5% B and increased to 30% B in 5 minutes, kept at 30% B for 5 minutes., returned to 5% B in 3 minutes and held at 5% B for 2 minutes before the next injection for column re-equilibrium.

The positive ion ESI mass spectrometric parameters were as follow: capillary voltage; 5.5 kV, temperature; 300 °C, declustering potential (DP); 100 V, and collision cell exit potential (CXP); 15 V. LC-MS/MS was performed with MRM transitions of m/z 300.6 → 371.2 (Ang-(1-7)), m/z 349.7 → 400.2 (Ang II), and m/z 516.5 → 769.4 (IS). Nitrogen was used as collision gas, and the collision energies were set at 20-30 eV. A calibration curves using peak height ratio (analyte over IS) were constructed over the range of 500 pg/mL to 10 ng/mL in plasma was used to measure the Ang peptides' levels in plasma samples.

5.4.10 Sample Preparation and LC-MS/MS Analysis of ArA Metabolites

The method for ArA metabolites extraction was obtained from a previously-done method (185); however, we validated the method in our lab. Briefly, previously-stored samples were thawed at room temperature. Then, they were centrifuged at 10,000 revolutions per minute for 10 minutes at 0 °C and 300 μL of resultant supernatant was transferred to 1.7 mL Eppendorf tubes. Then 100 μL of 200 ng/mL deuterated 8, 9-eicosatrienoic acid (8, 9-EET-d₁₁) was added as internal standard to each sample. 0.5% formic acid was added to the samples for acidifying them.

ArA metabolites were extracted using a liquid-liquid extraction method with ethyl acetate. First, 500 μ L of ethyl acetate was added to the samples following by centrifuging at 10,000 revolutions per minute at 0 $^{\circ}$ C for 10 minutes. 300 μ L of the supernatant was collected and the extraction was done for the second time with 500 μ L of ethyl acetate followed by centrifugation and taking 600 μ L of the supernatant. Samples were dried under stream of nitrogen and reconstituted in 100 μ L methanol. 10 μ L of the reconstituted sample was injected into the LC-MS/MS. A published reverse-phase HPLC method was validated and used in our lab (185). The separation and detection were done on a Shimadzu (Columbia, MD, USA) HPLC system with a controller (CBM-20A), two binary pumps (LC-30AD), an autosampler (SIL-20AC), and a DGU-20A5 degasser, coupled with an AB Sciex (Foster City, CA, USA) QTRAP 5500 quadrupole mass spectrometer equipped with electrospray ionization (ESI) probe. Data were acquired and analyzed using AB Sciex Analyst software (version 1.7) provided with the system. Reverse phase chromatographic separation was achieved on a C18 Synergi™ Fusion-RP LC column (2.5 μ m, 100 \times 2 mm) (Phenomenex, Torrance) and maintained at 40 $^{\circ}$ C. A C18 guard column (2.1 mm) (Phenomenex, Torrance, CA, USA) attached to a holder (Phenomenex, Torrance, CA, USA) was attached prior to the analysis column. The mobile phase A was 0.1% formic acid in water and mobile phase B was 0.1% formic acid in acetonitrile. Separation of ArA metabolites was done using a gradient at flow rate of 0.2 mL/min. The gradient started at time 0 with 5% B, then, it was increased to 20% B at 2 minutes following by an increase to 55% B for 0.5 minutes. It was held at 55% B for 2.5 minutes, and then increased to 100%B in two minutes and

was held at 100% B for another minute. The gradient was dropped down to initial 5% B at 9.5 minutes and held at 5% B for 1 minute to re-equilibrate the column.

The detection was done on a SCIEX QTRAP 5500 quadrupole mass spectrometer (Framingham, MA, USA) in negative electrospray ionization (ESI) mode. The negative ESI mass spectrometric parameters were as follows: capillary voltage, -4.5 kV; temperature, 400 °C; declustering potential (DP), 100 V; collision cell exit potential (CXP), 15 V. LC-MS/MS was performed with MRM transitions with the parameters shown in Table 6. Nitrogen was used as collision gas, and the collision energies were set at 20 eV.

The chromatograms were monitored and analyzed by the Analyst software version 1.7 from AB SCIEX (Framingham, MA, USA).

Table 6. Compound parameters for arachidonic acid metabolites, and their internal standard with MRM in negative electrospray ionization mode.

Analyte	Q1 Mass (Da)	Q3 Mass (Da)	DP (volts)	CE (volts)	CXP (volts)
5, 6-EET	319	191	-30	-14	-11
8, 9-EET	319	155	-30	-14	-11
11, 12-EET	319	208	-120	-18	-11
14, 15-EET	319	167	-120	-18	-11
8, 9-EET-d ₁₁	330	155	-25	-18	-19
20-HETE	319	245	-95	-22	-15
5, 6-DHT	337	145	-115	-22	-11
8, 9-DHT	337	127	-105	-26	-11
11, 12-DHT	337	187	-115	-24	-19
14, 15-DHT	337	207	-40	-24	-13

A standard curve ranging from 0.625-160 ng/mL was constructed in plasma to extract the unknown concentration of samples from. The method was validated with performing intra-day and inter-day assays for each ArA metabolite.

5.4.11 Statistical Analysis

The results of the Ang peptides concentration assays are presented as mean \pm standard error of mean (SEM) in rat and human plasma (ng/mL). The Ang-(1-7)/Ang-II ratios are calculated individually for each rat, for plasma samples and then mean \pm SEM was calculated. For multiple comparison in all groups, one-way analysis of variance (ANOVA) followed by Tukey's adjustment was used.

The results of the qPCR study were analyzed using $2^{-\Delta\Delta Ct}$ where each gene is compared to the control (GAPDH) and then the values for each group is calculated in comparison to the control. The results are shown as mean \pm SD and for multiple comparison in all groups, we used one-way ANOVA followed by Tukey's adjustment.

The Western blot results analyses are presented as mean \pm standard deviation (SD) of ratio of OD of the bands obtained for target protein and loading control beta-actin or tubulin. The values optical densities were obtained by processing the Western blot images through ImageJ software (developed by multiple contributors worldwide and available through University of Wisconsin-Madison). For multiple comparison between along all groups we used one-way ANOVA followed by Bonferroni adjustment.

5.5 Results

5.5.1 Effect of Ang. Conj. Treatment on Body Weight and Arthritis Index

AIA appeared 8-10 days post-adjuvant injection. It manifested as paw redness and erythema of the ankle joints, followed by involvement of the metatarsophalangeal and interphalangeal joints. Over time, the symptoms gradually extended to other areas of the hind and forepaws. Three times each week, the weight, paw, and joint measurements were taken. The paw and joint diameters on day 24 relative to day 0 are provided as percentage changes (Fig. 14).

The percentage change of animals' body weight gain was significantly reduced in AIA animals and treatment with Ang-(1-7) and Ang. Conj. restored the body weight gain over time (Fig. 14A). The weight gain percentage value in the inflamed (12.6 ± 5.5) and Ang-(1-7)-treated group (31.6 ± 5.3) was significantly lower than the control group (50.1 ± 2.5). However, the value in the Ang. Conj.-treated group (34.2 ± 4.5) was comparable to that of the control group (Fig. 14A). As a measure of signs and symptoms of arthritis, the arthritis index (AI) was significantly higher in the inflamed group indicating efficacious arthritis induction. Therapeutic efficacy of Ang-(1-7) and Ang. Conj. was noticeable after administration of three consecutive doses (~6 days), but it was statistically significant at 10 days post-dose (Fig. 14A and B). The right and left joints diameter percent changes at the end of the experiment compared to day 0 in non-treated inflamed rats (29.0 ± 9.0 and 27.7 ± 7.4) were significantly higher than in the control group (2.7 ± 1.2 and 3.8 ± 0.8). The drug treatment impacted the swelling of right and left joints as it was substantially lower in Ang. Conj. (3.6 ± 1.6 and 2.5 ± 1.4) group than Ang-(1-7) (9.6 ± 2.5 and 12.4 ± 7.4) group (Table 7 and Figure 14C and E).

The same trend was seen for the left and right paw diameter percent changes but did not reach a significant difference (Table 7, Fig. 14D and F).

Table 7. The percentage change in paw and joint diameters in different treatment groups at the end of the experiment compared to day 0. Adapted from reference (186) with permission.

Animal group	Paw diameter percentage change Mean (SEM)		Joint diameter percentage change Mean (SEM)	
	Left hind	Right hind	Left hind	Right hind
Control (n=6)	2.7 (2.0) ^a	0.0 (1.3) ^a	2.7 (1.2) ^a	3.8 (0.8) ^a
Inflamed (n=6)	22.7 (10.6) ^a	23.7 (10.5) ^a	29.0 (9.0) ^b	27.7 (7.4) ^b
Ang-(1-7) (n=5)	4.8 (1.3) ^a	10.0 (10.7) ^a	9.6 (2.5) ^{a,b}	12.4 (4.6) ^a
Ang. Conj. (n=5)	3.1 (1.5) ^a	1.8 (0.6) ^a	3.6 (1.6) ^a	2.5 (1.4) ^a

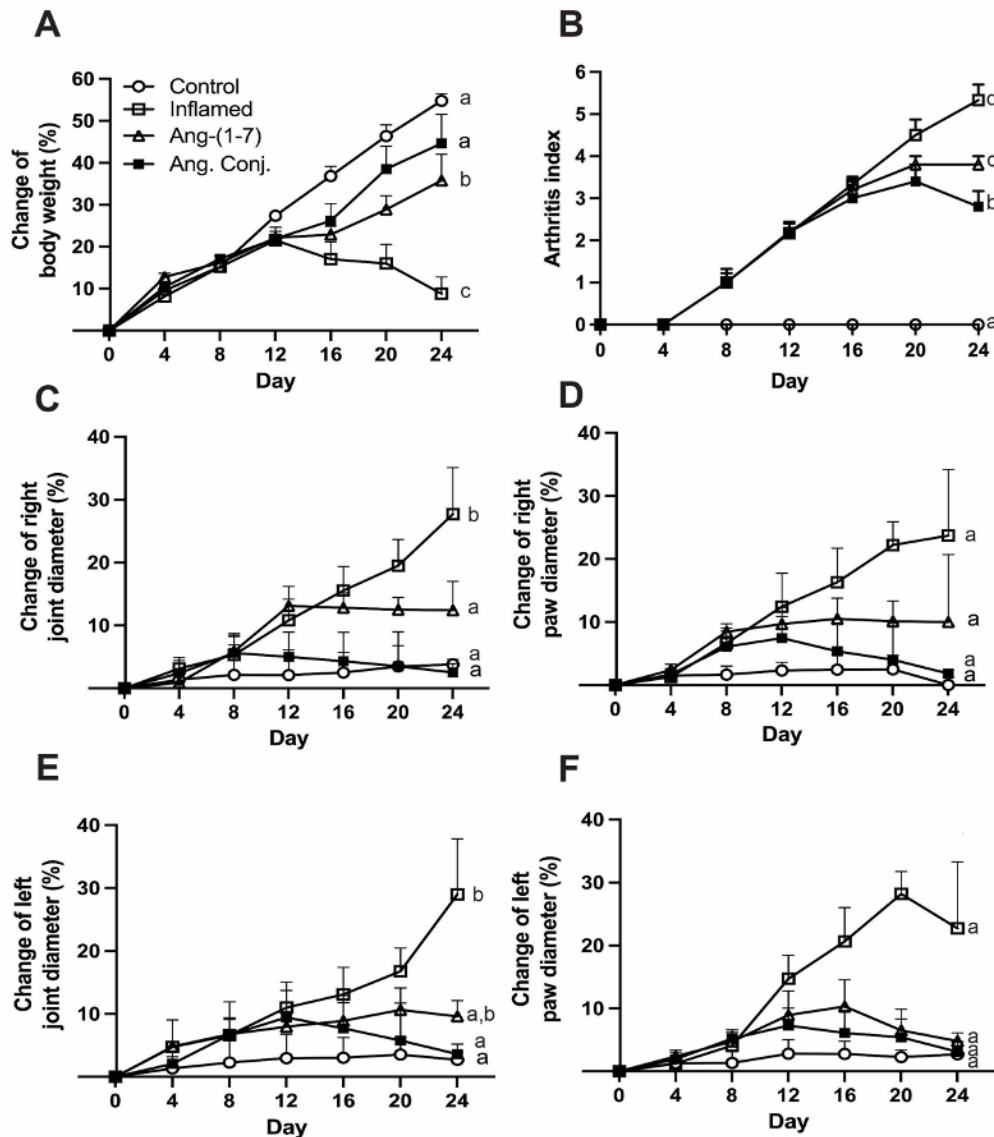


Figure 14. Effect of AIA and treatment with Ang-(1-7) and Ang. Conj. on the percentage change of body weight (A) and the arthritis index (B) in the rats (n = 5-6). The percentage change in the right joint (C), right paw (D), left joint (E), and left paw (F) diameters compared to day 0. Different letters denote significant differences between groups ($p < 0.05$), one-way ANOVA followed by Tukey's post hoc test. Adapted from reference (186) with permission.

5.5.2 Serum Nitrate and Nitrite Levels

The serum nitrate and nitrite levels were significantly elevated in inflamed animals (5.15 ± 1.02 ng/mL) compared to healthy control rats (0.22 ± 0.13 ng/mL). Ang. Conj.

treatment significantly reduced the NO concentration to 0.95 ± 0.52 ng/mL, which was

comparable to the control group. Although Ang-(1-7) treatment reduced the NO concentration to 2.35 ± 0.73 ng/mL, this reduction did not happen to the same extent as after treatment with Ang. Conj. The NO level in Ang-(1-7) treated rats was not significantly different from the inflamed or control group (Fig. 15).

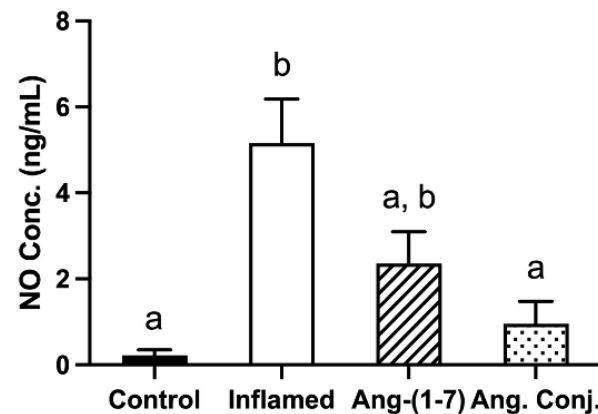


Figure 15. Effect of AIA and Ang-(1-7) or Ang. Conj. treatment on serum NO concentrations (n = 5-6). Different letters denote significant differences between groups ($p < 0.05$), one-way ANOVA followed by Tukey post hoc test. Adapted from reference (186) with permission.

5.5.3 Measuring the Plasma Levels of Ang-(1-7) and Ang. Conj.

Plasma extraction and LC-MS/MS detection methods were validated for Ang-(1-7) and Ang II and the validation parameters results are reported in Table 8.

Table 8. Inter- and intra-day precision and accuracy of Ang peptides. Adapted from reference (187) with permission.

Peptide	Conc. (ng/mL)	Intra-day		Inter-day	
		(CV%)	Accuracy%	(CV%)	Accuracy%
Ang-(1-7)	0.31	≤ 9.39	105.6 ± 5.7	≤ 6.64	102.7 ± 1.3
	1.25	≤ 3.42	95.1 ± 6.3	≤ 1.29	108.0 ± 3.4
	5	≤ 1.34	100.7 ± 0.8	≤ 2.17	98.9 ± 8.2

	0.2	≤ 5.05	102.9 ± 7.3	≤ 3.24	96.81 ± 15.4
Ang II	0.8	≤ 2.39	102.5 ± 1.8	≤ 8.37	100.9 ± 11.7
	3.2	≤ 1.07	99.1 ± 9.2	≤ 7.83	101.0 ± 6.8

The level of Ang-(1-7) and Ang II peptides and their ratio is presented in Fig. 16. These data confirmed the treatment of AIA rats with Ang. Conj. significantly increases the Ang-(1-7) plasma levels (1.45 ± 0.22 ng/mL) compared with the control (0.75 ± 0.08 ng/mL), inflamed (0.19 ± 0.05 ng/mL), and Ang-(1-7)-treatment (0.90 ± 0.17 ng/mL) groups (Figure 16A). The Ang II plasma levels, on the other hand, present a reverse trend. The AIA significantly elevates Ang II levels in the inflamed group (1.70 ± 0.37 ng/mL), which reduced to a comparable level to the control group (0.27 ± 0.02 ng/mL) after treatment with Ang-(1-7) (0.30 ± 0.036 ng/mL) or Ang. Conj. (0.21 ± 0.02 ng/mL) (Fig. 16B). Ang-(1-7)/Ang II ratio was significantly higher in the Ang. Conj.-treated group (6.30 ± 1.89) compared with the healthy-control (4.10 ± 1.42), inflamed (0.1 ± 0.03), and Ang-(1-7) (2.00 ± 0.60) groups (Fig. 16C).

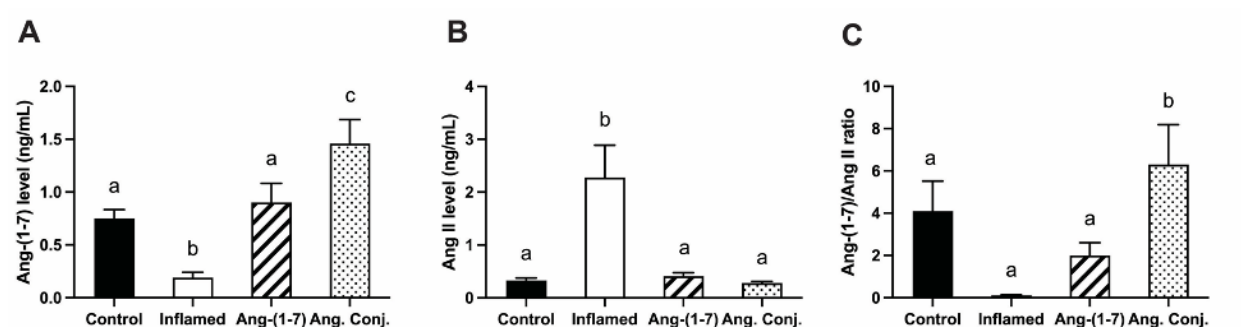


Figure 16. Ang-(1-7) (A), Ang II (B), levels and their ratio in plasma in control (n=6), inflamed (n=6), Ang-(1-7)-treated (n=5), and Ang. Conj.-treated (n=5) groups. Values are reported as mean ± SEM, and statistical analysis was done using one-way ANOVA with the Tukey post hoc

test. Different letters denote significant differences between groups ($p < 0.05$). Adapted from reference (186) with permission.

5.5.4 Measuring the Plasma Levels of ArA Metabolites

ArA metabolites were measured in plasma using validated LC-MS/MS methods for each (Table 9). The coefficient of variance, and accuracy measurements are within the accepted range of less than 20% and between 80-120%, respectively.

Table 9. Inter- and intra-day precision and accuracy of ArA metabolites. Adapted from reference (187) with permission.

Metabolite	Conc. (ng/mL)	Intra-day		Inter-day	
		(CV%)	Accuracy%	(CV%)	Accuracy%
5,6-EET	0.62	8.76	101.88	4.53	100.73
	5	2.1	100.5	3.8	103.4
	40	7.2	98.3	6.4	99.3
	160	0.7	100.3	0.7	100.0
8,9-EET	0.62	3.1	106.1	7.8	101.9
	5	6.5	99.9	6.8	101.7
	40	4.9	100.7	4.3	99.9
	160	0.34	100.2	0.2	100.6
11,12-EET	0.62	3.6	103.6	7.6	97.7
	5	0.41	102.4	9.8	98.0
	40	1.9	98.9	2.31	96.7
	160	0.1	100.4	1.7	101.8
14,15-EET	0.62	7.5	100.3	6.7	96.5
	5	6.9	96.5	7.6	103.1
	40	6.5	99.5	5.7	101.3

	160	2.3	101.6	1.1	102.6
20-HETE	0.62	4.9	105.5	3.4	106.6
	5	4.0	113.1	3.1	109.7
	40	2.9	106.9	1.9	106.9
	160	1.1	101.6	1.5	102.8
5,6-DHT	0.62	6.0	101.3	9.4	97.1
	5	5.1	107.9	9.5	99.6
	40	2.9	103.1	5.85	104.4
	160	0.6	102.3	1.3	101.8
8,9-DHT	0.62	9.7	101.3	9.3	100.3
	5	9.1	105.3	5.2	102.0
	40	3.1	102.3	3.1	100.2
	160	1.1	101.6	1.8	101.4
11,12-DHT	0.62	5.0	104.8	7.9	101.5
	5	3.2	110.3	2.2	105.9
	40	2.7	106.2	2.4	103.4
	160	2.0	100.3	1.8	101.2
14,15-DHT	0.62	4.8	99.6	3.9	103.8
	5	3.2	105.2	2.4	102.2
	40	2.2	103.4	4.5	101.9
	160	0.3	101.7	1.7	102.3

Analyzing the level of total EETs, total DHTs, and 20-HETE in plasma reveals that the level of the total EETs and DHTs decreased in inflamed group and treatment with Ang. Conj. restored its level significantly. Total EETs level consists of the sum of 4,5-EET,

8,9-EET, 11,12-EET, and 14,15-EET, measured in plasma by LC-MS/MS, separately. Total EETs mean \pm SEM level in control, inflamed, Ang-(1-7)-treated, and Ang. Conj.-treated groups were 98.2 ± 7.9 , 12.5 ± 2.9 , 80.12 ± 7.2 , and 123.9 ± 13.1 ng/mL, respectively (Fig. 17A).

Total DHTs level consists of the sum of 4,5-DHT, 8,9-DHT, 11,12-DHT, and 14,15-DHT, measured in plasma by LC-MS/MS, separately. Total DHTs mean \pm SEM level in control, inflamed, Ang-(1-7)-treated, and Ang. Conj.-treated groups were 13.3 ± 1.6 , 3.1 ± 1.2 , 7.8 ± 0.7 , and 12.8 ± 2.4 ng/mL, respectively (Fig. 17B).

20-HETE concentrations in plasma of in control, inflamed, Ang-(1-7)-treated, and Ang. Conj.-treated rats were $15.5 \pm 2.$, 111.1 ± 4.0 , 26.0 ± 3.8 , and 18.0 ± 3.3 ng/mL, respectively (Fig. 17C).

Total EETs/20-HETE ratio was significantly lower in inflamed rats (0.10 ± 0.02 unit), whereas this ratio was higher in Ang-(1-7) (3.48 ± 0.65), and Ang. Conj. (7.73 ± 1.21) groups compared to the control group (6.90 ± 1.03) (Fig. 17D).

We observed a positive correlation between the Ang II vs total EETs/20-HETE ratio. This trend was reversed when Ang II was correlated with the ratio of total EETs/20-HETE (Fig. 17E and F).

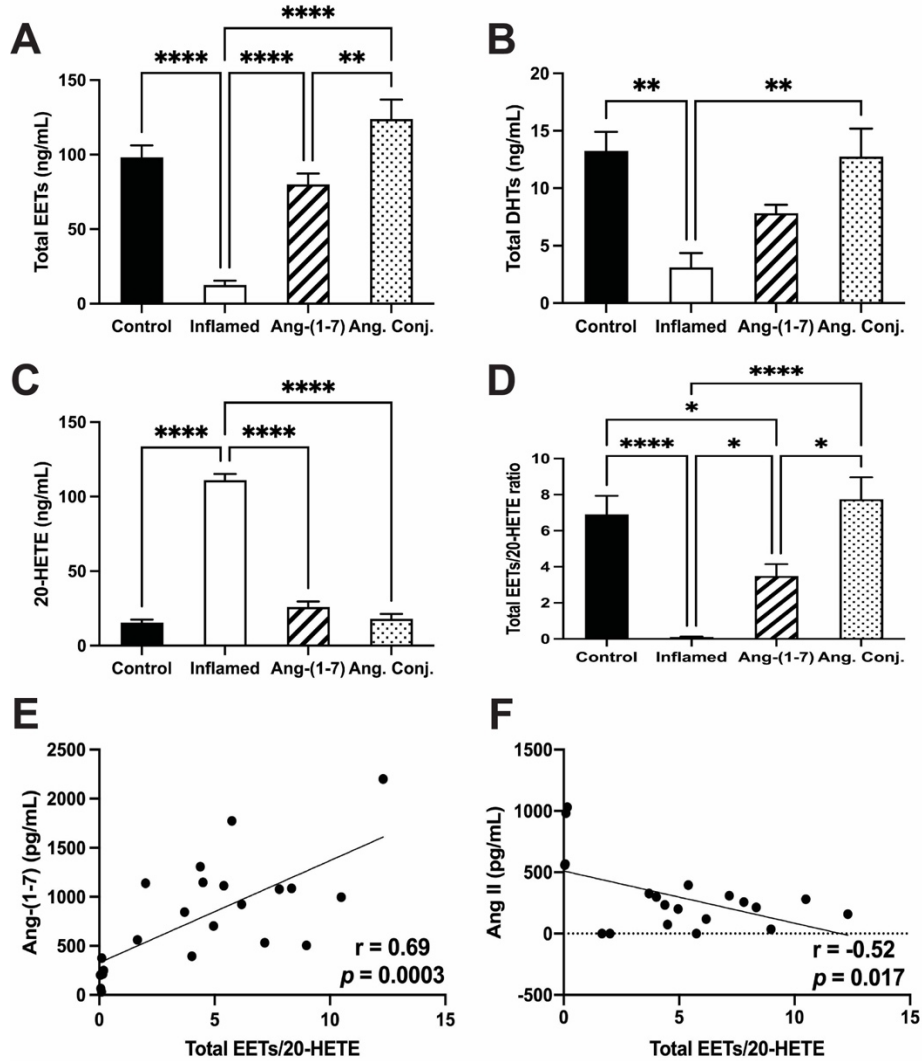


Figure 17. Total EETs (A), DHTs (B), and 20-HETE (C) levels in rat plasma samples from control (n=6), inflamed (n=6), Ang-(1-7)-treated (n=5), and Ang. Conj.-treated (n=5) rats. Ratio of the total EETs to 20-HETE in the same groups (D). Correlation between the RAS peptide and ArA metabolites (E&F). Values are reported as mean \pm SEM, and statistical analysis was done using one-way ANOVA with the Tukey post hoc test. * Significantly different from another group, $p < 0.05$. Adapted from reference (188) with permission.

5.5.5 Gene Expression of the RAS Components in Different Tissues

The mRNA expression of ACE1, ACE2, AT1R, and MasR in the heart, lung, liver, and kidney, are shown in Fig. 18. ACE1 and AT1R gene expression levels increased significantly in all inflamed rat tissues examined, and ACE2 gene expression was reduced in the heart, lung, liver and kidney. The expression of the MasR gene

increased in the heart and decreased in the lung and kidney, with no change observed in the liver. All changes were significantly reversed by treatment with Ang-(1-7) and Ang. Conj. (in a higher magnitude). However, in the heart tissue, the increased MasR expression due to AIA was further increased by Ang. Conj. ACE2/ACE1 and MasR/AT1R gene expression ratios in all four tissues reduced, and treatment with Ang-(1-7) normalized them while Ang. Conj. increased them several folds.

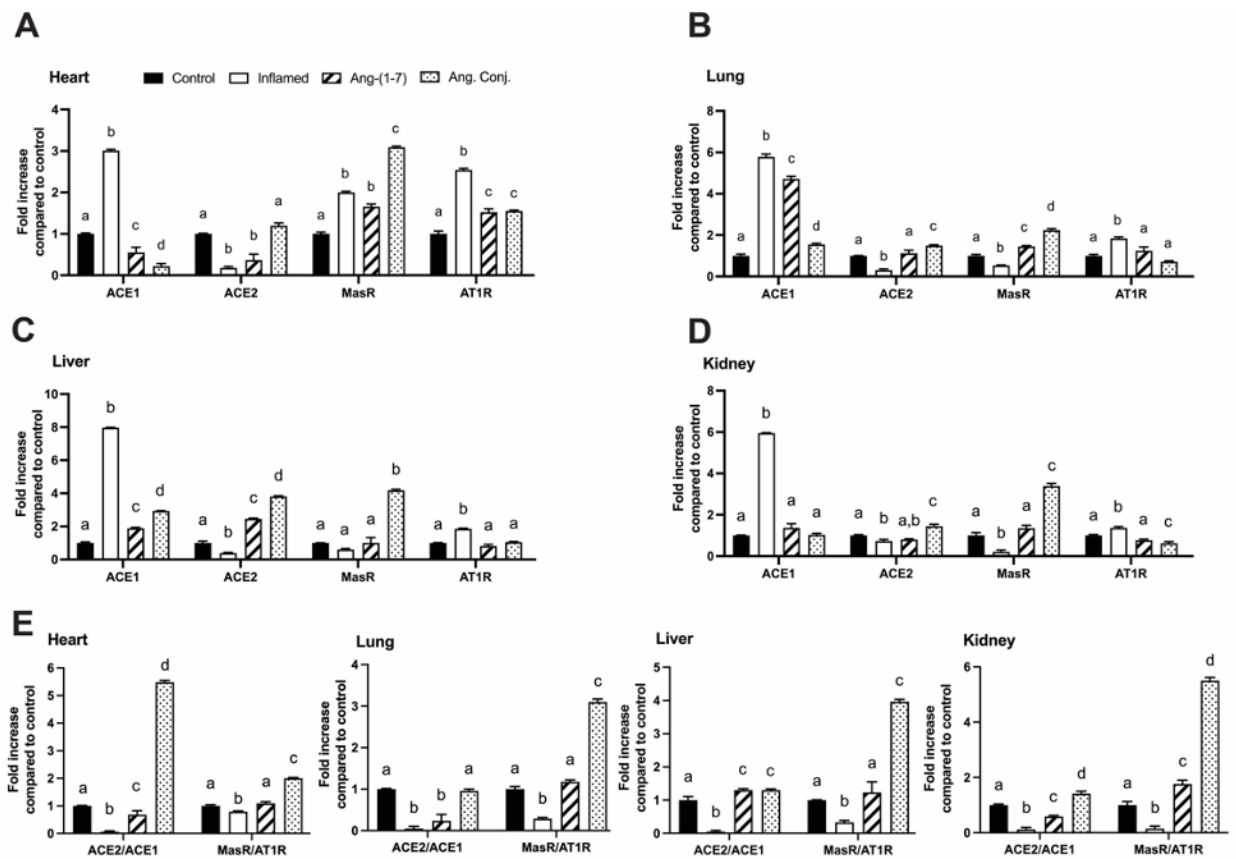


Figure 18. Gene expression of ACE1, ACE2, MasR, and AT1R levels in the heart (A), lung (B), liver (C), kidney (D) tissues, and the ratio of ACE2/ACE1 and MasR/AT1R in those tissues (E) in control (n=6), inflamed (n=6), Ang-(1-7)-treated (n=5), and Ang. Conj.-treated (n=5) groups. ACE1; angiotensin-converting enzyme 1, ACE2; angiotensin-converting enzyme 2, MasR; Mas receptor, AT1R; angiotensin II type 1 receptor. Values are reported as mean \pm SEM, and statistical analysis was done using one-way ANOVA with the Tukey post hoc test. Different letters denote significant differences between groups ($p < 0.05$). Adapted from reference (186) with permission.

5.5.6 Protein Expression of the RAS Components in Different Tissues

Data shown in Fig. 19 represent the significant changes in relative protein density of ACE1, ACE2, MasR, and AT1R in the heart, lung, liver, and kidney tissues due to AIA. These changes were normalized by Ang-(1-7) or Ang. Conj. treatment and the effects were more pronounced in the case of the latter. The individual proteins WB results indicate i) AIA caused a significant increase in the ACE1 protein expression in the heart, liver, and kidney tissues of the inflamed rats and Ang-(1-7) or Ang. Conj. treatment reversed it, which was more efficient in the case of treatment with Ang. Conj., and brought it back to the control group level. ii) AIA significantly reduced the ACE2 expression in the heart and lung tissues, and treatment with Ang-(1-7) or Ang. Conj. normalized it. In the case of the liver and kidney, AIA resulted in a similar change trend but was not significant. iii) MasR's expression was significantly reduced in inflamed animals' lung, liver, and kidney tissues, which were again normalized by Ang-(1-7) or Ang. Conj. treatments. iv) The AT1R expression was significantly increased in all tissues other than the kidney in the inflamed group and Ang. Conj. treatment reversed the expression more efficiently than Ang-(1-7). v) ACE2/ACE1 and MasR/AT1R protein expression ratios in all tested tissues were reduced by AIA, and treatment with Ang-(1-7) or Ang. Conj. normalized them.

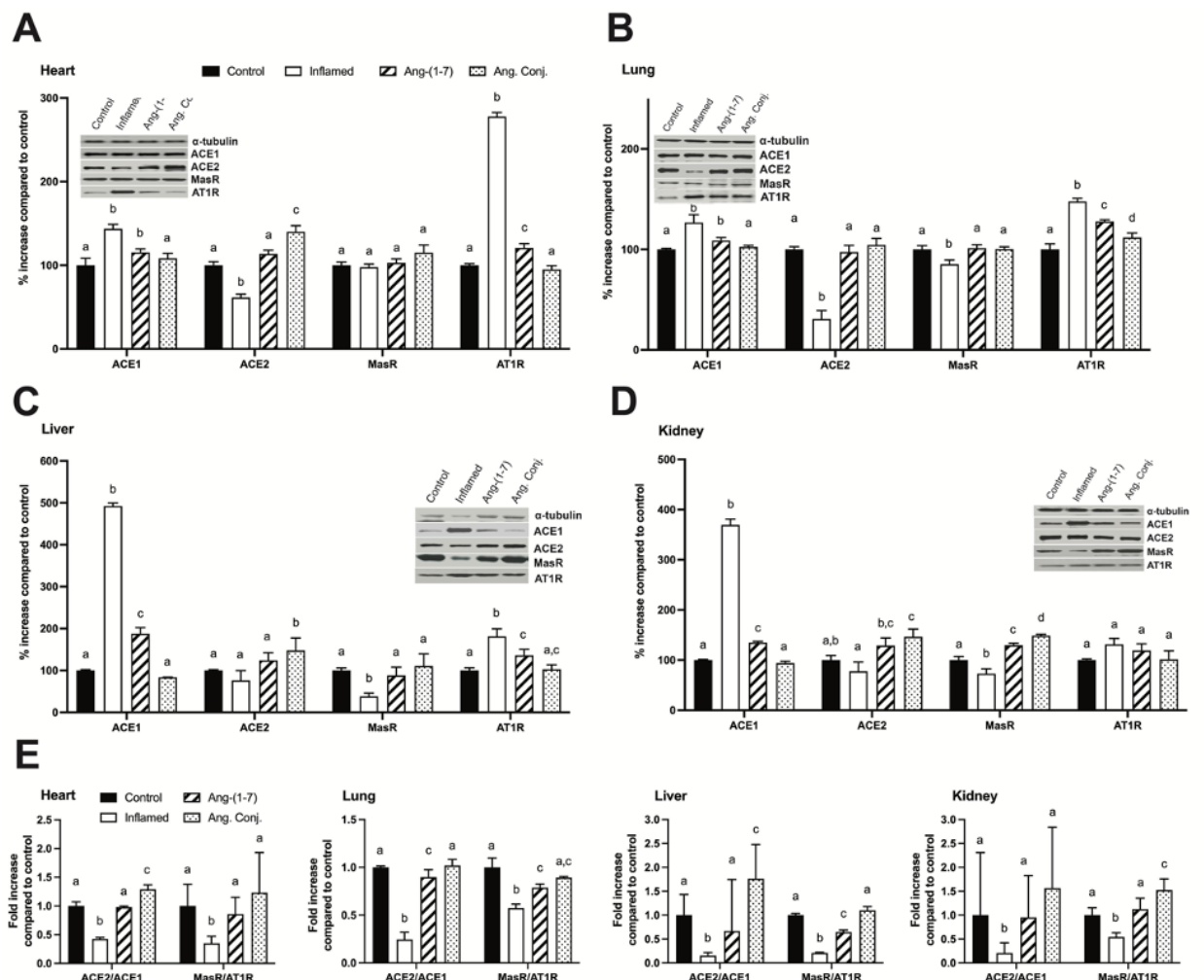


Figure 19. Protein expression of ACE1, ACE2, MasR, and AT1R, levels in the heart (A), lung (B), liver (C), kidney (D) tissues, and the ratio of ACE2/ACE1 and MasR/AT1R (E) in control (n=6), inflamed (n=6), Ang-(1-7)-treated (n=5), and Ang. Conj.-treated (n=5) groups. ACE1; angiotensin-converting enzyme 1, ACE2; angiotensin-converting enzyme 2, MasR; Mas receptor, AT1R; angiotensin II type 1 receptor. Values are reported as mean \pm SEM, and statistical analysis was done using one-way ANOVA with the Tukey post hoc test. Different letters denote significant differences between groups ($p < 0.05$). Adapted from reference (186) with permission.

5.5.7 Statistical Analysis

The results of ArA metabolites are presented as concentration mean \pm SD of concentration of respective metabolites (EETs, 20-HETE, and DHTs) in the rat plasma (ng/mL). The total EETs/20-HETE ratios are calculated individually for each rat plasma,

and reported as mean \pm SEM. The mean values obtained for each group is compared with mean of other group using one-way ANOVA followed by Tukey's adjustment.

5.6 Discussion

The anti-inflammatory effects of Ang-(1-7) have been reported previously (49). The administration of Ang-(1-7) or Ang. Conj. impacted the activated RAS, which was more pronounced in the case of Ang. Conj. Using an AIA model of RA, our results demonstrates that exogenous delivery of Ang-(1-7) as a stable conjugate, Ang. Conj., augments the RAS protective arm. This enhancement has considerable anti-inflammatory benefits by restoring weight gain, lowering paw and joint edema, and decreasing the elevated NO level and AI caused by inflammation (Fig. 14). By reducing NO concentration, the anti-inflammatory effect of Ang. Conj. followed the same trend as the shift in Ang-(1-7) and Ang II plasma levels (Fig. 16). NO serum levels did not differ significantly between the control and Ang. Conj. groups (Fig. 15). The effect of Ang-(1-7) and Ang. Conj. on AI were not significantly different until 10 days after therapy started. This may be owing to the time needed for Ang-(1-7) concentration to reach a steady-state level. These effects were largely consistent with restoring the disrupted equilibrium between the classical and protective arms, as measured by ratios of Ang-(1-7)/Ang II peptides, or ACE2/ACE1 and MasR/AT1R at the gene or protein levels. In agreement with previous reports (139), the findings of our study illustrates that induced inflammation in AIA rats modifies the ratio of the RAS components in plasma peptides, enzyme, and receptor levels in all investigated tissues. Changes in ACE1 and ACE2 enzyme expression affect plasma Ang-(1-7) and Ang II levels, as well as their ratio (Fig. 16). These findings demonstrate that the reduced expression of ACE2 led to a decrease

in plasma concentration of the vasodilator peptide, Ang-(1-7). This effect was observed in the heart and kidney tissues of the AIA rats and most likely applies to other tissues (139). Notably, Ang II supports pro-inflammatory effects and is raised in numerous cardiovascular disorders, including hypertension, atherosclerosis, and coronary heart disease, by increasing the synthesis of various inflammatory mediators and their migration into sites of tissue injury (189, 190). Consistent with the pro-inflammatory actions of Ang II, treatment with ACEIs and ARBs diminishes the production and release of inflammatory mediators in models of inflammation (191-196). ACE2, by degrading the Ang II to Ang-(1-7) and MasR signaling, counters Ang II pro-inflammatory effects (197, 198). MasR gene expression was unaffected by AIA in any of the studied tissues, whereas AT1R gene expression was considerably elevated in the heart and liver tissues. These variations in gene expression resulted in variable alterations in protein expression, with the lung, liver, and kidney tissues exhibiting reduced MasR density and all tissues except the kidney exhibiting higher AT1R expression. In contrast, the MasR/AT1R protein ratio was decreased in all AIA-untreated tissues. This observation further shifts the balance of the activated RAS components toward their detrimental classical arm effects. The observed significant increase in AT1R and decrease in MasR/AT1R supports the hypothesis that arthritis can alter the vasodilation-vasoconstriction balance, as there will be less MasR for coupling with already reduced vasodilator Ang-(1-7). As a result, more AT1R will be available to be activated by a higher concentration of a vasoconstrictor, Ang II. We only examined the quantities of Ang peptides in plasma, which were dramatically reduced in AIA rats; however, given the decreased ratio of ACE2/ACE1 expressions, this is most likely true for all tissues.

Animals with AIA could be treated with Ang-(1-7) to mitigate the negative effects of an active RAS and its shift toward the classical arm. The RAS exerts its physiological effects through AT1R, AT2R, and MasR. Ang II has an affinity for AT1R and AT2R (with offsetting responses), but most Ang II effects are mediated through AT1R (199). In the present study, we focused only on the AT1R and MasR; however, the AT2R receptor gene and protein expressions can also be affected by inflammation and should be taken into account when interpreting the data. When Ang. Conj. was administered, the restoration of equilibrium and exertion of anti-inflammatory effects were more significant and apparent. The improved efficacy can be attributed to the intermittently prolonged effect of Ang-(1-7) through MasR signaling. The Ang. Conj. thrice-weekly application for two weeks significantly increased the reduced plasma Ang-(1-7), reduced the increased level of Ang II, and restored the healthy control ratio of those peptides (Fig. 16). The gene and protein expression of ACE1 and ACE2 were consistent with observed modification of Ang peptides, resulting in an overall considerable improvement of the ACE2/ACE1 ratio in tested tissues. The MasR/AT1R has a similar pattern in all tissues, however their expressions differ slightly. Moreover, as one of the majors' contributors of inflammation, CYP-mediated ArA metabolites physiological balance and the RAS components are disturbed by the inflammation, resulting in the augmentation of pro-inflammatory arms of both pathways. ArA metabolites has been shown to yield potent pathological components that induce inflammation. Our approach of using Ang-(1-7) and its long-acting bone targeting conjugate reversed such an effect and promoted anti-inflammatory effect in the AA animal model (200). These results suggest that treatment of Ang. Conj. resembles treatment with ACEIs and ARBs and reduces the pro-

inflammatory effects of Ang II in various tissues in order to treat arthritic, renal, cardiovascular, pulmonary, and hepatic disorders. A head-to-head comparative research is necessary for confirming these results.

5.7 Conclusions

In conclusion, the results of the *in vivo* study of RA study suggest that at the plasma and tissue levels, inflammation alters the equilibrium of the RAS components, such as enzymes, peptides, and receptors. Exogenous administration of Ang-(1-7) and Ang. Conj. corrects the imbalances in the activated RAS caused by inflammation. The superior Ang. Conj. protective benefits that have been seen in in different tissue imply that the bone-targeted delivery of Ang-(1-7) improves its efficacy and can be a valuable therapeutic option for inflammatory diseases such as RA, renal, cardiovascular, pulmonary, and hepatic diseases. The physiological balance of CYP-mediated ArA metabolites and the RAS components are disturbed by the inflammation, resulting in the augmentation of pro-inflammatory arms of both pathways. Our approach of using Ang-(1-7) and its long-acting bone targeting conjugate reversed such an effect and promoted anti-inflammatory effect in the AA animal model.

6 Chapter VI: *In vitro* and *In vivo*

Pharmacodynamics of Ang. Conj. in Cancer

6.1 Background

6.1.1 The RAS and Cancer

Years after the discovery of the RAS, several researchers helped us to better understand the regulatory mechanisms of each of its components and their effect in cancer initiation, progression, and inhibition (141). Thus, research into the role of the RAS has gained attention as a result of observed dysregulation of the RAS in several types of cancers (201, 202). Interestingly, these observations were more confirmed when patients receiving ACEIs showed a reduced risk of developing certain cancers, suggesting the attribution of the RAS antagonism to the anti-cancer effect (202, 203). Cancers' development and spread in the body are caused by an interruption of the physiological systems influencing cell growth, migration and death. In addition, inflammation and the expansion of vascular networks are frequently seen. The RAS components expression and actions has shown to be influential in malignancy. This hypothesis is additionally analyzed by testing the RAS inhibitors (used to treat hypertension and cardiovascular disease) and their actions in augmenting cancer therapies. All these indicate RAS involvement and potential in cancer initiation and progression. As a result, comprehending the cellular actions of this system is needed (201). In what follows the role of different components of the RAS in cancer initiation, progression, and inhibition will be discussed in more details.

As an enzyme that converts Ang I to Ang II, ACE1 is present in endothelial cells types, such as lung capillaries and kidney epithelial cells (204). It is an important blood pressure, angiogenesis, and inflammation regulator and its expression in microvessels endothelium surrounding the tumor area, is inferred as its role in tumor angiogenesis (205-207). As an example, reports have shown the overexpression of the ACE1 in infantile hemangioma (the most common infancy tumor). Furthermore, different ACE1 alleles have shown different levels of activity, in a way that people with low ACE1 activity have a cancer-protective effect, and those with highly active ACE1 have higher incidence of cancer (11, 208). Accumulating evidence also shows that ACEIs, such as perindopril and captopril reduce tumor growth, metastasis, and angiogenesis in colorectal cancer and lung (202).

As a receptor for the Ang II peptide substrate, AT1R is primarily involved in regulating the blood pressure as a result of stimulating the release of vasopressin, reabsorption of water and sodium, fibrosis, cellular growth, migration (202, 209). AT1R is well-documented for its link with cancer, with a 20% overexpression in breast cancer and transition from benign to malignant tumors in the development of breast, ovarian, and gastric cancers (201, 202). AT1R overexpression in ovarian and cervical cancer is a sign of tumor invasiveness and blocking the AT1R action by ARBs is shown to be linked to lower occurrence of metastasis, reduction in tumor vascularization, and reduction in tumor size (210). AT1R releases more VEGF which can act on the tumor microenvironment by preventing immune cell infiltration which explains the low survival and great progression of the cancer (210).

AT2R is another receptor for Ang II which opposes its effects through AT1R (209). However, its expression does not seem to be very high especially in adulthood compared to AT1R (211). AT2R is found to counteract the effects of AT1R in cancer and cardiovascular implications. In one study, as a result of AT2R deficiency, the AT1R-mediated VEGF upregulation was higher in response to the Ang II, suggesting an inhibitory role for the actions of AT2R (202). The protective role of the AT2R was studied in a AT2R-functional transplanted pancreatic ductal mouse model that shows a lower degree of tumor vasculature compared to the non-functional AT2R ones (212).

6.1.2 Synovial Sarcoma (SS)

SS is a rare soft tissue sarcoma of uncertain differentiation that is caused by a translocation between SS18 and SSX 1, 2, 4 chromosomes. Although it can affect any age, it is mostly common in young adults between ages of 15 and 30 and every year about 800 to 1000 cases are diagnosed with SS in the United States and more commonly in males (213).

It was first found in the right knee of a 46-year-old man which was a combination of connective and epithelial tissue neoplasia. It is a deep-seated mass with or without local pain and tenderness with some patients suffering from limitation of movement. SS diameter is typically 3-10 cm and it irregularly penetrates to the adjacent soft tissue such as tendon (214). These lesions can occur anywhere and most of them occur in the extremities and especially lower limbs. Despite some large and fast-growing tumor, the majority of SSs are slow-growing and the average duration of signs and symptoms is approximately two years before diagnosis (215). SS requires a biopsy and pathological evaluation for defining the subtypes and tumor grade (216).

There are different approaches for the treatment of SS. First and the mainstay treatment is the **surgical excision** previously treated with amputation; however, cross-sectional imaging and adjuvant therapies advancements made it possible for many patients to circumvent the amputation in the surgery. Depending on the tumor margins and placement, radiotherapy may be needed to decrease the recurrence risk, locally (217). However, amputation is still considered in patients that a major structure of the functional bone is involved (218).

For the larger tumors, **radiotherapy** is recommended and shown to be effective and has local control improvement and overall survival benefit (216). Due to its postoperative complications such as fibrosis and joint stiffness, intensity-modulated radiation therapy was introduced to decrease the postoperative complications. This approach is used especially in with several medical comorbidities and metastatic cases in which the surgery risks are more than its benefit (219).

Chemotherapy has still some controversy despite the SS chemosensitive nature. Ifosfamide and doxorubicin are the most common agents used as adjuvant therapy in palliative care and high-risk adult and children cases (220).

Immunotherapy is an approach based on the fact that greater number of cancer antigens correlates to a better response and because of a low risk-reward ratio of immunotherapy in other cancers, they were tested for SS, as well. The first drug to be used with not promising results was ipilimumab (a cytotoxic T-lymphocyte-associate protein 4 inhibitor) (221). With more recognizing the immune system involvement in SS, NY-ESO-01 was found to be a uniquely-expressed antigen in SS more than 80% available in the cancer cells (222). The studies on using this antigen as a target to treat

the SS is still on-going and showing some promising results in different phases of clinical trials (223).

6.1.3 Osteosarcoma (OS)

OS is a form of malignant bone tumor in children and young adults accounting for 1% of all cancer diagnosis and 5-10% malignancies of the children and youth age group. U-2 OS and MNNG-HOS are considered OS cells lines that the RAS pathway was studied for their treatment. In a recent study by Lassig et al. it was found that knocking down the Ang-(1-7) receptor, MasR, using small interfering RNA, both U-2 OS and MNNG-HOS cell proliferation increases. They showed that a possible mechanism for this is through the canonical transient receptor potential channels expression which is regulated by the MasR and its ligands, such as Ang-(1-7) and almandine (224). As a result, direct and signaling pathway-specific therapeutic targeting of the canonical transient receptor potential channels may serve as an option for OS treatment improvement. In another study by Ding et al. Elemene, a natural compound extracted from a medicinal Chinese herb, *Rhizomazedoariae*, was tested *in vitro* on MG-63 and U-2 OS cell lines and *in vivo* on the MG-63 and U-2 OS-injected mice to show a potential involvement of the RAS. Based on their finding, Ang II and ACE1 were downregulated and the weight and volume of both xenograft tumors were reduced, following the elemene-therapy (225). The role of the RAS protective arm was studied on U-2 OS and MNNG-HOS cells to demonstrate the possible function and expression of the RAS protective axis. All the essential components of the RAS, including Ang-(1-7), ACE2, and MasR are expressed in both cell lines and their activation compromised the cell growth and migration. Moreover, measuring the pro-inflammatory cytokines involved in the RAS axes

modulation, particularly the protective arm demonstrating the RAS involvement in the tumor progression, growth, and metastasis (226).

6.1.4 Breast Cancer

Breast cancer is one of the leading causes of death and the second deadliest cancer in women worldwide. Statistics show that one out of eight women will develop breast cancer at some point in her life in the United States. Thus, looking for therapies which can effectively address this challenge is very crucial (227).

Some risk factors associated with the breast cancer are pregnancy at ages over 30, second and so forth pregnancies (228), age, reproductive, genetic, and epigenetic factors (229). Breast cancers with hormone receptor-positive represent 80% of all breast cancers which means that breast cancer cells express hormone receptors and the presence of estrogen (ER) or progesterone (PR) causes them to grow (230). ER and PR positive cancers are responsive to hormonal therapies, such as aromatase inhibitors, and tamoxifen in comparison with the hormone receptor-negative types (231). Roughly 20% of total breast cancers are human epidermal growth factor receptor 2 positive (HER2+) which metastasize early and grow rapidly (232). Another type of breast cancer which is a very aggressive subtype compared to others is triple negative breast tumors (ER-, PR-, HER2-) (233).

In recent years, the RAS has gained a significant importance due to its connection to different types of cancer, including breast cancer. The RAS imbalance linked to several malignancies has been shown in different animal and clinical studies (234). This is supported by showing evidences of cancer growth, metastasis, and angiogenesis inhibitions when the classical arm of the RAS is downregulated, and ACEIs, or ARBs

are used (201). Accumulating data suggests ACEIs or ARBs are plausible treatments candidates for cancer (235).

The expression of the RAS components in normal and cancerous breast tissue, suggests an important role of this system in development of breast cancer (236).

Moreover, breast cancer is seen in obese patients and the RAS imbalance is highly linked to weight gain (237). Ang II is a key components in dysregulation of metabolic processes by altering insulin signaling, cellular stress, and inflammatory pathways (238). These dysregulations have a great impact on tumor microenvironment and breast tumor cells are negatively impacted by the pro-inflammatory adipocytokines which are one of the most important hallmarks of breast cancer (239) and create an ideal breast tumor microenvironment. Accumulating data demonstrate the involvement of the RAS, especially Ang II overexpression in a detrimental manner in breast cancers (240).

Studies conducted in the past few decades have shown the overexpression of ACE, Ang II, AT1R in three different types of cancer cell lines (MDA-MB-231, MCF-7, and T-47D) compared to the normal breast cells (PCS-600 cells) in which the protective arm (Ang-(1-7), ACE2, and MasR) was predominantly activated. Additionally, they have found a lower level of Ang-(1-7) production in all cancer cell lines compared to normal breast cells (241). Arrieta et al. found a higher AT1R expression in seventy-seven surgically resected malignant breast tumors compared to benign lesions as control while they observed no differences in AT2R expression level. They also showed that a higher AT1R level was related to increased angiogenesis in breast cancer compared to the control (242). Therefore, a potential mechanism that the RAS is involved in breast cancer pathogenesis is through AT1R. Interestingly, an increased in AT1R expression

was shown in the study of Rhodes et al. (243) and Egami et al. showed that AT1R is associated with angiogenesis, tumor growth, and inflammation induction (244).

On the other hand, the components of the protective arm of the RAS have shown to be positively effective in the breast cancer. AT2R shows opposite functions in comparison to AT1R through reducing tumor progression and proliferation by activating tumor suppressor gene (245, 246) and reducing cancer cell migration by targeting AKT phosphorylation in human endothelial cells (247). Overall AT2R demonstrated a tumor suppressor effect and a potential target for cancer prevention (248). Ang-(1-7) though the activation of MasR provides a protective function against breast cancer progression. Rodgers et al. showed that 100 µg/kg Ang-(1-7) administration daily can attenuate the frequency of breast cancer therapy associated side effects in breast cancer patients (123). Moreover, Ang-(1-7) is reduced in breast cancer patients (241) and the protective arm of the RAS component downregulation causes metastasis (249).

In conclusion, breast cancer association with the activated RAS is shown in several studies and it is confirmed by use of RAS inhibitors and other therapies as options for breast cancer. Results indicate that inhibiting the Ang II-AT1R axis, with or without stimulating the Ang-(1-7)-MasR axis may help control cancer progression. Specifically, these approaches have shown to improve efficacy of chemotherapy, immunotherapy, and radiotherapy in animal models (250-252).

6.2 Rationale

Upon successful improvements in pharmacokinetic parameters, Ang. Conj. was designed to be tested *in vitro* first for ethical reasons. *In vitro* studies allow a substance to be studied safely before subjecting humans or animals to the possible side effects or

toxicity of a new drug. Efficacy and toxicity potentials can be learned from *in vitro* studies and the results can be used for moving forward to *in vivo*.

6.3 Hypotheses and Objectives

We hypothesized that Ang. Conj. due to its higher half-life can decrease the cancer cell proliferation in SS, OS, and breast cancer cell lines compared to vehicle and the native peptide. In current work we aimed at studying pharmacodynamic effects of Ang-(1-7) and its conjugate on cell proliferation in SS, OS, and breast cancer cell lines.

We speculated that Ang. Conj. due to its longer half-life can inhibit the tumor growth and decrease the tumor size compared to the vehicle in mice model of SS. Moreover, we hypothesized that the RAS components are affected by the cancer proliferation and treatment with Ang. Conj. could revert such imbalance at mRNA and protein levels. This study was performed to compare the efficacy of Ang-(1-7) and Ang. Conj. administration in SS-bearing mice model with vehicle on tumor size and to measure the RAS components at gene and protein level in tumor tissue.

6.4 Experimental Methods and Materials

6.4.1 Cancer Cell Lines and Culture Media

The *in vitro* efficacy of the Ang. Conj. compared to the native peptide was tested on different cancer cell lines. The cell lines tested were SS and OS plus breast cancer cells. Cells were purchased from American Type Culture Collection (ATCC, Manassas, VA, USA).

Sterile-filtered Dulbecco's modified Eagle Medium (DMEM), high glucose was purchased from Sigma Aldrich (Sigma Aldrich, St. Louis, MO, USA). It contained 4500 mg/L glucose, L-glutamine, and sodium bicarbonate, without sodium pyruvate. Penicillin/streptomycin antibiotics (Atlanta biologicals, Flowery Branch, GA, USA) and fetal bovine serum (Neuromics, Edina, MN, USA) were added at the final concentration of 1% (50 units) and 10% of the culture medium, respectively. DMEM was used for 4T1.2 and U2-OS cells.

Roswell Park Memorial Institute (RPMI) 1640 medium containing no phenol red was purchased from Fisher Scientific (Waltham, MA, USA). Concentration of the antibiotics and fetal bovine serum was the same for the RPMI 1640 medium. RPMI medium was used for T47D and SJSA-1 cells.

Cells were cultured in their corresponding culture medium and kept in an incubator equipped with 5% carbon dioxide at 37 °C and were passaged or collected for further assays when they were reaching about 80% confluency. For this purpose, culture media and trypsin-EDTA 0.25% solution containing 2.5 gr porcine trypsin and 0.2 gr EDTA with phenol red (Sigma Aldrich, St. Louis, MO, USA). Cells were removed from the incubator and their medium was removed. They were washed once with 5 mL PBS, and 2 mL trypsin-EDTA (used to detach the adherent cells from the surface) was added to the tissue culture flask containing the cells. Then, after cells were transferred to the incubator for 3 minutes, they were checked under the microscope for detachment and transferred to a sterile plastic tube. They were then centrifuged at 2000 ×rpm for 4 minutes to remove the trypsin-EDTA. Then, cells were reconstituted in the corresponding medium to achieve the desired concentration and prepared for further

analysis. All procedures were done under a BSL-2 biosafety hood to avoid any contamination of the cells' environments.

6.4.2 MTT Cell Viability Assay

The 3-(4,5-dimethylthiazol-2-yl)-2,5-diphenyl-2H-tetrazolium bromide (MTT) cell viability assay is based on the NAD(P)H-dependent cellular oxidoreductase enzymes ability in viable cells to convert the soluble substrate MTT into insoluble formazan crystals. After solubilization of crystals, the resulting purple formazan is used for quantification by spectrophotometry. Each well is normalized proportionally to the number of viable cells. Cells were first seeded in each well at the concentration of 10,000 cells/well, and incubated for 24 hours. For each treatment arm (Ang-(1-7) and Ang. Conj.), concentration of 10 μ M was tested. After 72 hours of incubation, cells were subjected to a quick wash with PBS, followed by addition of MTT substrate (10 μ L of 500 μ g/mL) diluted in the cell medium, and then the cells were maintained for 3 hours in a CO₂ incubator at 37 °C. After the incubation period, 100 μ L solution of isopropanol/HCl (solubilizing reagent) was added and the samples were agitated for 30 minutes on a horizontal shaker to promote the elution of the formazan crystals. The supernatant was quantified by measuring the absorbance values at 590 nm and 650 nm filter in VarioscanLux™ microplate reader (Thermofisher Scientific, Waltham, MA, USA). All experiments were performed in triplicate (253).

6.4.3 RealTimeGlo™ MT Cell Viability Assay

Studying the real time cell viability of the breast cancer cell lines was done using the RealTimeGlo™ MT Cell Viability Assay kit (Promega, Madison, WI). This assay is a

nonlytic, homogenous bioluminescent method. It determines the number of viable cells and thus metabolism (MT). The assay involves adding NanoLuc® luciferase and a cell-permeant pro-substrate, the MT Cell Viability Substrate, to cells in culture. This substrate diffuses from cells into the surrounding culture medium where it is rapidly used by the NanoLuc® Enzyme to produce a luminescent signal which correlates with the number of viable cells. Both the MT Cell Viability Substrate and NanoLuc® Enzyme are stable in complete cell culture medium at 37 °C for at least 72 hours. The assay can be performed in two formats: continuous-read measurement or endpoint measurement. We performed the assay for breast cancer cell lines in continuous-read measurement format. When the assay is set up in the continuous-read format, the RealTime-Glo™ reagents (i.e., MT Cell Viability Substrate and NanoLuc® Enzyme) can be added to the wells at the same time as the cells or test compound or at any point during the assay to start obtaining viability measurements. The reagents were made fresh each time before each experiment and the cell suspension, test compound diluent, and cell culture medium were equilibrated to 37 °C, in advance. For the continuous-read method, the substrate and enzyme should be added to cell culture medium to prepare a 1X dilution. The assay linearity should be determined with regard to a range of cell densities before the test to determine the varying capacities of cells to reduce the MT Cell Viability Substrate. The assay linearity was done for 4T1.2, MCF-7, and T47D breast cancer cell lines, and the best cell density was determined for each of those.

For performing the assay, reagents were equilibrated in 37 °C along with the media and cells. Cell suspensions were prepared in the corresponding cell culture media and the alive cell concentrations were determined using the 10 µL trypan blue and 10 µL cell

suspension. To prepare 1 mL of 2X concentration of RealTime-Glo™ reagents, 2 µL of MT Cell Viability Substrate, 1000X, and 2µl of NanoLuc® Enzyme, 1000X, were added to 996 µL of cell culture medium. If more amounts were needed, the calculations were done based on the needed volumes and number of the wells. An equal volume of the 2X RealTime-Glo™ reagent was added to the cells (that were made in the desired concentration determined based on the linearity assay). For example, if cells are plated in 40 µL, then add 40 µL of 2X RealTime-Glo™ reagent to the cells at the same time. Cells were incubated in a cell culture incubator at 37 °C and 5% CO₂ for 1 hour. Then, the test compounds (Ang-(1-7) and Ang. Conj.) were prepared in PBS in different concentrations in a way that their final concentrations in each well be 1 or 10 µM for each compound. The test compounds were added for 10 µL. The luminescence was determined in different time points using a plate-reading luminometer until 72 hours. All samples were done in triplicates.

6.4.4 Dose Calculation

In case of *in vivo* pharmacodynamic studies 0.6 mg/kg or an equivalent dose of Ang. Conj. was administered s.c. every other day. In this study, all doses were weight-normalized and equivalent to their average therapeutic recommended dose for cancer diseases.

6.4.5 Sample Collection

For the SS study, after 21 days of treatment, mice were euthanized with carbon dioxide and spine dislocation method using the Idaho State University Animal Facility protocol. The tumors were localized in the joint area, and they were cut precisely by removing the

skin. They were sectioned in 1.7 mL Eppendorf tubes for Western blot, and qPCR. They were then snap-frozen in liquid nitrogen and kept at -80 °C.

6.4.6 Statistical Analysis

The results of the MTT cell viability assay were reported as mean \pm SD by comparing the OD of the Ang-(1-7) and Ang. Conj.-treated groups with the buffer-treated cells. Then the viability percentage was calculated compared to time 0. The mean values obtained for each group is compared with mean of other group using one-way ANOVA followed by Bonferroni adjustment.

6.5 Results

6.5.1 Cell Proliferation Assay of SS and OS Cell Lines

The result of the single administration of either vehicle, Ang-(1-7) 10 μ M, or Ang. Conj. equivalent dose of Ang-(1-7) is shown in Fig. 20. After 72 hours of single administration of vehicle or test compounds, cells were treated with MTT to compare their proliferation percentage to day 0. Both OS and SS cell lines showed a greater anti-proliferation effect when treated with Ang. Conj. compared to control and Ang-(1-7). SJSA-1 and HSSY-1 cell viability percentage results were normalized to the control and Ang. Conj. ($80.9 \pm 4.3\%$) significantly reduced the cell viability compared to Ang-(1-7) ($97.9 \pm 4.9\%$) and control. The same trend was seen on HSSY-1 cells where Ang. Conj.-treated ($73.6 \pm 3.2\%$) cell proliferation was significantly different from Ang-(1-7) ($97.9 \pm 3.9\%$) (Fig. 20).

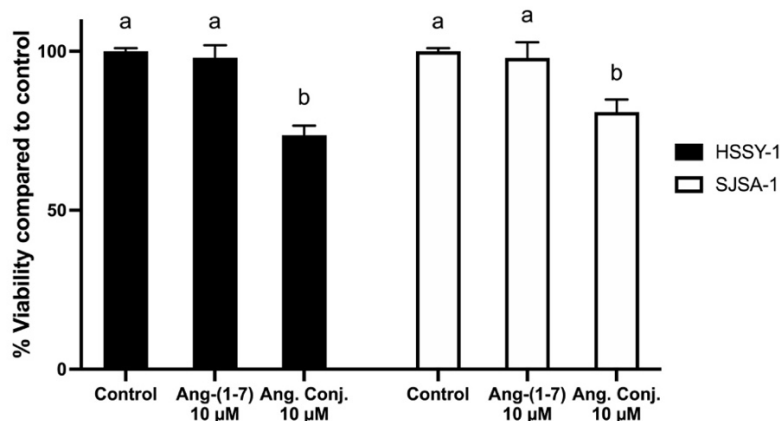


Figure 20. Effect of Ang. Conj. treatment on HSSY-1 and SJSA-1 cancer cells proliferation after 72 hours of a single administration of vehicle, Ang-(1-7) 10 µM, or Ang. Conj. 10 µM.

6.5.2 RealTime MT Assay on Breast Cancer Cell Lines

Three breast cancer cell lines (4T1.2, T47D, and MCF7) were used for studying the RealTime effect of vehicle, and Ang-(1-7), and the results were compared with Ang. Conj. and presented in Fig. 21. Absorbances were taken at different time points of 0, 6, 24, 48, and 72 hours and the results are normalized to the control and then highest absorbance. In 4T1.2 cell line, 48 hours after a single administration of vehicle, Ang-(1-7), or Ang. Conj., Ang. Conj.-treated cell viability ($53.3 \pm 10.1\%$) was significantly reduced compared to the vehicle ($97.0 \pm 1.6\%$), and Ang-(1-7)-treated cells ($83.0 \pm 3.4\%$) (Fig. 21A). This cell proliferation inhibition continued to 72 hours. In T47D cells, after 72 hr, Ang. Conj. significantly reduced the cell proliferation ($53.2 \pm 8.7\%$) compared to Ang-(1-7) ($85.2 \pm 8.8\%$) and control ($94.4 \pm 3.2\%$) (Fig. 21B). Fig. 21C shows a similar trend in MCF7 cell line to T47D except Ang. Conj. treatment ($58.3 \pm 15.6\%$) was only significantly different from vehicle ($81.5 \pm 9.6\%$) in cell viability percentage.

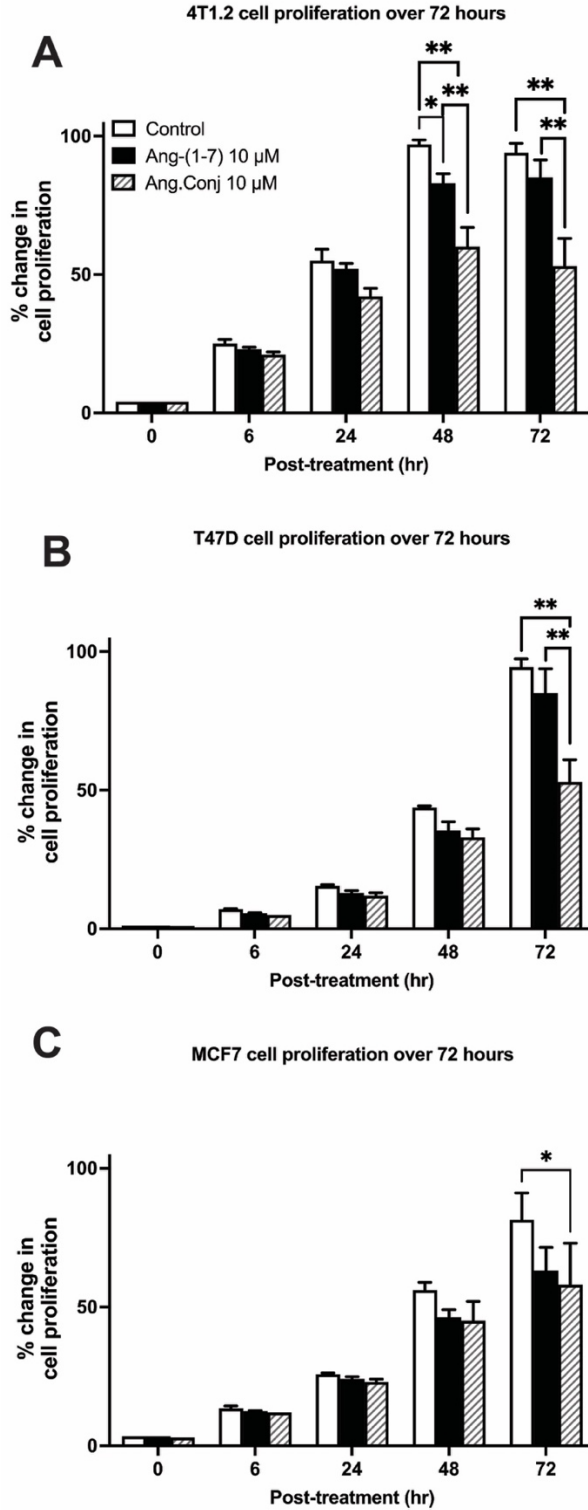


Figure 21. Cell proliferation in 4T1.2 (A), T47D (B), and MCF7 (C) breast cancer cell lines after 72 hours of a single administration of vehicle, Ang-(1-7) 10 μM, or Ang. Conj 10 μM. Results are reported as mean ± SEM. * Significant different with $p < 0.05$.

6.5.3 Tumor Size Change in SS-bearing Mice

Fig. 22 presents the tumor size increase in control mice bearing tumor treated with vehicle, Ang-(1-7), and Ang. Conj. Tumor size increased in control group and decreased in both Ang-(1-7) and Ang. Conj.-treated groups as shown in Fig. 22.

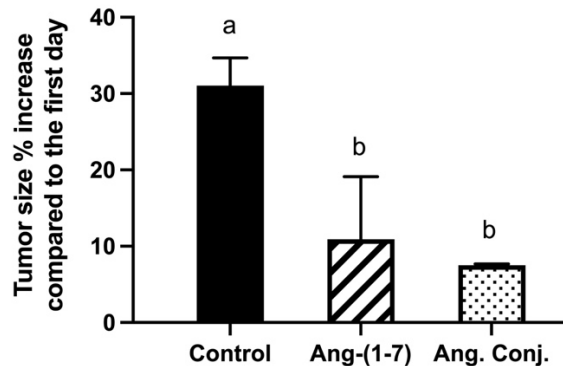


Figure 22. Effect of vehicle, Ang-(1-7), and Ang. Conj. treatment on percentage tumor size change compared to day one in SS-bearing mice. Different letters show significant difference between groups. Data are presented as relative to the value of control (mean \pm SD), * $p < 0.05$.

6.5.4 The RAS Gene Expression in Tumor Tissue from SS-bearing Mice

Fig. 23 presents the significant increase of ACE2 gene expression after Ang-(1-7) and Ang. Conj. treatments. Ang. Conj. increased MasR expression but it was not significantly different from other groups. There was also a nonsignificant trend on AT1R gene expression reduction due to treatment as well.

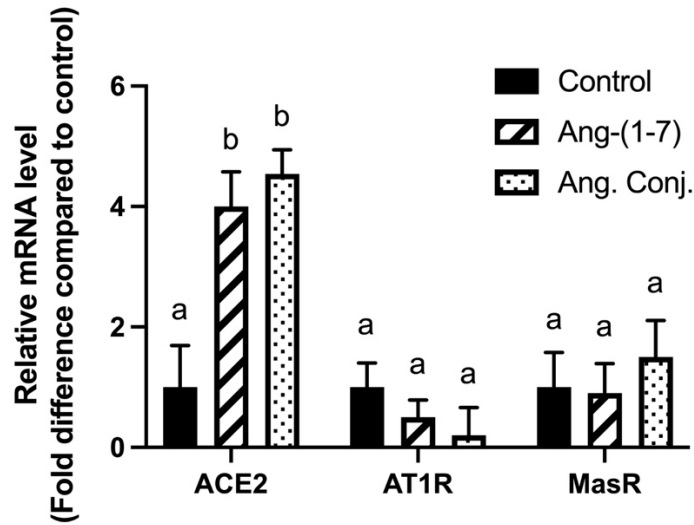


Figure 23. Effects of vehicle, Ang-(1-7) and Ang. Conj. treatment on the RAS components gene expression in tumor tissue from SS-bearing mice. Different letters show significant difference between groups. Data are presented as relative to the value of control (mean \pm SD), $p < 0.05$.

6.5.5 The RAS and Apoptosis Marker Protein Expression in Tumor Tissue from SS-bearing Mice

Fig. 24 presents the significant effect of Ang. Conj. and Ang-(1-7) on increasing of ACE2 and caspase-3 protein expression when they were compared with control group.

The AT1R expression was not impacted by Ang-(1-7), but significantly reduced after Ang. Conj. treatment. Such effects were significantly different when Ang. Conj. and Ang-(1-7) groups were compared.

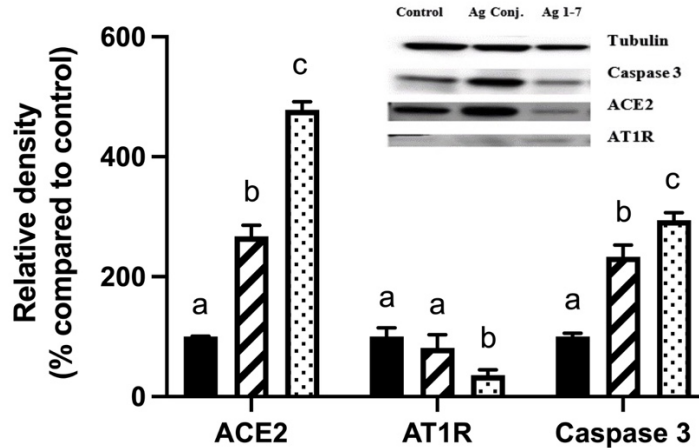


Figure 24. Effect of vehicle, Ang. Conj. and Ang-(1-7) on the RAS and apoptosis maker protein expression in tumor tissue from SS-bearing mice. Different letters show significant difference between groups. Data are presented as relative to the value of control (mean \pm SD), * $p < 0.05$.

6.6 Discussion

Ang II is the major effector peptide of the classical RAS axis which is best known for its role in systemic volume homeostasis and blood pressure control. Ang II affects important processes, including proliferation, apoptosis, fibrosis and inflammation (11). Having a strong angiogenic activity (254), the classical arm has also been implicated in tumorigenesis (11), induction of proangiogenic factors (255), and platelet-derived growth factor (PDGF) (256). Invasion and angiogenesis are correlated to AT1R expression levels in ovarian carcinoma (257). Accordingly, ACEIs have shown to suppress the growth and angiogenic activity of head and neck carcinoma (258). In another study in a mouse model of colorectal carcinoma, AT1R blockade and ACEIs reduced liver metastasis and angiogenesis (259). Early gastric cancer has also been linked to the ACE insertion/deletion polymorphism (ACE I/D) (260), and increased lymph node metastasis (261). An independent risk factor for nodal spread in gastric cancer is the AT1R expression status and ACE I/D (262). For OS, a recent study

showed a decrease in tumor growth and lung and liver metastasis by using an AT1R antagonist, CV11974, in a mice model of OS (263). On the other hand reinforcing the protective arm of the RAS has shown to be a treatment option in many cancer types (200). It was shown that in U2 OS and MNNG-HOS cells which are considered OS cell lines, express a functional protective arm axis that its induction exerts beneficial effects towards OS treatment by preventing cancer metastasis (226). In breast cancer, it is reported that Ang-(1-7) production in is attenuated and classical arm components are produced more (241). Studies indicated the beneficial role of ACE2 in breast cancer angiogenesis inhibition, where the ACE2 level is significantly lower in cancer tissue than in normal breast tissue (264). Ang-(1-7) has been shown to limit the migration and invasion of lung carcinoma cells and lung cancer, in contrast to the tumor-promoting effect of Ang II/ AT1R described before (200, 265). The *in vitro* cancer cell study was performed to determine the cell proliferation and potential functional significance of the ACE2/ Ang-(1-7)/ MasR pathway of the RAS in OS, SS (Fig. 20), and breast cancer cell lines. The results of this study show that SJSA-1 (OS), HSSY-1 (SS), 4T1.2, T47D, and MCF7 (breast cancer) cell lines' proliferation is decreased by the Ang-(1-7) and to a greater extent by its bone-targeted delivery. Similar results were reported when ACE2 was overexpressed (266, 267). At 72 hours, all three cell lines showed a significantly less proliferation in Ang. Conj.-treated group compared to control. Ang-(1-7) was not capable of exerting such action (Fig. 21). This can be attributed to the longer half-life of Ang. Conj. Considering the lack of target (bone) for binding of bone-seeking moiety of Ang. Conj., the enhanced observed efficacy compared with native Ang-(1-7) can be attributed to its improved stability and sustained release of native peptide.

The cancer study of *in vivo* results using a mice model of SS indicates that Ang. Conj. has better stability and efficacy than native peptide on suppressing the cancer progression which is presented as reducing the tumor size (Fig. 22). This effect could be attributed to switching the balance between two arms of the RAS in favor of protective arm which are anti-proliferation, anti-angiogenesis, vasodilation and anti-inflammation effects (Fig. 23). This switch in balance was done by increasing the ACE2 and decreasing of AT1R gene and protein expression due to Ang. Conj. treatment. Additionally, overexpression of caspase-3 protein as an apoptosis marker is correlated with reduction in tumor size (Fig. 23). The observed milder effects after treatment with Ang-(1-7) in comparison with Ang. Conj. could be attributed to different half-life and stability of these compounds. The improved stability through conjugation of Ang-(1-7) resulted in a profound anti-proliferation and anti-cancer action of Ang. Conj.

6.7 Conclusions

OS and SS cell lines express critical components of classical and alternative RAS axes. The activation of the ACE2/ Ang-(1-7)/ MasR axis inhibited cancer cell proliferation, and so may constitute a viable treatment strategy. In conclusion, Ang-(1-7) is known to exert its therapeutic effects, including anti-proliferative action, through binding to the MasR. So, the observed anti-proliferative effects can be explained by the ability of Ang. Conj. to boost the gene expression of the ACE2 enzyme, which is responsible for the conversion of Ang II to Ang-(1-7), as well as the expression of the MasR. Studying the effect of Ang. Conj. on SS, and breast cancer cell lines, showed that this compound is capable of inhibiting the proliferation of certain cancer cell lines. Moving to the *in vivo* study using a mice model of SS, the results reveal that Ang. Conj. has more stability

and efficacy than native peptide in inhibiting the progression of cancer, as seen by a considerable reduction in tumor size. This effect may be due to a shift in the balance between the two arms of the RAS in favor of the protective arm, which includes anti-proliferation, anti-angiogenesis, vasodilation, and anti-inflammatory actions. This was shown at cellular level, as well. The difference in half-life and stability between Ang-(1-7) and Ang. Conj. may account for the milder effects found after treatment with Ang-(1-7) versus Ang. Conj. In conclusion, Ang. Conj. exhibited a potent anti-proliferative and anti-cancer effect as a result of Ang-(1-7) conjugation's enhanced stability.

7 Summary

7.1 General Conclusions

The RAS regulates multiple tissues' and organs' functions by maintaining blood pressure, and electrolyte homeostasis (268). RAS is a great contributor to vascular, cardiac, renal, liver, reproductive, and musculoskeletal system physiology and some its pathophysiological effects include inflammation and fibrosis that link the RAS to the initiation, development, and progression of several diseases (269).

The RAS has two arms: the classical arm containing ACE1/Ang II /AT1R and the protective arm composed of ACE2 /Ang-(1-7) /MasR (Figure 1). In healthy individuals, these two arms are in a dynamic balance (12). Ang II is the RAS major vasoactive effector peptide and is produced mainly through enzymatic actions of ACE1 in plasma and various tissues (14). The resulting effects include vasoconstriction, cardiac hypertrophy and remodeling, inflammation, and fibrosis (15). Ang II is additionally associated with the initiation, proliferation, and metastasis of several cancers (16-18). Formation of Ang II from Ang I has been considered the final product of the RAS for a long time. However, recent studies have shown that there are other Ang peptides in the RAS that oppose the actions of Ang II (24). ACE2 acts as a major enzyme involved in the conversion of Ang II to Ang-(1-7). Thus, ACE2 effectively inhibits Ang II formation by stimulating alternate pathways for Ang I and, particularly, Ang II degradation (27). MasR, a specific receptor of Ang-(1-7), is a member of G protein-coupled receptors (GPCRs) family (26).

The RAS is considered an interesting therapeutic target and has been studied for several decades. Accumulating evidence proves that Ang-(1-7), the main peptide of the protective arm, counteracts the actions of Ang II (270). Due to Ang-(1-7)'s rapid systemic clearance, its short half-life (3-15min) restricts its potential therapeutic benefits. In this work a structurally-modified bone drug delivery system was proposed to extend the peptide circulation half-life.

The bone targeted delivery of Ang-(1-7) was successfully characterized and its *in vitro* stability and bone binding capacity were determined. The pharmacokinetic parameters of the Ang. Conj. was done after i.v. and s.c. bolus administration and compared with i.v. Ang-(1-7). A longer half-life was achieved. Due to a longer half-life, we tested the efficacy of Ang. Conj. with Ang-(1-7) in *in vivo* model of RA and *in vitro* and *in vivo* models of breast cancer, SS, and OS.

The results of this study show that Ang. Conj. modulates both RAS and ArA pathway and regulate the detrimental effects of inflammation imposed on these systems. Based on these findings, GlcN with an optimal safety profile and positive effects on RAS and ArA pathway on higher doses could be considered as an alternative for the NSAIDs in treatment of inflammatory conditions such as RA.

7.2 Future Directions

For validation of observed effects of Ang. Conj. in reducing inflammation, *in vivo* studies using different animal models of inflammatory diseases could be conducted with histological evaluation of different pro- and anti-inflammatory cytokines in several tissues, including joints.

The next step in introducing Ang. Conj. as a therapeutic agent would be to test it in pre-clinical species such as non-human primates and study its pharmacokinetics and pharmacodynamics. In order to address the Ang. Conj. effectiveness, a clinical trial in patient population with moderate to severe RA could be helpful.

7.3 Strength and Limitations

Conjugating the short-lived therapeutic molecules to a BP moiety is a unique method for improving the stability, pharmacokinetics, and accumulation in bone tissue for peptides such as Ang-(1-7). This strategy has the potential to provide a reliable therapy option for a variety of clinical disorders linked to the active classical arm of the RAS. The most significant weakness of the pharmacokinetic study is the feasibility of detecting Ang. Conj. by LC-MS/MS due to its high ionization state. So, to overcome this issue, we used the Ang-(1-7) released from Ang. Conj. as a surrogate compound to define the Ang. Conj. release profile and Ang-(1-7) pharmacokinetic parameters after administration of Ang. Conj.

Human pilot study present with several limitations. Although statistical significance was demonstrated for nearly all associations, clustered data rather than correlation was reported for CRP. Its interpretation should be approached with caution. In addition, if the sample size was greater and more persons with RA participated in the study, the results would be more robust and persuasive. Incorporating additional disease index scores could also strengthen the association between RAS biomarkers and the CRP and RAPID3 indices.

8 References

1. Reid IA, Morris BJ, Ganong WF. The renin-angiotensin system. Annual review of physiology. 1978;40(1):377-410.
2. Unger T. The role of the renin-angiotensin system in the development of cardiovascular disease. The American journal of cardiology. 2002;89(2):3-9.
3. Johnston CI. Biochemistry and pharmacology of the renin-angiotensin system. Drugs. 1990;39(1):21-31.
4. Skov J, Persson F, Frøkiær J, Christiansen JS. Tissue renin–angiotensin systems: a unifying hypothesis of metabolic disease. Frontiers in endocrinology. 2014;5:23.
5. Karamyan VT, Speth RC. Enzymatic pathways of the brain renin–angiotensin system: unsolved problems and continuing challenges. Regulatory peptides. 2007;143(1):15.
6. Unger T, Badoer E, Ganten D, Lang R, Rettig R. Brain angiotensin: pathways and pharmacology. Circulation. 1988;77(6 Pt 2):140-54.
7. Wu Y, Lu X, Li M, Zeng J, Zeng J, Shen B, et al. Renin-angiotensin system in osteoarthritis: a new potential therapy. International immunopharmacology. 2019;75:105796.
8. Dias-Peixoto MF, Santos RA, Gomes ER, Alves MN, Almeida PW, Greco L, et al. Molecular mechanisms involved in the angiotensin-(1-7)/Mas signaling pathway in cardiomyocytes. Hypertension. 2008;52(3):542-8.

9. Santos RAS, Oudit GY, Verano-Braga T, Canta G, Steckelings UM, Bader M. The renin-angiotensin system: going beyond the classical paradigms. *American Journal of Physiology-Heart and Circulatory Physiology*. 2019.
10. Iwanami J, Mogi M, Tsukuda K, Wang X-L, Nakaoka H, Ohshima K, et al. Role of angiotensin-converting enzyme 2/angiotensin-(1-7)/Mas axis in the hypotensive effect of azilsartan. *Hypertension Research*. 2014;37(7):616-20.
11. Deshayes F, Nahmias C. Angiotensin receptors: a new role in cancer? *Trends in Endocrinology & Metabolism*. 2005;16(7):293-9.
12. South AM, Shaltout HA, Washburn LK, Hendricks AS, Diz DI, Chappell MC. Fetal programming and the angiotensin-(1-7) axis: a review of the experimental and clinical data. *Clinical Science*. 2019;133(1):55-74.
13. Santos RAS, Oudit GY, Verano-Braga T, Canta G, Steckelings UM, Bader M. The renin-angiotensin system: going beyond the classical paradigms. *American Journal of Physiology-Heart and Circulatory Physiology*. 2019;316(5):H958-H70.
14. Turner AJ, Hooper NM. The angiotensin-converting enzyme gene family: genomics and pharmacology. *Trends in pharmacological sciences*. 2002;23(4):177-83.
15. Hahn A, Regenass S, Kern F, Buhler F, Resink T. Expression of soluble and insoluble fibronectin in rat aorta: effects of angiotensin II and endothelin-1. *Biochemical and biophysical research communications*. 1993;192(1):189-97.
16. Penafuerte CA, Gagnon B, Sirois J, Murphy J, MacDonald N, Tremblay ML. Identification of neutrophil-derived proteases and angiotensin II as biomarkers of cancer cachexia. *British journal of cancer*. 2016;114(6):680-7.

17. Pei N, Mao Y, Wan P, Chen X, Li A, Chen H, et al. Angiotensin II type 2 receptor promotes apoptosis and inhibits angiogenesis in bladder cancer. *J Exp Clin Cancer Res*. 2017;36(1):77.
18. Ekambaram P, Lee J-YL, Hubel NE, Hu D, Yerneni S, Campbell PG, et al. The CARMA3–Bcl10–MALT1 Signalosome Drives NFκB Activation and Promotes Aggressiveness in Angiotensin II Receptor–Positive Breast Cancer. *Cancer research*. 2018;78(5):1225-40.
19. Lacolley P, Regnault V, Nicoletti A, Li Z, Michel J-B. The vascular smooth muscle cell in arterial pathology: a cell that can take on multiple roles. *Cardiovascular research*. 2012;95(2):194-204.
20. Kaschina E, Unger T. Prehypertension and the renin-angiotensin-aldosterone system. *Prehypertension and Cardiometabolic Syndrome*: Springer; 2019. p. 307-18.
21. Montezano AC, Touyz RM. Reactive oxygen species, vascular Noxs, and hypertension: focus on translational and clinical research. *Antioxidants & redox signaling*. 2014;20(1):164-82.
22. Wei C-C, Tian B, Perry G, Meng QC, Chen Y-F, Oparil S, et al. Differential ANG II generation in plasma and tissue of mice with decreased expression of the ACE gene. *American Journal of Physiology-Heart and Circulatory Physiology*. 2002;282(6):H2254-H8.
23. Dell'Italia LJ, Collawn JF, Ferrario CM. Multifunctional role of chymase in acute and chronic tissue injury and remodeling. *Circulation research*. 2018;122(2):319-36.
24. Arendse LB, Danser AJ, Poglitsch M, Touyz RM, Burnett JC, Llorens-Cortes C, et al. Novel therapeutic approaches targeting the renin-angiotensin system and

- associated peptides in hypertension and heart failure. *Pharmacological reviews*. 2019;71(4):539-70.
25. Santos RA, Campagnole-Santos MJ, Andrade SIP. Angiotensin-(1–7): an update. *Regulatory Peptides*. 2000;91(1-3):45-62.
26. Solinski HJ, Gudermann T, Breit A. Pharmacology and signaling of MAS-related G protein–coupled receptors. *Pharmacological reviews*. 2014;66(3):570-97.
27. Dong X, Han S-k, Zylka MJ, Simon MI, Anderson DJ. A diverse family of GPCRs expressed in specific subsets of nociceptive sensory neurons. *Cell*. 2001;106(5):619-32.
28. Hashimoto N, Maeshima Y, Satoh M, Odawara M, Sugiyama H, Kashihara N, et al. Overexpression of angiotensin type 2 receptor ameliorates glomerular injury in a mouse remnant kidney model. *American Journal of Physiology-Renal Physiology*. 2004;286(3):F516-F25.
29. Hakam AC, Hussain T. Renal angiotensin II type-2 receptors are upregulated and mediate the candesartan-induced natriuresis/diuresis in obese Zucker rats. *Hypertension*. 2005;45(2):270-5.
30. Nakanishi H, Yamamoto K. Cathepsin E in the central nervous system. *Aspartic Proteinases*: Springer; 1998. p. 213-7.
31. Kageyama T, Ichinose M, Yonezawa S. Processing of the precursors to neurotensin and other bioactive peptides by cathepsin E. *Journal of Biological Chemistry*. 1995;270(32):19135-40.
32. Hackenthal E, Hackenthal R, Hilgenfeldt U. Isorenin, pseudorenin, cathepsin D and renin. A comparative enzymatic study of angiotensin-forming enzymes. *Biochimica et Biophysica Acta (BBA)-Enzymology*. 1978;522(2):574-88.

33. Saavedra JM. Brain and pituitary angiotensin. *Endocrine reviews*. 1992;13(2):329-80.
34. Davies BJ, Pickard BS, Steel M, Morris RG, Lathe R. Serine proteases in rodent hippocampus. *Journal of Biological Chemistry*. 1998;273(36):23004-11.
35. Araujo RC, Lima MP, Lomez ES, Bader M, Pesquero JB, Sumitani M, et al. Tonin expression in the rat brain and tonin-mediated central production of angiotensin II. *Physiology & behavior*. 2002;76(2):327-33.
36. Ramaha A, Patston PA. Release and degradation of angiotensin I and angiotensin II from angiotensinogen by neutrophil serine proteinases. *Archives of biochemistry and biophysics*. 2002;397(1):77-83.
37. Hermann K, Phillips MI, Raizada MK. Metabolism of angiotensin peptides by neuronal and glial cultures from rat brain. *Journal of neurochemistry*. 1989;52(3):863-8.
38. Reaux A, Iturrioz X, Vazeux G, Fournie-Zaluski M-C, David C, Roques B, et al. Aminopeptidase A, which generates one of the main effector peptides of the brain renin-angiotensin system, angiotensin III, has a key role in central control of arterial blood pressure. *Biochemical Society Transactions*. 2000;28(4):435-40.
39. Shivakumar BR, Wang Z, Hammond TG, Harris RC. EP24. 15 interacts with the angiotensin II type I receptor and bradykinin B2 receptor. *Cell Biochemistry and Function: Cellular biochemistry and its modulation by active agents or disease*. 2005;23(3):195-204.
40. DAHMS P, MENTLEIN R. Purification of the main somatostatin-degrading proteases from rat and pig brains, their action on other neuropeptides, and their

identification as endopeptidases 24.15 and 24.16. *European Journal of Biochemistry*. 1992;208(1):145-54.

41. Welches WR, Brosnihan KB, Ferrario CM. A comparison of the properties and enzymatic activities of three angiotensin processing enzymes: angiotensin converting enzyme, prolyl endopeptidase and neutral endopeptidase 24.11. *Life sciences*. 1993;52(18):1461-80.

42. Turner AJ, Tanzawa K. Mammalian membrane metallopeptidases: NEP, ECE, KELL, and Pex. *The FASEB Journal*. 1997;11(5):355-64.

43. Roques BP, Noble F, Dauge V, Fournie-Zaluski M, Beaumont A. Neutral endopeptidase 24.11: structure, inhibition, and experimental and clinical pharmacology. *Pharmacological reviews*. 1993;45(1):87-146.

44. Khajeh Pour S, Scoville C, Tavernier SS, Aghazadeh-Habashi A. Plasma angiotensin peptides as biomarkers of rheumatoid arthritis are correlated with anti-ACE2 auto-antibodies level and disease intensity. *Inflammopharmacology*. 2022:1-8.

45. Giani JF, Mayer MA, Muñoz MC, Silberman EA, Hocht C, Taira CA, et al. Chronic infusion of angiotensin-(1–7) improves insulin resistance and hypertension induced by a high-fructose diet in rats. *American Journal of Physiology-Endocrinology and Metabolism*. 2009;296(2):E262-E71.

46. Giani JF, Burghi V, Veiras LC, Tomat A, Muñoz MC, Cao G, et al. Angiotensin-(1–7) attenuates diabetic nephropathy in Zucker diabetic fatty rats. *American Journal of Physiology-Renal Physiology*. 2012;302(12):F1606-F15.

47. Loot AE, Roks AJ, Henning RH, Tio RA, Suurmeijer AJ, Boomsma F, et al. Angiotensin-(1–7) attenuates the development of heart failure after myocardial infarction in rats. *Circulation*. 2002;105(13):1548-50.
48. Shenoy V, Kwon K-C, Rathinasabapathy A, Lin S, Jin G, Song C, et al. Oral delivery of Angiotensin-converting enzyme 2 and Angiotensin-(1-7) bioencapsulated in plant cells attenuates pulmonary hypertension. *Hypertension*. 2014;64(6):1248-59.
49. da Silveira KD, Coelho FM, Vieira AT, Sachs D, Barroso LC, Costa VV, et al. Anti-inflammatory effects of the activation of the angiotensin-(1–7) receptor, MAS, in experimental models of arthritis. *The Journal of Immunology*. 2010;185(9):5569-76.
50. Chen J-L, Zhang D-L, Sun Y, Zhao Y-X, Zhao K-X, Pu D, et al. Angiotensin-(1–7) administration attenuates Alzheimer's disease-like neuropathology in rats with streptozotocin-induced diabetes via Mas receptor activation. *Neuroscience*. 2017;346:267-77.
51. Jiang T, Zhang Y-D, Zhou J-S, Zhu X-C, Tian Y-Y, Zhao H-D, et al. Angiotensin-(1-7) is reduced and inversely correlates with tau hyperphosphorylation in animal models of Alzheimer's disease. *Molecular neurobiology*. 2016;53(4):2489-97.
52. Krishnan B, Torti FM, Gallagher PE, Tallant EA. Angiotensin-(1-7) reduces proliferation and angiogenesis of human prostate cancer xenografts with a decrease in angiogenic factors and an increase in sFlt-1. *The Prostate*. 2013;73(1):60-70.
53. Machado R, Santos R, Andrade S. Mechanisms of angiotensin-(1–7)-induced inhibition of angiogenesis. *American Journal of Physiology-Regulatory, Integrative and Comparative Physiology*. 2001;280(4):R994-R1000.

54. Pham H, Schwartz BM, Delmore JE, Reed E, Cruickshank S, Drummond L, et al. Pharmacodynamic stimulation of thrombogenesis by angiotensin (1–7) in recurrent ovarian cancer patients receiving gemcitabine and platinum-based chemotherapy. *Cancer chemotherapy and pharmacology*. 2013;71(4):965-72.
55. Soto-Pantoja DR, Menon J, Gallagher PE, Tallant EA. Angiotensin-(1-7) inhibits tumor angiogenesis in human lung cancer xenografts with a reduction in vascular endothelial growth factor. *Molecular cancer therapeutics*. 2009;8(6):1676-83.
56. Lula I, Denadai ÂL, Resende JM, de Sousa FB, de Lima GF, Pilo-Veloso D, et al. Study of angiotensin-(1–7) vasoactive peptide and its β -cyclodextrin inclusion complexes: complete sequence-specific NMR assignments and structural studies. *Peptides*. 2007;28(11):2199-210.
57. Marques FD, Ferreira AJ, Sinisterra RD, Jacoby BA, Sousa FB, Caliari MV, et al. An oral formulation of angiotensin-(1-7) produces cardioprotective effects in infarcted and isoproterenol-treated rats. *Hypertension*. 2011;57(3):477-83.
58. Hay M, Polt R, Heien ML, Vanderah TW, Largent-Milnes TM, Rodgers K, et al. A novel angiotensin-(1-7) glycosylated mas receptor agonist for treating vascular cognitive impairment and inflammation-related memory dysfunction. *Journal of Pharmacology and Experimental Therapeutics*. 2019;369(1):9-25.
59. Silva-Barcellos NM, Frézard F, Caligiorne S, Santos RA. Long-lasting cardiovascular effects of liposome-entrapped angiotensin-(1-7) at the rostral ventrolateral medulla. *Hypertension*. 2001;38(6):1266-71.

60. Ma X, Pang Z, Zhou J, He L, Hao Q, Li W, et al. Acetylation and amination protect angiotensin 1–7 from physiological hydrolyzation and therefore increases its antitumor effects on lung cancer. *Molecular pharmaceutics*. 2018;15(6):2338-47.
61. Khajehpour S, Aghazadeh-Habashi A. Targeting the Protective Arm of the Renin-Angiotensin System: Focused on Angiotensin-(1–7). *Journal of Pharmacology and Experimental Therapeutics*. 2021;377(1):64-74.
62. Seeman E. Bone quality: the material and structural basis of bone strength. *Journal of bone and mineral metabolism*. 2008;26(1):1-8.
63. Nakai T, Okuyama C, Kubota T, Yamada K, Ushijima Y, Taniike K, et al. Pitfalls of FDG-PET for the diagnosis of osteoblastic bone metastases in patients with breast cancer. *European journal of nuclear medicine and molecular imaging*. 2005;32(11):1253-8.
64. Lewiecki EM. Bisphosphonates for the treatment of osteoporosis: insights for clinicians. *Therapeutic advances in chronic disease*. 2010;1(3):115-28.
65. Poole KE, Compston JE. Bisphosphonates in the treatment of osteoporosis. *Bmj*. 2012;344.
66. Gil L, Han Y, Opas EE, Rodan GA, Ruel R, Seedor JG, et al. Prostaglandin E2-bisphosphonate conjugates: potential agents for treatment of osteoporosis. *Bioorganic & medicinal chemistry*. 1999;7(5):901-19.
67. Hirabayashi H, Fujisaki J. Bone-specific drug delivery systems. *Clinical pharmacokinetics*. 2003;42(15):1319-30.

68. Arns S, Gibe R, Moreau A, Morshed MM, Young RN. Design and synthesis of novel bone-targeting dual-action pro-drugs for the treatment and reversal of osteoporosis. *Bioorganic & medicinal chemistry*. 2012;20(6):2131-40.
69. Aghazadeh-Habashi A, Khajehpour S. Improved pharmacokinetics and bone tissue accumulation of Angiotensin-(1–7) peptide through bisphosphonate conjugation. *Amino Acids*. 2021;53(5):653-64.
70. Pullamsetti S, Savai R, Janssen W, Dahal B, Seeger W, Grimminger F, et al. Inflammation, immunological reaction and role of infection in pulmonary hypertension. *Clinical Microbiology and Infection*. 2011;17(1):7-14.
71. Brøchner AC, Toft P. Pathophysiology of the systemic inflammatory response after major accidental trauma. *Scandinavian journal of trauma, resuscitation and emergency medicine*. 2009;17(1):1-10.
72. Kumar V. Tissue renewal and repair: regeneration, healing, and fibrosis. *Pathologic basis of disease*. 2005:87-118.
73. Tortora GJ, Derrickson BH. *Principles of anatomy and physiology*: John Wiley & Sons; 2018.
74. Curtsinger JM, Mescher MF. Inflammatory cytokines as a third signal for T cell activation. *Current opinion in immunology*. 2010;22(3):333-40.
75. Sattar N, McCarey DW, Capell H, McInnes IB. Explaining how “high-grade” systemic inflammation accelerates vascular risk in rheumatoid arthritis. *Circulation*. 2003;108(24):2957-63.
76. Husby G. Amyloidosis and rheumatoid arthritis. *Clinical and experimental rheumatology*. 1985;3(2):173-80.

77. Shah SH, NEWBY KL. C-reactive protein: a novel marker of cardiovascular risk. *Cardiology in review*. 2003;11(4):169-79.
78. De Luigi A, Fragiaco C, Lucca U, Quadri P, Tettamanti M, De Simoni MG. Inflammatory markers in Alzheimer's disease and multi-infarct dementia. *Mechanisms of ageing and development*. 2001;122(16):1985-95.
79. Kelsey JL, Hochberg MC. Epidemiology of chronic musculoskeletal disorders. *Annual review of public health*. 1988;9(1):379-401.
80. Lawrence RC, Helmick CG, Arnett FC, Deyo RA, Felson DT, Giannini EH, et al. Estimates of the prevalence of arthritis and selected musculoskeletal disorders in the United States. *Arthritis & Rheumatism: Official Journal of the American College of Rheumatology*. 1998;41(5):778-99.
81. Cellucci T, Guzman J, Petty RE, Batthish M, Benseler SM, Ellsworth JE, et al. Management of Juvenile Idiopathic Arthritis 2015: a position statement from the pediatric Committee of the Canadian Rheumatology Association. *The Journal of rheumatology*. 2016;43(10):1773-6.
82. Jessar RA, Hollander JL. Types of arthritis and their medical treatment. *The American journal of nursing*. 1955:426-9.
83. Smolen JS, Aletaha D, Koeller M, Weisman MH, Emery P. New therapies for treatment of rheumatoid arthritis. *The Lancet*. 2007;370(9602):1861-74.
84. Silman AJ, Hochberg MC. *Epidemiology of the rheumatic diseases*: Oxford University Press; 2001.
85. Butcher L. Rheumatoid arthritis: prevalence, economics, and implications for payers and purchasers. *Biotechnology healthcare*. 2008;5(2):16.

86. Bombardier C, Hawker G, Mosher D. The Impact of Arthritis in Canada: Today and Over the Next 30 Years. Toronto (ON): Arthritis Alliance of Canada; 2011. 2011.
87. Gibofsky A. Overview of epidemiology, pathophysiology, and diagnosis of rheumatoid arthritis. The American journal of managed care. 2012;18(13 Suppl):S295-302.
88. Isaacs JD. The changing face of rheumatoid arthritis: sustained remission for all? Nature Reviews Immunology. 2010;10(8):605-11.
89. Huppa JB, Davis MM. T-cell-antigen recognition and the immunological synapse. Nature Reviews Immunology. 2003;3(12):973-83.
90. Ferucci ED, Templin DW, Lanier AP, editors. Rheumatoid arthritis in American Indians and Alaska Natives: a review of the literature. Seminars in arthritis and rheumatism; 2005: Elsevier.
91. Silman AJ, Pearson JE. Epidemiology and genetics of rheumatoid arthritis. Arthritis research & therapy. 2002;4(3):1-8.
92. Morgan AW, Robinson JI, Conaghan PG, Martin SG, Hensor EM, Morgan MD, et al. Evaluation of the rheumatoid arthritis susceptibility loci HLA-DRB1, PTPN22, OLIG3/TNFAIP3, STAT4 and TRAF1/C5 in an inception cohort. Arthritis research & therapy. 2010;12(2):1-10.
93. Division of Adult and Community Health CfDCaP. What is rheumatoid arthritis (RA)? : National Center for Chronic Disease Prevention and Health Promotion; 2020 July 27 [Available from: <http://www.cdc.gov/arthritis/basics/rheumatoid.htm>].

94. Metsios GS, Kitas GD. Physical activity, exercise and rheumatoid arthritis: effectiveness, mechanisms and implementation. *Best Practice & Research Clinical Rheumatology*. 2018;32(5):669-82.
95. Phillips C, Contreras E, Oswald J. NSAIDs, Opioids, and Beyond. *Pain Management-Practices, Novel Therapies and Bioactives*: IntechOpen; 2020.
96. Abbasi M, Mousavi MJ, Jamalzahi S, Alimohammadi R, Bezvan MH, Mohammadi H, et al. Strategies toward rheumatoid arthritis therapy; the old and the new. *Journal of cellular physiology*. 2019;234(7):10018-31.
97. Cruz BH, Garnica IU, Parera RS, Romero ER, Gutiérrez JC, Sánchez AG, et al. Disease-modifying antirheumatic drug prescription patterns in adult rheumatoid arthritis patients in routine clinical practice in Spain. *European Journal of Rheumatology*. 2020;7(4):149.
98. Fechtenbaum M, Nam JL, Emery P. Biologics in rheumatoid arthritis: where are we going? *British Journal of Hospital Medicine*. 2014;75(8):448-56.
99. Kavanaugh A, Lipsky P. Biologics in the treatment of rheumatoid arthritis: Mechanisms of action. *Current directions in autoimmunity*. 2001;3:240-73.
100. Wu Y, Li M, Zeng J, Feng Z, Yang J, Shen B, et al. Differential expression of renin-angiotensin system-related components in patients with rheumatoid arthritis and osteoarthritis. *The American Journal of the Medical Sciences*. 2020;359(1):17-26.
101. Cobankara V, Öztürk MA, Kiraz S, Ertenli I, Haznedaroglu IC, Pay S, et al. Renin and angiotensin-converting enzyme (ACE) as active components of the local synovial renin-angiotensin system in rheumatoid arthritis. *Rheumatology international*. 2005;25(4):285-91.

102. Mahmood NMA, Hussain SA, Mirza RR. Azilsartan improves the effects of etanercept in patients with active rheumatoid arthritis: a pilot study. *Therapeutics and Clinical Risk Management*. 2018;14:1379.
103. Wassmann S, Stumpf M, Strehlow K, Schmid A, Schieffer B, Böhm M, et al. Interleukin-6 induces oxidative stress and endothelial dysfunction by overexpression of the angiotensin II type 1 receptor. *Circulation research*. 2004;94(4):534-41.
104. Zhang Y, Ding H, Song Q, Wang Z, Yuan W, Ren Y, et al. Angiotensin II inhibits osteogenic differentiation of isolated synoviocytes by increasing DKK-1 expression. *The international journal of biochemistry & cell biology*. 2020;121:105703.
105. Silveira KD, Coelho FM, Vieira AT, Barroso LC, Queiroz-Junior CM, Costa VV, et al. Mechanisms of the anti-inflammatory actions of the angiotensin type 1 receptor antagonist losartan in experimental models of arthritis. *Peptides*. 2013;46:53-63.
106. Walsh DA, Catravas J, Wharton J. Angiotensin converting enzyme in human synovium: increased stromal [125I] 351A binding in rheumatoid arthritis. *Annals of the rheumatic diseases*. 2000;59(2):125-31.
107. Sagawa K, Nagatani K, Komagata Y, Yamamoto K. Angiotensin receptor blockers suppress antigen-specific T cell responses and ameliorate collagen-induced arthritis in mice. *Arthritis & Rheumatism*. 2005;52(6):1920-8.
108. Forrester SJ, Booz GW, Sigmund CD, Coffman TM, Kawai T, Rizzo V, et al. Angiotensin II signal transduction: an update on mechanisms of physiology and pathophysiology. *Physiological reviews*. 2018;98(3):1627-738.
109. Fernandez LA, Twickler J, Mead A. Neovascularization produced by angiotensin II. *The Journal of laboratory and clinical medicine*. 1985;105(2):A2.

110. Walsh NC, Gravallesse EM. Bone remodeling in rheumatic disease: a question of balance. *Immunological reviews*. 2010;233(1):301-12.
111. Asaba Y, Ito M, Fumoto T, Watanabe K, Fukuhara R, Takeshita S, et al. Activation of renin-angiotensin system induces osteoporosis independently of hypertension. *Journal of bone and mineral research*. 2009;24(2):241-50.
112. Diarra D, Stolina M, Polzer K, Zwerina J, Ominsky MS, Dwyer D, et al. Dickkopf-1 is a master regulator of joint remodeling. *Nature medicine*. 2007;13(2):156-63.
113. Nakai K, Kawato T, Morita T, Iinuma T, Kamio N, Zhao N, et al. Angiotensin II induces the production of MMP-3 and MMP-13 through the MAPK signaling pathways via the AT1 receptor in osteoblasts. *Biochimie*. 2013;95(4):922-33.
114. Yewle JN, Puleo DA, Bachas LG. Bifunctional bisphosphonates for delivering PTH (1-34) to bone mineral with enhanced bioactivity. *Biomaterials*. 2013;34(12):3141-9.
115. De Mello WC, Ferrario CM, Jessup JA. Beneficial versus harmful effects of Angiotensin (1-7) on impulse propagation and cardiac arrhythmias in the failing heart. *Journal of the Renin-Angiotensin-Aldosterone System*. 2007;8(2):74-80.
116. Sasaki S, Higashi Y, Nakagawa K, Matsuura H, Kajiyama G, Oshima T. Effects of angiotensin-(1-7) on forearm circulation in normotensive subjects and patients with essential hypertension. *Hypertension*. 2001;38(1):90-4.
117. Zhang J, Noble NA, Border WA, Huang Y. Infusion of angiotensin-(1-7) reduces glomerulosclerosis through counteracting angiotensin II in experimental glomerulonephritis. *American Journal of Physiology-Renal Physiology*. 2010;298(3):F579-F88.

118. Klein N, Gembardt F, Supé S, Kaestle SM, Nickles H, Erfinanda L, et al. Angiotensin-(1–7) protects from experimental acute lung injury. *Critical Care Medicine*. 2013;41(11):e334-e43.
119. Santos SHS, Braga JF, Mario EG, Pôrto LCJ, Rodrigues-Machado MdG, Murari A, et al. Improved lipid and glucose metabolism in transgenic rats with increased circulating angiotensin-(1-7). *Arteriosclerosis, thrombosis, and vascular biology*. 2010;30(5):953-61.
120. Kang JS, DeLuca PP, Lee KC. Emerging pegylated drugs. *Expert opinion on emerging drugs*. 2009;14(2):363-80.
121. Petty WJ, Miller AA, McCoy TP, Gallagher PE, Tallant EA, Torti FM. Phase I and pharmacokinetic study of angiotensin-(1-7), an endogenous antiangiogenic hormone. *Clinical Cancer Research*. 2009;15(23):7398-404.
122. Petty WJ, Aklilu M, Varela VA, Lovato J, Savage PD, Miller AA. Reverse translation of phase I biomarker findings links the activity of angiotensin-(1–7) to repression of hypoxia inducible factor-1 α in vascular sarcomas. *Bmc Cancer*. 2012;12(1):1-7.
123. Rodgers KE, Oliver J, dizerega GS. Phase I/II dose escalation study of angiotensin 1-7 [A (1-7)] administered before and after chemotherapy in patients with newly diagnosed breast cancer. *Cancer chemotherapy and pharmacology*. 2006;57(5):559-68.
124. Kluskens LD, Nelemans SA, Rink R, de Vries L, Meter-Arkema A, Wang Y, et al. Angiotensin-(1-7) with thioether bridge: an angiotensin-converting enzyme-resistant,

- potent angiotensin-(1-7) analog. *Journal of Pharmacology and Experimental Therapeutics*. 2009;328(3):849-54.
125. Carter CS, Morgan D, Verma A, Lobaton G, Aquino V, Sumners E, et al. Therapeutic delivery of Ang (1–7) via genetically modified probiotic: a dosing study. *The Journals of Gerontology: Series A*. 2020;75(7):1299-303.
126. Habashi AA, Khajeh pour SA, Ranjit A. Prevention and treatment of rheumatoid arthritis using bone-targeted angiotensin peptide in rats. *The FASEB Journal*. 2020;34(S1):1-.
127. Soro-Paavonen A, Gordin D, Forsblom C, Rosengard-Barlund M, Waden J, Thorn L, et al. Circulating ACE2 activity is increased in patients with type 1 diabetes and vascular complications. *Journal of hypertension*. 2012;30(2):375-83.
128. Varagic J, Ahmad S, Nagata S, Ferrario CM. ACE2: angiotensin II/angiotensin-(1–7) balance in cardiac and renal injury. *Current hypertension reports*. 2014;16(3):1-9.
129. Park SE, Kim WJ, Park SW, Park JW, Lee N, Park C-Y, et al. High urinary ACE2 concentrations are associated with severity of glucose intolerance and microalbuminuria. *Eur J Endocrinol*. 2013;168(2):203-10.
130. Takahashi Y, Haga S, Ishizaka Y, Mimori A. Autoantibodies to angiotensin-converting enzyme 2 in patients with connective tissue diseases. *Arthritis research & therapy*. 2010;12(3):1-8.
131. Pincus T, Swearingen CJ, Bergman M, Yazici Y. RAPID3 (Routine Assessment of Patient Index Data 3), a rheumatoid arthritis index without formal joint counts for routine care: proposed severity categories compared to disease activity score and

clinical disease activity index categories. *The Journal of rheumatology*.

2008;35(11):2136-47.

132. Schwenger V, Sis J, Breitbart A, Andrassy K. CRP levels in autoimmune disease can be specified by measurement of procalcitonin. *Infection*. 1998;26(5):274-6.

133. Cui L, Nithipatikom K, Campbell WB. Simultaneous analysis of angiotensin peptides by LC–MS and LC–MS/MS: metabolism by bovine adrenal endothelial cells.

Analytical biochemistry. 2007;369(1):27-33.

134. Porstmann T, Kiessig S. Enzyme immunoassay techniques an overview. *Journal of immunological methods*. 1992;150(1-2):5-21.

135. Saag KG, Teng GG, Patkar NM, Anuntiyo J, Finney C, Curtis JR, et al. American College of Rheumatology 2008 recommendations for the use of nonbiologic and biologic disease-modifying antirheumatic drugs in rheumatoid arthritis. *Arthritis Care & Research: Official Journal of the American College of Rheumatology*. 2008;59(6):762-84.

136. Arthur JM, Forrest JC, Boehme KW, Kennedy JL, Owens S, Herzog C, et al. Development of ACE2 autoantibodies after SARS-CoV-2 infection. *PloS one*. 2021;16(9):e0257016.

137. Braz NFT, Pinto MRC, Vieira ÉLM, Souza AJ, Teixeira AL, Simões-e-Silva AC, et al. Renin–angiotensin system molecules are associated with subclinical atherosclerosis and disease activity in rheumatoid arthritis. *Modern Rheumatology*. 2021;31(1):119-26.

138. Alexanian A, Miller B, Roman RJ, Sorokin A. 20-HETE-producing enzymes are up-regulated in human cancers. *Cancer genomics & proteomics*. 2012;9(4):163-9.

139. Asghar W, Aghazadeh-Habashi A, Jamali F. Cardiovascular effect of inflammation and nonsteroidal anti-inflammatory drugs on renin–angiotensin system in experimental arthritis. *Inflammopharmacology*. 2017;25(5):543-53.
140. Moreira FRC, de Oliveira TA, Ramos NE, Abreu MAD, Simões e Silva AC. The role of renin angiotensin system in the pathophysiology of rheumatoid arthritis. *Molecular Biology Reports*. 2021;48(9):6619-29.
141. Munro MJ, Wickremesekera AC, Davis PF, Marsh R, Tan ST, Itinteang T. Renin-angiotensin system and cancer: a review. *Integr Cancer Sci Ther*. 2017;4(2):1-6.
142. Ribeiro-Oliveira Jr A, Nogueira AI, Pereira RM, Boas WWV, Dos Santos RAS, e Silva ACS. The renin–angiotensin system and diabetes: an update. *Vascular health and risk management*. 2008;4(4):787.
143. Ferrario CM, Ahmad S, Groban L. Mechanisms by which angiotensin-receptor blockers increase ACE2 levels. *Nature Reviews Cardiology*. 2020;17(6):378-.
144. Wester A, Devocelle M, Tallant E, Chappell MC, Gallagher PE, Paradisi F. Stabilization of Angiotensin-(1–7) by key substitution with a cyclic non-natural amino acid. *Amino Acids*. 2017;49(10):1733-42.
145. Samuelsson B. Arachidonic acid metabolism: role in inflammation. *Zeitschrift fur Rheumatologie*. 1991;50:3-6.
146. Theken KN, Deng Y, Kannon MA, Miller TM, Poloyac SM, Lee CR. Activation of the acute inflammatory response alters cytochrome P450 expression and eicosanoid metabolism. *Drug metabolism and disposition*. 2011;39(1):22-9.
147. Roman RJ. P-450 metabolites of arachidonic acid in the control of cardiovascular function. *Physiological reviews*. 2002;82(1):131-85.

148. Carroll MA, McGiff JC. A new class of lipid mediators: cytochrome P450 arachidonate metabolites. *Thorax*. 2000;55(suppl 2):S13-S6.
149. Kehl F, Cambj-Sapunar L, Maier KG, Miyata N, Kametani S, Okamoto H, et al. 20-HETE contributes to the acute fall in cerebral blood flow after subarachnoid hemorrhage in the rat. *American Journal of Physiology-Heart and Circulatory Physiology*. 2002;282(4):H1556-H65.
150. Roman RJ, Renic M, Dunn KM, Takeuchi K, Hacein-Bey L. Evidence that 20-HETE contributes to the development of acute and delayed cerebral vasospasm. *Neurological research*. 2006;28(7):738-49.
151. Tanaka Y, Omura T, Fukasawa M, Horiuchi N, Miyata N, Minagawa T, et al. Continuous inhibition of 20-HETE synthesis by TS-011 improves neurological and functional outcomes after transient focal cerebral ischemia in rats. *Neuroscience research*. 2007;59(4):475-80.
152. Gebremedhin D, Yamaura K, Harder DR. Role of 20-HETE in the hypoxia-induced activation of Ca²⁺-activated K⁺ channel currents in rat cerebral arterial muscle cells. *American Journal of Physiology-Heart and Circulatory Physiology*. 2008;294(1):H107-H20.
153. Campbell WB, Harder DR. Endothelium-derived hyperpolarizing factors and vascular cytochrome P450 metabolites of arachidonic acid in the regulation of tone. *Circulation research*. 1999;84(4):484-8.
154. Schwartzman M, Abraham N, Carroll M, Levere R, McGiff J. Regulation of arachidonic acid metabolism by cytochrome P-450 in rabbit kidney. *Biochemical Journal*. 1986;238(1):283-90.

155. Sarkis A, Lopez B, Roman RJ. Role of 20-hydroxyeicosatetraenoic acid and epoxyeicosatrienoic acids in hypertension. *Current opinion in nephrology and hypertension*. 2004;13(2):205-14.
156. Miyata N, Roman RJ. Role of 20-hydroxyeicosatetraenoic acid (20-HETE) in vascular system. *Journal of Smooth Muscle Research*. 2005;41(4):175-93.
157. Walkowska A, Thumová M, Škaroupková P, Husková Z, Vaňourková Z, Chábová VČ, et al. Intrarenal CYP-450 metabolites of arachidonic acid in the regulation of the nonclipped kidney function in two-kidney, one-clip Goldblatt hypertensive rats. *Journal of hypertension*. 2010;28(3):582.
158. Sacerdoti D, Gatta A, McGiff JC. Role of cytochrome P450-dependent arachidonic acid metabolites in liver physiology and pathophysiology. *Prostaglandins & other lipid mediators*. 2003;72(1-2):51-71.
159. Adam A-C, Lie KK, Whatmore P, Jakt LM, Moren M, Skjærven KH. Profiling DNA methylation patterns of zebrafish liver associated with parental high dietary arachidonic acid. *PloS one*. 2019;14(8):e0220934.
160. Rutting S, Papanicolaou M, Xenaki D, Wood LG, Mullin AM, Hansbro PM, et al. Dietary ω -6 polyunsaturated fatty acid arachidonic acid increases inflammation, but inhibits ECM protein expression in COPD. *Respiratory research*. 2018;19(1):1-12.
161. Yaghi A, Bradbury JA, Zeldin DC, Mehta S, Bend JR, McCormack DG. Pulmonary cytochrome P-450 2J4 is reduced in a rat model of acute *Pseudomonas pneumonia*. *American Journal of Physiology-Lung Cellular and Molecular Physiology*. 2003;285(5):L1099-L105.

162. Capra V, Bäck M, Barbieri SS, Camera M, Tremoli E, Rovati GE. Eicosanoids and their drugs in cardiovascular diseases: focus on atherosclerosis and stroke. *Medicinal research reviews*. 2013;33(2):364-438.
163. Kundumani-Sridharan V, Dyukova E, Hansen DE, Rao GN. 12/15-Lipoxygenase mediates high-fat diet-induced endothelial tight junction disruption and monocyte transmigration: a new role for 15 (S)-hydroxyeicosatetraenoic acid in endothelial cell dysfunction. *Journal of Biological Chemistry*. 2013;288(22):15830-42.
164. Ishizuka T, Cheng J, Singh H, Vitto MD, Manthathi VL, Falck JR, et al. 20-Hydroxyeicosatetraenoic acid stimulates nuclear factor- κ B activation and the production of inflammatory cytokines in human endothelial cells. *Journal of Pharmacology and Experimental Therapeutics*. 2008;324(1):103-10.
165. Anwar-mohamed A, Zordoky BN, Aboutabl ME, El-Kadi AO. Alteration of cardiac cytochrome P450-mediated arachidonic acid metabolism in response to lipopolysaccharide-induced acute systemic inflammation. *Pharmacological research*. 2010;61(5):410-8.
166. Chen S. Natural products triggering biological targets-a review of the anti-inflammatory phytochemicals targeting the arachidonic acid pathway in allergy asthma and rheumatoid arthritis. *Current drug targets*. 2011;12(3):288-301.
167. Zeldin DC. Epoxygenase pathways of arachidonic acid metabolism. *Journal of Biological Chemistry*. 2001;276(39):36059-62.
168. Node K, Huo Y, Ruan X, Yang B, Spiecker M, Ley K, et al. Anti-inflammatory properties of cytochrome P450 epoxygenase-derived eicosanoids. *Science*. 1999;285(5431):1276-9.

169. Gross GJ, Hsu A, Falck JR, Nithipatikom K. Mechanisms by which epoxyeicosatrienoic acids (EETs) elicit cardioprotection in rat hearts. *Journal of molecular and cellular cardiology*. 2007;42(3):687-91.
170. Chiamvimonvat N, Ho C-M, Tsai H-J, Hammock BD. The soluble epoxide hydrolase as a pharmaceutical target for hypertension. *Journal of cardiovascular pharmacology*. 2007;50(3):225-37.
171. Qiu H, Li N, Liu JY, Harris TR, Hammock BD, Chiamvimonvat N. Soluble epoxide hydrolase inhibitors and heart failure. *Cardiovascular therapeutics*. 2011;29(2):99-111.
172. Gorin Y, Kim NH, Feliers D, Bhandari B, Choudhury GG, Abboud HE. Angiotensin II activates Akt/protein kinase B by an arachidonic acid/redox-dependent pathway and independent of phosphoinositide 3-kinase. *The FASEB Journal*. 2001;15(11):1909-20.
173. Zafari AM, Ushio-Fukai M, Minieri CA, Akers M, Lassègue B, Griendling KK. Arachidonic acid metabolites mediate angiotensin II-induced NADH/NADPH oxidase activity and hypertrophy in vascular smooth muscle cells. *Antioxidants & redox signaling*. 1999;1(2):167-79.
174. Chu Z, Croft K, Kingsbury D, Falck J, Reddy K, Beilin L. Cytochrome P450 metabolites of arachidonic acid may be important mediators in angiotensin II-induced vasoconstriction in the rat mesentery in vivo. *Clinical science*. 2000;98(3):277-82.
175. Whiteley PE, Dalrymple SA. Models of inflammation: adjuvant-induced arthritis in the rat. *Current protocols in pharmacology*. 2001;13(1):5.. 1-5.. .

176. Piquette-Miller M, Jamali F. Influence of severity of inflammation on the disposition kinetics of propranolol enantiomers in ketoprofen-treated and untreated adjuvant arthritis. *Drug Metab Dispos.* 1995;23(2):240-5.
177. Bamgbose S, Noamesi B. Studies on cryptolepine. *Planta medica.* 1981;41(04):392-6.
178. Di Rosa M, Radomski M, Carnuccio R, Moncada S. Glucocorticoids inhibit the induction of nitric oxide synthase in macrophages. *Biochemical and biophysical research communications.* 1990;172(3):1246-52.
179. Barrott JJ, Illum BE, Jin H, Zhu J-F, Mosbrugger T, Monument MJ, et al. β -catenin stabilization enhances SS18-SSX2-driven synovial sarcomagenesis and blocks the mesenchymal to epithelial transition. *Oncotarget.* 2015;6(26):22758.
180. Dai S-Y, Peng W, Zhang Y-P, Li J-D, Shen Y, Sun X-F. Brain endogenous angiotensin II receptor type 2 (AT2-R) protects against DOCA/salt-induced hypertension in female rats. *Journal of neuroinflammation.* 2015;12(1):1-11.
181. Liu CX, Hu Q, Wang Y, Zhang W, Ma ZY, Feng JB, et al. Angiotensin-converting enzyme (ACE) 2 overexpression ameliorates glomerular injury in a rat model of diabetic nephropathy: a comparison with ACE inhibition. *Molecular Medicine.* 2011;17(1):59-69.
182. Liu J, Chen Q, Liu S, Yang X, Zhang Y, Huang F. Sini decoction alleviates E. coli induced acute lung injury in mice via equilibrating ACE-AngII-AT1R and ACE2-Ang-(1-7)-Mas axis. *Life sciences.* 2018;208:139-48.
183. Exner EC, Geurts AM, Hoffmann BR, Casati M, Stodola T, Dsouza NR, et al. Interaction between Mas1 and AT1RA contributes to enhancement of skeletal muscle

angiogenesis by angiotensin-(1-7) in Dahl salt-sensitive rats. *PloS one*.

2020;15(4):e0232067.

184. Wang T, Lian G, Cai X, Lin Z, Xie L. Effect of prehypertensive losartan therapy on AT1R and ATRAP methylation of adipose tissue in the later life of high-fat-fed spontaneously hypertensive rats. *Molecular medicine reports*. 2018;17(1):1753-61.

185. Edpuganti V, Mehvar R. UHPLC–MS/MS analysis of arachidonic acid and 10 of its major cytochrome P450 metabolites as free acids in rat livers: effects of hepatic ischemia. *Journal of Chromatography B*. 2014;964:153-63.

186. Khajeh pour S, Ranjit A, Summerill EL, Aghazadeh-Habashi A. Anti-Inflammatory Effects of Ang-(1-7) Bone-Targeting Conjugate in an Adjuvant-Induced Arthritis Rat Model. *Pharmaceuticals*. 2022;15(9):1157.

187. Ranjit A, Khajeh Pour S, Aghazadeh-Habashi A. Bone-Targeted Delivery of Novokinin as an Alternative Treatment Option for Rheumatoid Arthritis. *Pharmaceutics*. 2022;14(8):1681.

188. Khajehpour S, Aghazadeh-Habashi A. Anti-inflammatory effects of Angiotensin-(1-7) through Renin-Angiotensin System and Arachidonic Acid Pathway. *The FASEB Journal*. 2022;36.

189. Lemarié CA, Schiffrin EL. The angiotensin II type 2 receptor in cardiovascular disease. *Journal of the renin-angiotensin-aldosterone system*. 2010;11(1):19-31.

190. Ruiz-Ortega M, Lorenzo O, Suzuki Y, Rupérez M, Egido J. Proinflammatory actions of angiotensins. *Current opinion in nephrology and hypertension*. 2001;10(3):321-9.

191. Kortekaas KE, Meijer CA, Hinnen JW, Dalman RL, Xu B, Hamming JF, et al. ACE inhibitors potently reduce vascular inflammation, results of an open proof-of-concept study in the abdominal aortic aneurysm. *PloS one*. 2014;9(12):e111952.
192. Benicky J, Sánchez-Lemus E, Pavel J, Saavedra JM. Anti-inflammatory effects of angiotensin receptor blockers in the brain and the periphery. *Cellular and molecular neurobiology*. 2009;29(6):781-92.
193. Taguchi I, Toyoda S, Takano K, Arikawa T, Kikuchi M, Ogawa M, et al. Irbesartan, an angiotensin receptor blocker, exhibits metabolic, anti-inflammatory and antioxidative effects in patients with high-risk hypertension. *Hypertension research*. 2013;36(7):608-13.
194. Price A, Lockhart J, Ferrell W, Gsell W, McLean S, Sturrock R. Angiotensin II type 1 receptor as a novel therapeutic target in rheumatoid arthritis: in vivo analyses in rodent models of arthritis and ex vivo analyses in human inflammatory synovitis. *Arthritis & Rheumatism: Official Journal of the American College of Rheumatology*. 2007;56(2):441-7.
195. Mateo T, Nabah YNA, Taha MA, Mata M, Cerdá-Nicolás M, Proudfoot AE, et al. Angiotensin II-induced mononuclear leukocyte interactions with arteriolar and venular endothelium are mediated by the release of different CC chemokines. *The Journal of Immunology*. 2006;176(9):5577-86.
196. Nabah YNA, Mateo T, Estellés R, Mata M, Zagorski J, Sarau H, et al. Angiotensin II induces neutrophil accumulation in vivo through generation and release of CXC chemokines. *Circulation*. 2004;110(23):3581-6.

197. Schlüter K-D, Wenzel S. Angiotensin II: a hormone involved in and contributing to pro-hypertrophic cardiac networks and target of anti-hypertrophic cross-talks. *Pharmacology & therapeutics*. 2008;119(3):311-25.
198. Parajuli N, Ramprasath T, Patel VB, Wang W, Putko B, Mori J, et al. Targeting angiotensin-converting enzyme 2 as a new therapeutic target for cardiovascular diseases. *Canadian Journal of Physiology and Pharmacology*. 2014;92(7):558-65.
199. Xianwei W, Magomed K, Ding Z, Sona M, Jingjun L, Shijie L, et al. Cross-talk between inflammation and angiotensin II: studies based on direct transfection of cardiomyocytes with AT1R and AT2R cDNA. *Experimental biology and medicine*. 2012;237(12):1394-401.
200. Gallagher PE, Tallant EA. Inhibition of human lung cancer cell growth by angiotensin-(1-7). *Carcinogenesis*. 2004;25(11):2045-52.
201. George AJ, Thomas WG, Hannan RD. The renin–angiotensin system and cancer: old dog, new tricks. *Nature Reviews Cancer*. 2010;10(11):745-59.
202. Ager EI, Neo J, Christophi C. The renin–angiotensin system and malignancy. *Carcinogenesis*. 2008;29(9):1675-84.
203. Lever AF, Hole DJ, Gillis CR, McCallum IR, McInnes GT, MacKinnon PL, et al. Do inhibitors of angiotensin-I-converting enzyme protect against risk of cancer? *The Lancet*. 1998;352(9123):179-84.
204. Riordan JF. Angiotensin-I-converting enzyme and its relatives. *Genome biology*. 2003;4(8):1-5.
205. Featherston T, Yu HH, Dunne JC, Chibnall AM, Brasch HD, Davis PF, et al. Cancer stem cells in moderately differentiated buccal mucosal squamous cell

- carcinoma express components of the renin–angiotensin system. *Frontiers in Surgery*. 2016;3:52.
206. Bradshaw AR, Wickremesekera AC, Brasch HD, Chibnall AM, Davis PF, Tan ST, et al. Glioblastoma multiforme cancer stem cells express components of the renin–angiotensin system. *Frontiers in Surgery*. 2016;3:51.
207. Itinteang T, Dunne JC, Chibnall AM, Brasch HD, Davis PF, Tan ST. Cancer stem cells in moderately differentiated oral tongue squamous cell carcinoma express components of the renin–angiotensin system. *Journal of clinical pathology*. 2016;69(10):942-5.
208. Rosenthal T, Gavras I. Angiotensin inhibition and malignancies: a review. *Journal of human hypertension*. 2009;23(10):623-35.
209. Fyhrquist F, Saijonmaa O. Renin-angiotensin system revisited. *Journal of internal medicine*. 2008;264(3):224-36.
210. Ino K, Shibata K, Kajiyama H, Yamamoto E, Nagasaka T, Nawa A, et al. Angiotensin II type 1 receptor expression in ovarian cancer and its correlation with tumour angiogenesis and patient survival. *British Journal of Cancer*. 2006;94(4):552-60.
211. Shanmugam S, Corvol P, Gasc J-M. Angiotensin II type 2 receptor mRNA expression in the developing cardiopulmonary system of the rat. *Hypertension*. 1996;28(1):91-7.
212. Doi C, Egashira N, Kawabata A, Maurya DK, Ohta N, Uppalapati D, et al. Angiotensin II type 2 receptor signaling significantly attenuates growth of murine pancreatic carcinoma grafts in syngeneic mice. *BMC cancer*. 2010;10(1):1-13.

213. Stacchiotti S, Van Tine BA. Synovial sarcoma: current concepts and future perspectives. *Journal of Clinical Oncology*. 2018;36(2):180-7.
214. Fisher C. Synovial sarcoma. *Annals of diagnostic pathology*. 1998;2(6):401-21.
215. Chotel F, Unnithan A, Chandrasekar C, Parot R, Jeys L, Grimer R. Variability in the presentation of synovial sarcoma in children: a plea for greater awareness. *The Journal of Bone and Joint Surgery British volume*. 2008;90(8):1090-6.
216. Von Mehren M, Randall RL, Benjamin RS, Boles S, Bui MM, Conrad EU, et al. Soft tissue sarcoma, version 2.2016, NCCN clinical practice guidelines in oncology. *Journal of the National Comprehensive Cancer Network*. 2016;14(6):758-86.
217. Gundle KR, Gupta S, Kafchinski L, Griffin AM, Kandel RA, Dickson BC, et al. An analysis of tumor-and surgery-related factors that contribute to inadvertent positive margins following soft tissue sarcoma resection. *Annals of surgical oncology*. 2017;24(8):2137-44.
218. Ghert MA, Abudu A, Driver N, Davis AM, Griffin AM, Pearce D, et al. The indications for and the prognostic significance of amputation as the primary surgical procedure for localized soft tissue sarcoma of the extremity. *Annals of Surgical Oncology*. 2005;12(1):10-7.
219. Ramu EM, Houdek MT, Isaac CE, Dickie CI, Ferguson PC, Wunder JS. Management of soft-tissue sarcomas; treatment strategies, staging, and outcomes. *Sicot-j*. 2017;3.
220. Ferrari A, Chi Y-Y, De Salvo GL, Orbach D, Brennan B, Randall RL, et al. Surgery alone is sufficient therapy for children and adolescents with low-risk synovial

sarcoma: a joint analysis from the European paediatric soft tissue sarcoma Study Group and the Children's Oncology Group. *European Journal of Cancer*. 2017;78:1-6.

221. Maki RG, Jungbluth AA, Gnjatic S, Schwartz GK, D'Adamo DR, Keohan ML, et al. A pilot study of anti-CTLA4 antibody ipilimumab in patients with synovial sarcoma. *Sarcoma*. 2013;2013.

222. Pollack SM, Jungbluth AA, Hoch BL, Farrar EA, Bleakley M, Schneider DJ, et al. NY-ESO-1 is a ubiquitous immunotherapeutic target antigen for patients with myxoid/round cell liposarcoma. *Cancer*. 2012;118(18):4564-70.

223. Mitsis D, Francescutti V, Skitzki J. Current immunotherapies for sarcoma: clinical trials and rationale. *Sarcoma*. 2016;2016.

224. Lässig F, Klann A, Bekeschus S, Lendeckel U, Wolke C. Expression of canonical transient receptor potential channels in U-2 OS and MNNG-HOS osteosarcoma cell lines. *Oncology Letters*. 2021;21(4):1-8.

225. Ding L, Zhang G, Hou Y, Chen J, Yin Y. Elemene inhibits osteosarcoma growth by suppressing the renin-angiotensin system signaling pathway. *Molecular Medicine Reports*. 2018;17(1):1022-30.

226. Ender SA, Dallmer A, Lässig F, Lendeckel U, Wolke C. Expression and function of the ACE2/angiotensin (1-7)/Mas axis in osteosarcoma cell lines U-2 OS and MNNG-HOS. *Molecular Medicine Reports*. 2014;10(2):804-10.

227. DeSantis C, Ma J, Bryan L, Jemal A. Breast cancer statistics, 2013. *CA: a cancer journal for clinicians*. 2014;64(1):52-62.

228. MacMahon B, Cole P, Brown J. Etiology of human breast cancer: a review. *Journal of the National Cancer Institute*. 1973;50(1):21-42.

229. Tao Z, Shi A, Lu C, Song T, Zhang Z, Zhao J. Breast cancer: epidemiology and etiology. *Cell biochemistry and biophysics*. 2015;72(2):333-8.
230. Society AC. Breast cancer facts & figures. Cancer Society. 2019:1-44.
231. Osborne CK. Tamoxifen in the treatment of breast cancer. *New England Journal of Medicine*. 1998;339(22):1609-18.
232. Dean-Colomb W, Esteva FJ. Her2-positive breast cancer: herceptin and beyond. *European Journal of Cancer*. 2008;44(18):2806-12.
233. Al-Ejeh F, Simpson P, Sanus J, Klein K, Kalimutho M, Shi W, et al. Meta-analysis of the global gene expression profile of triple-negative breast cancer identifies genes for the prognostication and treatment of aggressive breast cancer. *Oncogenesis*. 2014;3(4):e100-e.
234. de Miranda FS, Guimarães JPT, Menikdiwela KR, Mabry B, Dhakal R, Iayeequr Rahman R, et al. Breast cancer and the renin-angiotensin system (RAS): Therapeutic approaches and related metabolic diseases. *Molecular and Cellular Endocrinology*. 2021;528:111245.
235. Shen J, Huang Y-M, Wang M, Hong X-Z, Song X-N, Zou X, et al. Renin–angiotensin system blockade for the risk of cancer and death. *Journal of the Renin-Angiotensin-Aldosterone System*. 2016;17(3):1470320316656679.
236. Puddefoot J, Udeozo U, Barker S, Vinson G. The role of angiotensin II in the regulation of breast cancer cell adhesion and invasion. *Endocrine-related cancer*. 2006;13(3):895-903.

237. Picon-Ruiz M, Morata-Tarifa C, Valle-Goffin JJ, Friedman ER, Slingerland JM. Obesity and adverse breast cancer risk and outcome: Mechanistic insights and strategies for intervention. *CA: a cancer journal for clinicians*. 2017;67(5):378-97.
238. Menikdiwela KR, Ramalingam L, Allen L, Scoggin S, Kalupahana NS, Moustaid-Moussa N. Angiotensin II increases endoplasmic reticulum stress in adipose tissue and adipocytes. *Scientific reports*. 2019;9(1):1-14.
239. Rose D, Komninou D, Stephenson G. Obesity, adipocytokines, and insulin resistance in breast cancer. *Obesity reviews*. 2004;5(3):153-65.
240. Rasha F, Ramalingam L, Menikdiwela K, Hernandez A, Moussa H, Gollahon L, et al. Renin angiotensin system inhibition attenuates adipocyte-breast cancer cell interactions. *Experimental Cell Research*. 2020;394(1):112114.
241. Bujak-Gizycka B, Madej J, Bystrowska B, Toton-Zuranska J, Kus K, Kolton-Wroz M, et al. Angiotensin 1-7 formation in breast tissue is attenuated in breast cancer-a study on the metabolism of angiotensinogen in breast cancer cell lines. *J Physiol Pharmacol*. 2019;70(4):503-14.
242. Arrieta O, Villarreal-Garza C, Vizcaíno G, Pineda B, Hernández-Pedro N, Guevara-Salazar P, et al. Association between AT1 and AT2 angiotensin II receptor expression with cell proliferation and angiogenesis in operable breast cancer. *Tumor Biology*. 2015;36(7):5627-34.
243. Rhodes DR, Ateeq B, Cao Q, Tomlins SA, Mehra R, Laxman B, et al. AGTR1 overexpression defines a subset of breast cancer and confers sensitivity to losartan, an AGTR1 antagonist. *Proceedings of the National Academy of Sciences*. 2009;106(25):10284-9.

244. Egami K, Murohara T, Shimada T, Sasaki K-i, Shintani S, Sugaya T, et al. Role of host angiotensin II type 1 receptor in tumor angiogenesis and growth. *The Journal of clinical investigation*. 2003;112(1):67-75.
245. Rasha F, Ramalingam L, Gollahon L, Rahman RL, Rahman SM, Menikdiwela K, et al. Mechanisms linking the renin-angiotensin system, obesity, and breast cancer. *Endocrine-related cancer*. 2019;26(12):R653-R72.
246. Song S, Su Z, Xu H, Niu M, Chen X, Min H, et al. Luteolin selectively kills STAT3 highly activated gastric cancer cells through enhancing the binding of STAT3 to SHP-1. *Cell death & disease*. 2017;8(2):e2612-e.
247. Benndorf R, Böger RH, Ergün SI, Steenpass A, Wieland T. Angiotensin II type 2 receptor inhibits vascular endothelial growth factor–induced migration and in vitro tube formation of human endothelial cells. *Circulation research*. 2003;93(5):438-47.
248. Rodrigues-Ferreira S, Nahmias C. G-protein coupled receptors of the renin-angiotensin system: new targets against breast cancer? *Frontiers in pharmacology*. 2015;6:24.
249. Yu C, Tang W, Wang Y, Shen Q, Wang B, Cai C, et al. Downregulation of ACE2/Ang-(1–7)/Mas axis promotes breast cancer metastasis by enhancing store-operated calcium entry. *Cancer letters*. 2016;376(2):268-77.
250. Namazi S, Rostami-Yalmeh J, Sahebi E, Jaberipour M, Razmkhah M, Hosseini A. The role of captopril and losartan in prevention and regression of tamoxifen-induced resistance of breast cancer cell line MCF-7: An in vitro study. *Biomedicine & Pharmacotherapy*. 2014;68(5):565-71.

251. Chu D-T, Nguyen Thi Phuong T, Tien NLB, Tran D-K, Nguyen T-T, Thanh VV, et al. The effects of adipocytes on the regulation of breast cancer in the tumor microenvironment: an update. *Cells*. 2019;8(8):857.
252. Chauhan VP, Chen IX, Tong R, Ng MR, Martin JD, Naxerova K, et al. Reprogramming the microenvironment with tumor-selective angiotensin blockers enhances cancer immunotherapy. *Proceedings of the National Academy of Sciences*. 2019;116(22):10674-80.
253. Sá M, Ribeiro H, Valverde T, Sousa B, Martins-Júnior P, Mendes R, et al. Single-walled carbon nanotubes functionalized with sodium hyaluronate enhance bone mineralization. *Brazilian journal of medical and biological research*. 2015;49.
254. Tamarat R, Silvestre J-S, Durie M, Levy BI. Angiotensin II angiogenic effect in vivo involves vascular endothelial growth factor-and inflammation-related pathways. *Laboratory investigation*. 2002;82(6):747-56.
255. Pupilli C, Lasagni L, Romagnani P, BELLINI F, MANNELLI M, MISCIGLIA N, et al. Angiotensin II stimulates the synthesis and secretion of vascular permeability factor/vascular endothelial growth factor in human mesangial cells. *Journal of the American Society of Nephrology*. 1999;10(2):245-55.
256. Fujita M, Hayashi I, Yamashina S, Itoman M, Majima M. Blockade of angiotensin AT1a receptor signaling reduces tumor growth, angiogenesis, and metastasis. *Biochemical and biophysical research communications*. 2002;294(2):441-7.
257. Suganuma T, Ino K, Shibata K, Kajiyama H, Nagasaka T, Mizutani S, et al. Functional expression of the angiotensin II type1 receptor in human ovarian carcinoma

cells and its blockade therapy resulting in suppression of tumor invasion, angiogenesis, and peritoneal dissemination. *Clinical Cancer Research*. 2005;11(7):2686-94.

258. Yasumatsu R, Nakashima T, Masuda M, Ito A, Kuratomi Y, Nakagawa T, et al. Effects of the angiotensin-I converting enzyme inhibitor perindopril on tumor growth and angiogenesis in head and neck squamous cell carcinoma cells. *Journal of cancer research and clinical oncology*. 2004;130(10):567-73.

259. Neo JH, Malcontenti-Wilson C, Muralidharan V, Christophi C. Effect of ACE inhibitors and angiotensin II receptor antagonists in a mouse model of colorectal cancer liver metastases. *Journal of gastroenterology and hepatology*. 2007;22(4):577-84.

260. Ebert MP, Lendeckel U, Westphal S, Dierkes J, Glas J, Folwaczny C, et al. The angiotensin I-converting enzyme gene insertion/deletion polymorphism is linked to early gastric cancer. *Cancer Epidemiology Biomarkers & Prevention*. 2005;14(12):2987-9.

261. Röcken C, Diebler E, Carl-McGrath S, Lendeckel U, Malfertheiner P, Roessner A, et al. The Number of Lymph Node Metastases in Gastric Cancer correlates with the Angiotensin II-receptor 1 (AT1R). *Zeitschrift für Gastroenterologie*. 2005;43(05):P001.

262. Röcken C, Röhl F-W, Diebler E, Lendeckel U, Pross M, Carl-McGrath S, et al. The angiotensin II/angiotensin II receptor system correlates with nodal spread in intestinal type gastric cancer. *Cancer Epidemiology Biomarkers & Prevention*. 2007;16(6):1206-12.

263. Wasa J, Sugiura H, Kozawa E, Kohyama K, Yamada K, Taguchi O. The tumor suppressive effect of angiotensin II type 1 receptor antagonist in a murine osteosarcoma model. *Anticancer research*. 2011;31(1):123-7.

264. Zhang Q, Lu S, Li T, Yu L, Zhang Y, Zeng H, et al. ACE2 inhibits breast cancer angiogenesis via suppressing the VEGFa/VEGFR2/ERK pathway. *Journal of Experimental & Clinical Cancer Research*. 2019;38(1):1-12.
265. Ni L, Feng Y, Wan H, Ma Q, Fan L, Qian Y, et al. Angiotensin-(1-7) inhibits the migration and invasion of A549 human lung adenocarcinoma cells through inactivation of the PI3K/Akt and MAPK signaling pathways. *Oncology reports*. 2012;27(3):783-90.
266. Feng Y, Ni L, Wan H, Fan L, Fei X, Ma Q, et al. Overexpression of ACE2 produces antitumor effects via inhibition of angiogenesis and tumor cell invasion in vivo and in vitro. *Oncology Reports*. 2011;26(5):1157-64.
267. Qian Y-R, Guo Y, Wan H-Y, Fan L, Feng Y, Ni L, et al. Angiotensin-converting enzyme 2 attenuates the metastasis of non-small cell lung cancer through inhibition of epithelial-mesenchymal transition. *Oncology reports*. 2013;29(6):2408-14.
268. Carey RM, Padia SH. Physiology and regulation of the renin–angiotensin–aldosterone system. *Textbook of nephro-endocrinology*: Elsevier; 2018. p. 1-25.
269. Ko B, Bakris G. The renin–angiotensin–aldosterone system and the kidney. *Textbook of Nephro-Endocrinology*: Elsevier; 2018. p. 27-41.
270. Santos R, Campagnole-Santos MJ, and Andrade SP. Angiotensin-(1–7): an update *Regul Pept*. 2000;91:45-62.